VOLUME 25 OCTOBER, 1937 NUMBER 10

# PROCEEDINGS
*of*
# The Institute of Radio Engineers

Application Blank for Associate Membership on Page XIX

# Institute of Radio Engineers Forthcoming Meetings

ROCHESTER FALL MEETING
Sagamore Hotel
Rochester, New York
November 8, 9, and 10, 1937

ATLANTA SECTION
October 21, 1937

CINCINNATI SECTION
October 19, 1937

CLEVELAND SECTION
October 28, 1937

DETROIT SECTION
October 15, 1937

LOS ANGELES SECTION
October 19, 1937

NEW YORK MEETING
November 3, 1937

PHILADELPHIA SECTION
November 4, 1937

WASHINGTON SECTION
October 11, 1937

## Pacific Coast Meeting

The Pacific Coast meeting of the Institute which was held in conjunction with the Pacific Coast Convention of the American Institute of Electrical Engineers attracted an attendance of ninety-five Institute members. There were nineteen technical papers presented and the summaries of these were given in the August, 1937, PROCEEDINGS. September 1 and 2 were devoted to the technical sessions at which the papers were presented. The various technical sessions were presided over by H. H. Beverage, president of the Institute; F. E. Terman, chairman of the Pacific Coast Committee; A. V. Eastman, vice chairman of the committee; and J. W. Wallace, chairman of the Seattle Section. A number of those in attendance were present at the annual banquet of the American Institute of Electrical Engineers. Many also took advantage of the full-day trip to Grand Coulee Dam which was arranged by the electrical engineering group.

## Committee Work

### ADMISSIONS

A meeting of the Admissions Committee was held in the Institute office on September 14 and attended by R. A. Heising, acting chairman; F. W. Cunningham, L. C. F. Horle, C. W. Horn, E. R. Shute, A. F. Van Dyck, and H. P. Westman, secretary.

Three applications for transfer to Fellow grade were approved. Eleven applications for transfer to Member were accepted and two were rejected. There were two applications for admission to the grade of Member approved.

### NEW YORK PROGRAM

R. R. Beal, G. C. Connor, D. E. Foster, R. A. Heising, Keith Henney, H. C. Likel (representing L. G. Pacent), and H. P. Westman, secretary, attended a meeting of the New York Program Committee which was held in the Institute office on September 2. The meeting was devoted to the preparation of a list of papers for presentation at the fall meetings of the Institute to be held in New York City.

## Institute Meetings

### INDIANAPOLIS SECTION

On June 24, V. C. McNabb, chairman, presided at a meeting of the Indianapolis Section held at the Indianapolis Athletic Club. There were eighty-six present.

A paper on "A New Inductive Tuning System" was presented by Paul Ware of P. R. Mallory and Company and discussed by Messrs. Callahan, French, and Passow. Described among the more important features of the system was a slide-contact variable inductance wherein the contact travels along the length of the turns of a rigid rotatable helix. A carriage assembly having insulated trolley wheels which ride on the wire is compressed between a fixed bar and the coil. The life of the contact is equal to several hundred miles of travel and corresponds to a million or more rotations. A terminal inductance having a $Q$ superior to a mechanically stopped-off portion of the rotating coil considerably improves operation at the high-frequency end of the range when used with a fixed condenser as a resonant circuit. Two or three times the usual tuning range may be obtained. The effects of varying the axial pitch, various coil geometries, and the use of high-frequency iron were described. The operating range of the coil is limited by the natural period of the shorted unused portion and in the low-frequency region by the impedance obtained. High-frequency oscillator design is simplified as at the low-frequency end of the range the circuit impedance continuously rises. Feed-back coupling at the high-frequency end may be made sufficient to maintain approximately uniform oscillation strength through a reactive range of a hundred to one. Comparisons were made between inductance and capacitance tuned superheterodyne input systems. A new oscillator tracking expedient produces a fourth tracking crossover for wide range tuning. The large range of motion of the multiturn coil over the half turn of a variable condenser permits much more accurate scale indication particularly in the high-frequency ranges. The system is virtually nonmicrophonic so far as the variable inductance is concerned.

An ultra-high-frequency oscillator capable of supplying a strong uniform voltage to frequencies above one hundred and fifty megacycles was described. A signal generator using the inductive tuning system was described and covered the range from ninety kilocycles to thirty-five megacycles with long accurate scales and only three switch positions. A receiving set was demonstrated and covered all frequencies between five hundred and forty kilocycles and sixty-five megacycles with three switch positions. In the discussion, it was pointed out that the antenna step-up and the tuned radio-frequency gain in the broadcast region were of the order of three to four and ten to fifteen, respectively. These gains depend on the coil size and increase with the inductance of the rotatable coil.

*Proceedings of the Institute of Radio Engineers*
*Volume 25, Number 10* *October, 1937*

## TECHNICAL PAPERS

# A NEGATIVE GRID TRIODE OSCILLATOR AND AMPLIFIER FOR ULTRA-HIGH FREQUENCIES*

By
A. L. Samuel
(Bell Telephone Laboratories, Inc., New York City)

***Summary***—*A description is given of some negative grid triodes of unusual design which operate both as oscillators and as amplifiers at frequencies higher than those previously reported. These tubes differ from the conventional primarily in the number and arrangement of the leads. When used as oscillators the upper frequency limits are increased by this arrangement to approximately 1.3 times the values otherwise obtained. Stable operations are secured as amplifiers at somewhat lower frequencies, the stability outputs and distortion ratios being comparable with those obtained from pentodes of similar ratings.*

IT IS an interesting and perhaps significant fact that the simple three-element vacuum tube is still used extensively as an oscillator and as a high power radio-frequency amplifier in spite of recent advances made in the design of multielement tubes. Some may see in this only the failure of the tube engineer to apply existing knowledge. The tube engineer, on the other hand, while not entirely unwilling to admit the truth of this accusation, is inclined to wonder if there may not still exist a field of usefulness for the triode. If such a field exists most certainly it must lie either in the region of very small tubes where the mechanics of fabrication prove difficult, or in the region of very large power tubes where the problems of the screen power dissipation become acute. What then could be more logical than to expect to find triodes used for power oscillators and amplifiers at ultra-high frequencies where the electron transit time considerations dictate small interelectrode spacings and where the relatively large power ratings require high dissipation rates?

As a matter of fact, the negative grid triode has appeared to lag behind the magnetron as an oscillator at frequencies above roughly 500 megacycles while the only successful power amplifiers which have been described for frequencies of the order of 300 megacycles are multielement tubes.[1] One is led to suspect that those factors which limit the

* Decimal classification: R330. Original manuscript received by the Institute, June 1, 1937. Presented before I.R.E.-U.R.S.I. Meeting, Washington, D. C., April 30, 1937.

[1] A. L. Samuel and N. E. Sowers, "A power amplifier for ultra-high frequencies," Proc. I.R.E., vol. 24, pp. 1464–1483; November, (1936), also in *Bell Sys. Tech. Jour.*, vol. 16, pp. 10–34; January, (1937).

frequency range of the triode as an amplifier may also limit its frequency range as an oscillator.

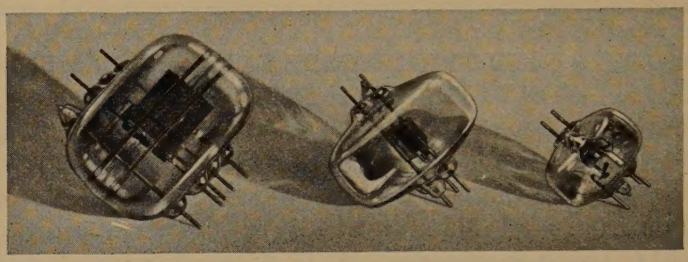

Fig. 1—Experimental double-lead tubes.

The triode as used at radio frequencies differs from the multi-element tube chiefly in the manner in which interaction is prevented

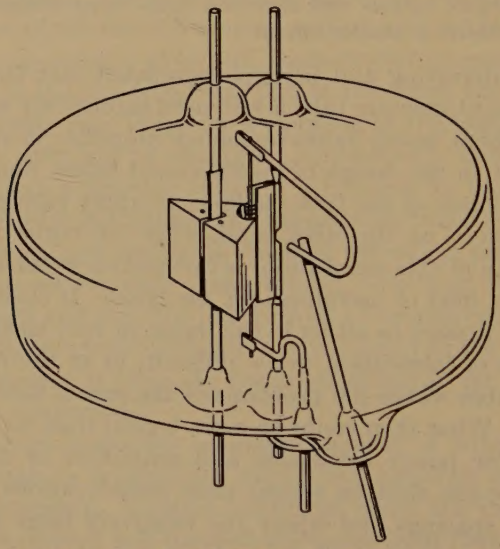

Fig. 2—Section view of a double-lead tube showing lead arrangement.

between the input and output circuits. This is obviously a circuit limitation, as contrasted with the electron-transit-time limitation which has received so much attention.[2] The greatest opportunity for

[2] F. B. Llewellyn, "Operation of ultra-high-frequency vacuum tubes," *Bell Sys. Tech. Jour.*, vol. 14, pp. 632–665; October, (1935).
W. R. Ferris, "Input resistance of vacuum tubes as ultra-high-frequency amplifiers," PROC. I.R.E., vol. 24, pp. 82–107; January, (1936).
D. O. North, "Analysis of the effects of space charge on grid impedance," PROC. I.R.E., vol. 24, pp. 108–136; January, (1936).
H. Rothe, "Input and output resistance of thermionic valves at high frequencies," *Telef. Rohre Supp.*, July, (1936).

improvement, therefore, seems to be in the direction of improved circuit design. The tubes described in this paper were developed from this point of view.

Sample tubes are shown in Fig. 1. They differ from tubes previously described[3] primarily in the lead arrangement. From the sketch of one of these tubes shown in Fig. 2, it will be observed that the grid and plate elements are supported by wires which in effect go straight

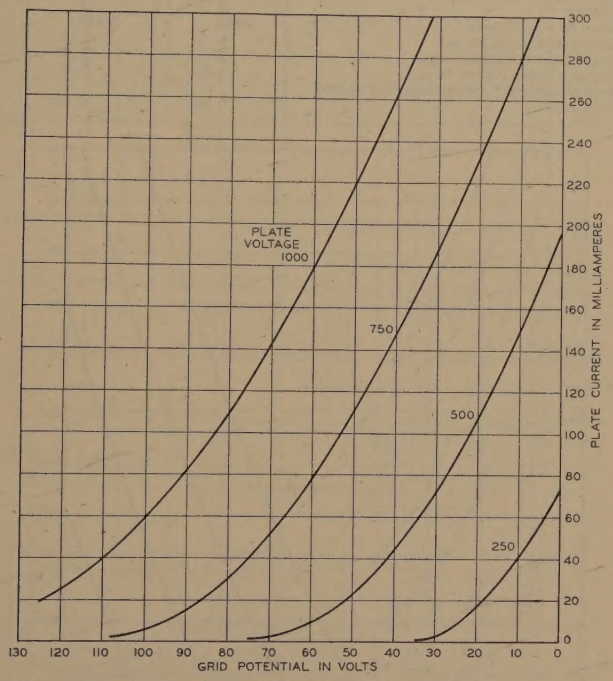


Fig. 3—Static characteristics of large tube.

through the tube envelope providing two independent leads to each of these elements. Although this arrangement has been used in Barkhausen tubes to reduce circuit losses,[3] it apparently has not previously been applied to the case of the negative grid tube. The filament leads are at one end only and one of these leads is extremely short. This unusual lead arrangement possesses a number of unique advantages which will be discussed in detail later.

The operating characteristics of these three tubes are listed in

[3] M. J. Kelly and A. L. Samuel, "Vacuum tubes as high-frequency oscillators," *Elec. Eng.*, vol. 53, pp. 1504–1517; November, (1934), also in *Bell Sys. Tech. Jour.*, vol. 14, pp. 97–134; January, (1936).

Table I. Special attention is directed to the values of interelectrode capacitances and lead inductances. The usual static characteristics,

TABLE I
CHARACTERISTICS

| | Large Tube | Intermediate Tube | Small Tube |
|---|---|---|---|
| Filament current in amperes | 10 | 8.5 | 4 |
| Filament potential in volts | 3 | 1.5 | 1 |
| Anode potential in volts | 750 | 500 | 300 |
| Maximum anode dissipation in watts | 150 | 50 | 25 |
| Amplification factor | 9 | 8 | 9 |
| Transconductance in micromhos | 4000 | 3000 | 2500 |
| Direct grid-plate capacitance in $\mu\mu f$ | 3.5 | 1.6 | 0.9 |
| Direct filament-grid capacitance in $\mu\mu f$ | 2 | 1.3 | 1 |
| Direct filament-plate capacitance in $\mu\mu f$ | 1.3 | 0.9 | 0.7 |
| Approximate grid-plate lead inductance in microhenrys (on each side) | 0.05 | 0.03 | 0.01 |

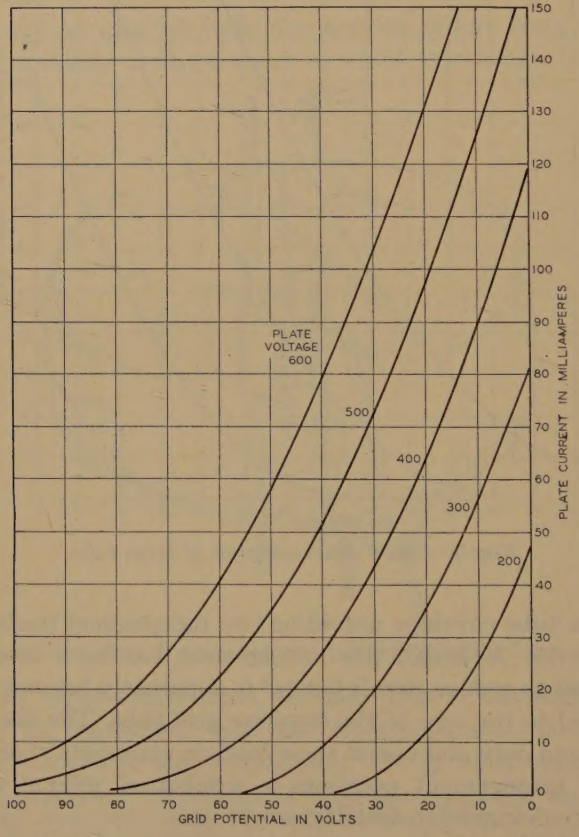


Fig. 4—Static characteristics of intermediate size tube.

shown in Figs. 3, 4, and 5 are quite typical for tubes of comparable rating.

One or two constructional features aside from the lead arrangement are worthy of note. All of the grids are of the so-called fin type. The filament of the large tube is in the form of a ribbon. This shape was adopted to provide the necessary emitting area while keeping the filament heating current demands within bounds. It also minimizes the

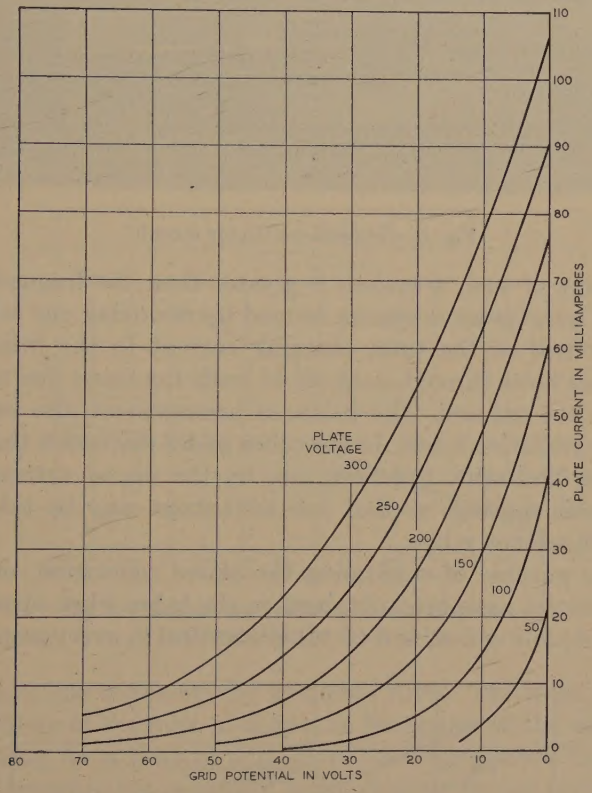


Fig. 5—Static characteristics of small tube.

objectionable end cooling which occurs with large size filaments. The filament in the small tube, although in the form of a wire, is tapered near the ends, again to minimize end cooling. Carbon has been used for the anodes, primarily because of the ease of fabrication for a limited number of experimental tubes.

## The Double-Lead Tube as an Oscillator

The double-lead arrangement is responsible for an increase in the upper frequency limit of the tube as an oscillator by a factor of from 1.2

to approximately 1.4. A typical oscillator circuit is shown in Fig. 6. Here the tube is mounted at the center of an equivalent half-wave Lecher system. It may be shown by a simple calculation that the natu-

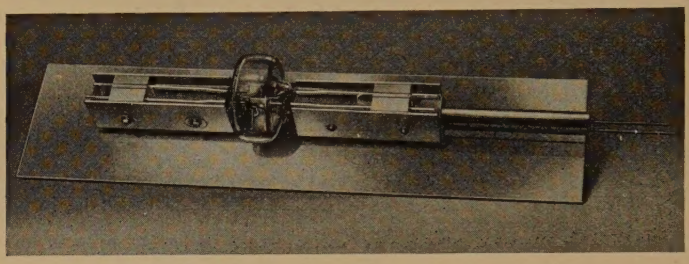

Fig. 6—Typical oscillator circuit.

ral frequency of such a system is greater than the frequency of the equivalent quarter-wave system formed by removing one set of leads. Since only half of the total charging current to the interelectrode capacitances flows through each set of leads the losses due to the lead resistances are reduced. The balanced arrangement also results in a decrease in radiation losses. In the tubes under discussion the electron-transit-time limitation has been met by the use of extremely small interelectrode spacings so that full advantage may be taken of the increased frequency range.

For the purpose of confirming the above conclusion, output and efficiency curves have been obtained on the tubes when operated both single and double ended, and on tubes identical in every respect except

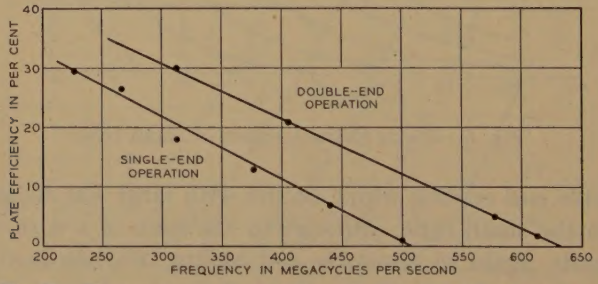


**Fig. 7—Comparison plot of the efficiencies of a large tube operated single and double ended.**

for omission of the extra set of leads. Typical results for the large tube are shown in Fig. 7. It will be observed that the efficiencies for double ended operation are always higher than for the single ended case over the range covered by the experimental data. In fact, usable outputs are

obtained at frequencies well beyond the point where the single ended tube fails to operate. The ratio of the cutoff frequencies for the two modes of operation happened to be 1.23 for the particular conditions under which these data were obtained.

Output and efficiency curves for the large size tube are shown in Fig. 8. The values of 60 watts at 300 megacycles and 40 watts at 400 megacycles compare quite favorably with outputs reported from radiation cooled magnetrons.[4] When the problems of modulation and the complications of the magnetron's magnetic field are considered, the advantages of the negative grid triodes become more apparent. Fig. 9 is a comparison plot of the outputs obtainable from these tubes and

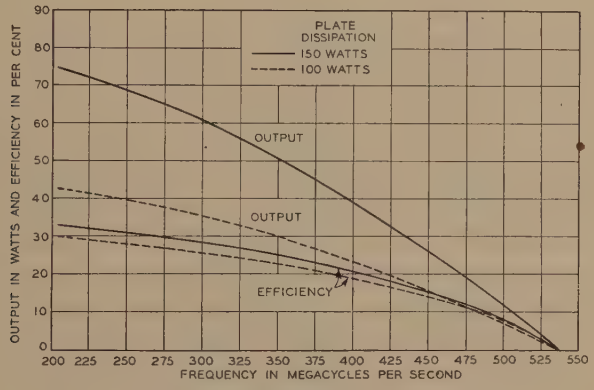


Fig. 8—Output and efficiency as a function of frequency for the large tube.

from some of the commercially available tubes. The sloping lines are for fixed values of the ratio of output to the square of the wave length, one line being for a ratio of four times that represented by the other line. The improvement in output made possible by the present departure in design is at once evident. Special attention is called to the output and the upper frequency limit of the small tubes. Typical values are 3 watts at 1200 megacycles, 2 watts at 1500 megacycles, and 1 watt at 1700 megacycles, with a limiting frequency of 1870 megacycles corresponding to a wave length of 16 centimeters. While the results so far obtained are obviously not conclusive, they do suggest that the negative grid tube is still a strong contender for the supremacy as an oscillator at frequencies as high as 1500 megacycles.

[4] G. R. Kilgore, "Magnetron oscillators for the generation of frequencies between 300 and 600 megacycles," Proc. I.R.E., vol. 24, pp. 1140–1157; August, (1936).

## The Double-Lead Tube as an Amplifier

The double-lead arrangement is also responsible for an increase in the upper frequency limit at which stable operation as an amplifier may be secured. To understand how this comes about it will be necessary to consider briefly the causes for instability as an amplifier.

The primary cause for instability of the triode is the interaction between the input and output circuits which results from the coupling between these circuits provided by the grid-plate capacitance. A second

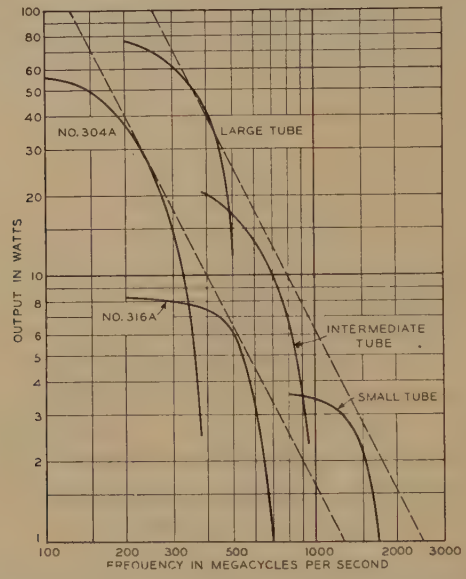


Fig. 9—Comparison plot of the outputs of the double-lead tubes and of commercially available tubes.

source of coupling is that caused by common impedances in the two circuits in the nature of the self and mutual inductance of the tube leads. This second form of coupling will be referred to as impedance coupling as contrasted with admittance coupling caused by the inter-electrode capacitances. At moderately high frequencies this impedance coupling is usually of negligible importance. Stable operation is thus possible when suitable means are provided to compensate or "neutralize" the admittance coupling. At ultra-high frequencies impedance coupling can no longer be neglected. It may, of course, be minimized by the use of short leads. As a consequence, triodes designed for use as oscillators at ultra-high frequencies are also good amplifiers.

The ultimate solution to the problem is to provide independent

leads for the input, output, and admittance neutralizing circuits so that impedance coupling because of common leads is definitely eliminated. Coupling because of mutual impedances will still be present but may be minimized by the proper arrangement of the leads. The double-lead tube is an attempt to fulfill these conditions. It will be observed that the only common impedance remaining is that introduced by one filament lead and that this lead is extremely short.

One additional refinement in circuit design is required before full advantage may be taken of this lead arrangement. In general, two methods of neutralizing admittance coupling are possible. One is to compensate for the potential, which the disturbing admittance introduces in the input circuit, by means of another potential of opposite polarity derived from a second and similar admittance properly connected. All of the more common capacitance neutralization schemes fall in this category. The second method, first disclosed by H. W. Nichols in U. S. Patent 1,325,879, is to resonate the offending admittance at the desired operating frequency so that the resulting parallel admittance is reduced to a very low value. In the triode circuit this takes the form of an inductance connected between the grid and plate of the tube and adjusted to resonate with the grid-plate capacitance. For ease of adjustment a somewhat lower fixed inductance may be used and tuned by the adjustment of a small variable condenser in parallel. This form of neutralization is commonly referred to as "coil" neutralization. At ultra-high frequencies where unavoidable inductances are already present in the form of lead inductances, this "coil" scheme possesses outstanding advantages over the more usual "capacitance" schemes. These advantages become even more pronounced with the availability of the double-lead tube.

In order to verify this analysis a "coil-neutralized" two-stage amplifier was constructed by R. J. Kircher using two of the larger sized tubes. An output of 60 watts at 144 megacycles with an efficiency of 30 per cent for class B operation is obtained with this amplifier. For an output of 20 watts at 144 megacycles the third order distortion products are 43 decibels below the fundamental. The stability and band width are quite comparable with results obtained on a pentode of similar ratings. Results of a comparable nature have been obtained on the intermediate size tube. The full capabilities of the small size tube as an amplifier have not been completely evaluated. From a comparison of its characteristics and performance as an oscillator with data available for the larger tubes, it seems reasonable to assume that stable operation as an amplifier will prove possible at frequencies as high as 1000 megacycles.

The encouraging nature of these results leads one to suspect that the negative grid triode will prove to be a strong contender for supremacy as an amplifier at ultra-high frequencies particularly in the range of large outputs just as it is still supreme for very large outputs at somewhat lower frequencies. Of course, much remains to be done before even the results here reported on experimental laboratory tubes can be duplicated on a practical scale.

In conclusion the double-lead tube is seen to possess a number of distinct advantages as both an oscillator and an amplifier in the frequency range from 100 megacycles to 1000 megacycles. While the ultimate limit to which such developments may be pushed is entirely a matter of conjecture it seems safe to predict that the triode will be able to meet the demands of the circuit designer at least for some time to come.

### Acknowledgment

The writer wishes to express his appreciation for the contributions of Mr. J. P. Laico toward the solution of the many difficult problems of mechanical designs and fabrication which have arisen in the course of this development.

*Proceedings of the Institute of Radio Engineers*
*Volume 25, Number 10* *October, 1937*

# SUDDEN DISTURBANCES OF THE IONOSPHERE*

By

J. H. Dellinger

(National Bureau of Standards, Washington, D.C.)

***Summary***—*The phenomenon described in this paper is the occurrence of a very sudden change in ionization of a portion of the ionosphere. It manifests itself by the complete fading out of high-frequency radio transmission for a period of a few minutes to an hour or more, and by perturbations of terrestrial magnetism and earth currents. The effect was discovered in 1935, and found to occur simultaneously everywhere throughout the illuminated half of the globe but not in the night half. The results of a world-wide investigation of the phenomenon which followed this discovery are presented in this paper.*

*The radio and magnetic effects have been shown to be of a distinct type, quite different from previously known vagaries in these fields. They are of maximum intensity in that region of the earth where the sun's radiation is perpendicular.*

*Many of the occurrences are simultaneous with great eruptions on the sun. Such eruptions emit vast quantities of ultraviolet light. These radiations are sometimes of such frequencies as to cause intense ionization of part of the ionosphere below the E layer. This sudden ionization causes the radio and other perturbations. Their characteristics are explained. Study of this effect is leading to new understanding of the nature of the ionosphere, the processes of radio wave transmission, the mechanisms of terrestrial magnetism, and the phenomena occurring in the sun.*

## I. Introduction

THIS paper presents the conclusions and data up to the end of 1936 of an investigation, started about the middle of 1935, of a hitherto unknown phenomenon. The phenomenon is the occurrence of a sudden intense increase in the ionization of a part of the earth's upper atmosphere, with resultant transient disturbances in such phenomena as radio wave transmission, terrestrial magnetism, and earth currents. The radio effect is of serious practical import, as it manifests itself principally as a sudden disappearance of radio signals received on high frequencies, the period of silence ranging from a few minutes to an hour or more. The whole phenomenon is of scientific interest particularly because it appears to have its origin in sudden bursts of radiation from the sun, and is opening the way to increased understanding of the sun, the ionosphere, radio transmission, terrestrial magnetism and related phenomena.

* Decimal classification: R113.5. Original manuscript received by the Institute, June 11, 1937. Presented before American Physical Society, Denver, Colo., June 25, 1937. Published in *Nat. Bur. Stand. Jour. Res.*, vol. 19, pp. 111–142; August, (1937). Publication approved by the Director of the National Bureau of Standards of the U. S. Department of Commerce.

In October, 1935, the author reported[1] the occurrence of radio fade-outs on March 20, May 12, July 6, and August 30 of that year. He pointed out that they occurred throughout the illuminated half of the globe but not the dark half, advanced the hypothesis that they depend on some solar emanation lasting only a few minutes, and suggested observations by workers in other sciences with a view to learning of the possible occurrence of effects in terrestrial magnetism, earth currents, solar radiation, etc., simultaneous with radio fade-outs. The suggestion met with widespread interest, and the author has had the collaboration of numerous individuals and organizations in this investigation.

Evidence followed rapidly that the postulated simultaneous effects do occur. The astronomers at Mt. Wilson Observatory of the Carnegie Institution of Washington were asked to examine their spectrohelioscopic data for the dates in question, and in November, 1935, R. S. Richardson of that Observatory informed the author that on July 6 and August 30 bright eruptions had been observed on the sun within a few minutes of the times of the radio fade-outs, and on the other two dates no observations had been made at the times of the fade-outs. These results were announced by Dr. Richardson and the author at the end of 1935.

The magnetograms of the Cheltenham, Maryland, Observatory of the U. S. Coast and Geodetic Survey were examined by the author for the times of all the fade-outs then known, and for several of them small abrupt pulses were found, beginning at a time within two minutes of the radio fade-out time. Also, H. H. Beverage of R.C.A. Communications, Inc., reported to the author the occurrence of a large sharp pulse on an earth-current recorder within a few minutes of the time of several of the radio fade-outs.

From these beginnings has grown an extensive research upon these interrelated phenomena. Through the kindness of many cordial co-operators I am able to present a summary of data on the known occurrences. Acknowledgments of the work of these co-operators are given in Section VII. Systematic recording of the phenomena has been carried on by the National Bureau of Standards, and complete reports have been furnished by a few other groups, but many of the reports from scattered places are sporadic and partial. Data are relatively meager for the Asiatic and Pacific regions. It is believed that the results are of sufficient value to provide encouragement for more widespread and systematic observations and for more intensive exploration of the several fields of inquiry opened up by this work.

Preliminary reports of the results, and explanation in terms of

[1] See first two references in Bibliography at end of paper.

ionosphere effects, were given by the author in papers presented at the Washington meeting of the American Section, International Scientific Radio Union, May 1, 1936, and at the Cleveland Convention of the Institute of Radio Engineers, May 11, 1936. A number of brief papers have been published by the author and others, giving some of the results and preliminary conclusions. (See Bibliography at end of paper.)

This paper presents a compressed summary of the known facts regarding 118 sudden disturbances of the ionosphere, many of which were accompanied by solar eruptions, many of which were manifested by perturbations of terrestrial magnetism and earth currents, and each of which was manifested by the wiping out of hundreds or thousands of radio transmissions.

## II. Data

In this Section a summary of the available data is presented. In Sections III, IV, and V the facts regarding particular aspects of the data are presented and discussed. In Section VI is given a discussion and explanation of the entire phenomenon.

The data considered in this paper are given in very condensed form in Table I, and are essentially for the years 1935 and 1936. One earlier occurrence is included, that of November 28, 1934, as it was clearly the same phenomenon. There is little reliable information on earlier occurrences of this type. Some records indicate occurrences which may or may not be the same phenomenon. Thus, the logs of radio operating companies show radio traffic interruptions on many occasions in 1934 and earlier but there is very little information at hand to judge whether they were of the type due to the sudden ionosphere disturbances here studied or to others of the various radio wave vagaries mentioned at the beginning of Section III below. Information on a number of such traffic interruptions in 1928 have been given by T. L. Eckersley.[2] From the data given in his paper, the failure of radio transmission on October 10, 1928, from 1100 to 1200, G.M.T., may have been a case of the phenomenon here studied. Likewise, from data reported to the author of the present paper, the failure of radio transmission from 1305 to 1400, G.M.T., on May 11, 1934, may also have been a case.

Similarly, there is some information on a few early occurrences of sudden terrestrial magnetic pulses simultaneous with visible solar eruptions, occasionally reported by astronomers many years ago. Some instances are given by G. E. Hale.[3] Interesting ones were ob-

[2] "An investigation of short waves," *Proc. I. E. E.* (London), vol. 67, p. 992, (1929)

[3] "The spectrohelioscope and its work, Part III; Solar eruptions and their apparent terrestrial effects," *Astrophys. Jour.*, vol. 73, p. 379, (1931).

served on August 3 and 5, 1872, by Prof. C. A. Young, as described in his book, "The Sun," (1884). These occurrences may have been of the type associated with the sudden ionosphere disturbances here studied.

Table I summarizes the data from all sources. It is regretted that only a summary can be given; the complete details are so voluminous that it is not practicable to tell the whole story of each of the occurrences. The complete details would occupy hundreds of pages. Thus in the case of numerous publications listed in the Bibliography the entire article is devoted to observations at a single place of a single one of these occurrences. Table I includes some information based on published articles. Most of the data, however, were derived from observations made at the National Bureau of Standards and from reports sent by other observers to the author. Acknowledgments of this assistance are given in Section VII below.

Even though they represent very extensive observations, the data we have do not give comprehensive information on the occurrences. In some cases we have knowledge of the disturbance from only two places of observation (and effects reported from only one place are included in two or three cases, where radio waves were received over numerous paths and the effects were extremely intense and clearly authentic). It would be desirable that we have for each occurrence information from numerous points all over the world, on the effects which occurred in radio transmission, terrestrial magnetism, and earth currents. In no case have we such complete information, and in many cases we also lack certainty as to whether a solar eruption occurred at the time. The incomplete character of our knowledge should be remembered in interpreting the data.

This investigation has dealt primarily with the radio aspects of the sudden ionosphere disturbances, as the form of Table I indicates. The table gives, for each receiving location reporting a radio fade-out, the average time of the fade-out of high-frequency radio waves for each of the locations of transmitting stations whose emissions were affected. For the terrestrial magnetic and earth-current pulses, the effects upon atmospherics, and solar eruptions, only the times of occurrence are given. All times given in this paper are in G.M.T., i.e., Greenwich Mean Time. Eastern Standard Time is five hours less than G.M.T.

In the second column of Table I, the first time given on each line is the time of beginning of the radio fade-out. Where three times are given, the second is the time when the radio signals began to come in again and the third is the time when the intensities had risen to normal. Where two times are given, the second is in most cases the time when the radio signals had risen to approximately normal.

TABLE I

DATA ON RADIO FADE-OUTS AND OTHER MANIFESTATIONS OF SUDDEN IONOSPHERE DISTURBANCES

| Date | Time, G.M.T. | Reported observed in | Reported locations of transmitting stations | Reported solar and magnetic effects, etc. |
|---|---|---|---|---|
| 1934 | | | | |
| Nov. 28 | 1710–1740 | Georgia | Eastern U.S.A. | Solar eruption, beginning about 1710. |
| | 1710–1745 | New York | S. America | Terrestrial magnetic pulse, 1707–1730. |
| | 1710–1730 | Washington, D.C. | D.C.* | Earth-current pulse, 1710–1740. |
| 1935 | | | | |
| Jan. 25 | 0335–0535 | California | Asia, Philippines, Java | |
| Mar. 20 | 0150–0200 | Philippines | California | |
| | 0148–0200 | California | Asia, Philippines, Java | |
| May 12 | 1157–1215 | France | (Numerous) | Ter. mag. pulse, 1157. |
| | 1156–1214 | New Jersey | England | |
| | 1200–1215 | New York | Europe, S. America | |
| July 6 | 1409–1437 | New York | England, U.S.A., S. America | Solar eruption, 1358–1418. Ter. mag. pulse, 1407–1412. |
| | 1408–1430 | France | N. & S. America, Asia | Earth-current pulse, 1400–1411. |
| Aug. 30 | 2320–2325–2335 | California | Asia, Philip., Java, Western U.S.A., California. | Solar eruption 2312 to after 2330. |
| | 2300–2329 | Philippines | | |
| Sept. 13 | 1630–1640–1650 | California | U.S.A., Manila, Shanghai, Tokyo | Solar eruption, 1635–1641. Ter. mag. pulse, 1630. |
| Sept. 27 | 1250–1350 | New York | Europe, S. America | Solar eruption, from before 1200 to after 1230. Ter. mag. pulse, 1250. |
| | 1245–1315 | England | (Numerous) | |
| Sept. 29 | 2055–2120–0150 | California | Tokyo, Shanghai, Hawaii, New York | |
| | 2050–2110 | D.C. | Massachusetts | |
| Oct. 24 | 1100–1200 | New York | (Numerous) | Earth-current pulse, 1130–1215 |
| Nov. 18 | 1755–1815 | Porto Rico | U.S.A. | |
| | 1757–1800 | D.C. | Ohio | |
| Nov. 29 | 1405–1415 | New York | S. America | Solar eruption, from before 1431 to 1445. |
| | 1405–1415 | Brazil | (All stations) | |
| Nov. 30 | 1721–1730–1815 | D.C. | Ohio, Massachusetts | Solar eruption, 1751–1830. |
| Nov. 30 | 1850–1908–1930 | D.C. | Ohio, Massachusetts | |
| | 1900–1925–1935 | Hawaii | California | |
| Dec. 16 | 2209–2230 | D.C. | Massachusetts | Solar eruption, 2210–2238. |
| | 2223–2225 | Hawaii | California | |
| Dec. 17 | 1615–1630 | New York | S. America | Solar eruption, beginning before 1609. |
| | 1630–1700 | New Jersey | England | Ter. mag. pulse, 1610–1630. |
| | 1610–1618–1630 | D.C. | Massachusetts, Ohio | |
| | 1620–1630–1655 | Texas | Numerous amateur stations. | |
| Dec. 18 | 0450–0615 | California | Asia, Philippines. Java | |
| Dec. 23 | 1730–1826–2000 | D.C. | Ohio, Mass., D.C.* | Solar eruption, from before 1757 to after 1805. |
| | 1730–2000 | California | Asia, Philippines, Java | |
| | 1730–1930 | New York | Europe, S. America | |
| | 1740–1930 | Georgia | Eastern U.S.A. | |
| | 1745 | Porto Rico | U.S.A. | |
| 1936 | | | | |
| Feb. 6 | 1520–1645–2040 | D.C. | Ohio, D.C.* | Ter. mag. pulse, 1520. |
| | 1520–1550–1645 | Georgia | Eastern U.S.A. | L-f atmos. increase, 1520–1600. |
| | 1515–1530–1700 | New York | S. America, Europe | |
| | 1520–1620 | England | Numerous | |
| Feb. 8 | 0130–0310 | Philippines | China, Guam, Hawaii | |
| | 0130–0230 | Japan | California, Brazil, Syria | |
| | 0205–0300 | California | Asia, Philippines, Java | |
| | 0200–0315 | Malaya | Asia | |
| | 0200–0325 | Siam | Asia | |
| | 0210–0330 | Fr. Indo China | Asia, Philippines, Java | |

* Disappearance or weakening of sky waves reflected vertically from ionosphere.

TABLE I—*Continued*

| Date | Time, G.M.T. | Reported observed in | Reported locations of transmitting stations | Reported solar and magnetic effects, etc. |
|---|---|---|---|---|
| 1936 | | | | |
| Feb. 8 | 1315–1402 | Porto Rico | U.S.A. | Solar eruption, 1330 to after 1400. |
| | 1325–1500 | England | Numerous | Ter. mag. pulse, about 1328. |
| | 1326–1350–1420 | D.C. | Ohio, Massachusetts | L-f atmos. increase, 1325 |
| | 1323–1358 | New York | Europe, S. Amer. | |
| Feb. 14 | 1515–1550–1730 | D.C. | Ohio, Mass., Calif., Ill., Texas, D.C.* | Solar eruption, 1530–1600. Ter. mag. pulse, 1515–1600 |
| | 1516–1540–1700 | New York | Europe, N. & S. America | L-f atmos. increase, 1526. |
| | 1518–1542 | New Jersey | England | |
| | 1518–1600 | Michigan | U.S.A. | |
| | 1517–1545 | Missouri | U.S.A. | |
| | 1515–1550 | Texas | U.S.A. | |
| | 1520–1540 | Pennsylvania | U.S.A. | |
| | 1516–1536–1546 | Arkansas | U.S.A. | |
| | 1519–1545–1600 | Holland | Dutch Indies, Europe, N. & S. America | |
| | 1518–1542 | England | S. Africa, Egypt, India, Europe, N. & S. America, Australia. | |
| | 1513–1545 | Spain | Europe, N. & S. America | |
| | 1516–1545 | France | Africa, N. & S. America, Japan, China. | |
| | 1519–1550 | Germany | N. & S. Amer. | |
| | 1520–1545 | Africa | France | |
| | 1515–1540 | Syria | France | |
| | 1515–1605 | Argentina | (Numerous) | |
| | 1520–1545 | Quebec, Canada | U.S.A. & Canada | |
| | 1515–1635 | Panama, C. Z. | N. & S. America | |
| | 1515–1545–1730 | Porto Rico | U.S.A. | |
| | 1518–1542 | Florida | Porto Rico | |
| | 1518–1548 | California | U.S.A. | |
| | 1518–1540 | Louisiana | U.S.A. | |
| | 1517–1550 | Illinois | U.S.A. | |
| | 1515–1533 | Idaho | U.S.A. | |
| | 1515–1545 | Nebraska | U.S.A. | |
| | 1520–1546 | Ohio | U.S.A. | |
| | 1515–1600 | Georgia | U.S.A. | |
| | 1515–1545 | Massachusetts | U.S.A. | |
| | 1515–1540 | Oklahoma | U.S.A. | |
| | 1517–1536 | Virginia | U.S.A. | |
| Feb. 16 | 1550–1613–1627 | D.C. | Ohio, Mass., D.C.* | Solar eruption, from before 1630 to after 1700. |
| | 1600–1630 | Rhode Island | New England States | L-f atmos. increase, 1545–1700. |
| | 1545 | France | (Numerous) | |
| Mar. 4 | 1956–2010 | California | Asia, Philip. Java, U.S.A. | Ter. mag. pulse, 1955–2005 |
| | 1956–2007–2020 | D.C. | Ohio, Mass., D.C.* | Slight earth-current pulse, 1956. |
| Mar. 10 | 0540–0600 | Japan | India, Syria, China, Siam, Java. | |
| Mar. 23 | 1545–1553–1603 | D.C. | Ohio, Mass., D.C.* | Solar eruption, 1530–1607. Ter. mag. pulse, 1545. L-f atmos. increase, 1545–1650. |
| Apr. 1 | 0930–0950 | England | (Numerous) | Solar eruption, 0926–1040. |
| | 0938 | France | (Numerous) | |
| Apr. 1 | 1200–1220 | England | (Numerous) | |
| | 1218–1223–1229 | D.C. | Ohio, Massachusetts | |
| Apr. 2 | 0405–0417–0640 | Malaya | Java, Malaya | |
| | 0400–0420 | Japan | Calif., Philippines, Asia | |
| | 0400–0415 | California | Asia, Philippines, Java | |
| | 0400–0420 | Argentina | Tokyo | |
| Apr. 6 | 1356–1403–1418 | D.C. | Ohio, Mass., D.C.* | Ter. mag. pulse, 1355–1402 |
| | 1353–1418 | New York | (Numerous) | L-f atmos. increase, 1357–1448. |
| | 1353–1359 | New Jersey | England | |
| | 1355–1405 | Holland | S. America, Portugal, Hungary | |
| | 1355–1405 | England | N. & S. America, Africa, Japan | |
| Apr. 7 | 0230–0430 | Japan | Europe | Solar eruption, starting before 0231. |

* Disappearance or weakening of sky waves reflected vertically from ionosphere.

TABLE I—*Continued*

| Date | Time, G.M.T. | Reported observed in | Reported locations of transmitting stations | Reported solar and magnetic effects, etc. |
|---|---|---|---|---|
| 1936 | | | | |
| Apr. 8 | 0920–0945 | Holland | Austria, Hungary | Solar eruption, 0810–1000.<br>Ter. mag. pulse, 0912–0925. |
| Apr. 8 | 1450–1520 | D.C. | Ohio, Mass., D.C.* | Ter. mag. pulse, 1450. |
| | 1450–1520 | Texas | U.S.A. | |
| | 1450–1520 | Arizona | U.S.A. | |
| Apr. 8 | 1646–1726–1815 | D.C. | Ohio, Mass., D.C.* | Solar eruption, 1645–1703 |
| | 1650–1700 | France | U.S.A., S. America | Ter. mag. pulse, 1645–1705. |
| | 1645–1657–1720 | New York | England, S. Amer., U.S.A. | Earth-current pulse, 1645–1700. |
| | 1650–1658–1704 | New Jersey | England | L-f atmos. increase, 1650–1745 |
| | 1645–1708 | Holland | Japan, Europe, N. & S. America | |
| | 1650–1706–1725 | Georgia | U.S.A | |
| | 1648–1705 | California | Asia, Philip., Java, U.S.A. | |
| | 1645–1657–1720 | England | N.Y., S. America, Africa | |
| | 1630–1655–1705 | Quebec | England, Australia | |
| | 1630–1655–1705 | British Columbia | Quebec, Australia | |
| | 1650–1710 | Spain | S. America | |
| | 1645–1740 | Peru | Peru* | |
| | 1703–1738 | Oklahoma | (Numerous) | |
| | 1650–1712 | Texas | (Numerous) | |
| | 1650–1703–1720 | Florida | (Numerous) | |
| | 1645–1655–1715 | Tennessee | (Numerous) | |
| | 1640–1720 | Illinois | (Numerous) | |
| | 1648–1704–1720 | Indiana | (Numerous) | |
| | 1658–1705–1730 | Iowa | (Numerous) | |
| | 1658–1704–1725 | Nebraska | (Numerous) | |
| | 1655–1718 | Missouri | (Numerous) | |
| Apr. 9 | 1320–1400 | D.C. | Ohio, Massachusetts | Solar eruption, from before 1330 to 1430. |
| | 1320–1330–1430 | New York | Europe | L-f atmos. increase, 1310–1440. |
| | 1325–1335–1345 | Holland | Europe, N. & S. America | |
| | 1340–1348 | England | (Numerous) | |
| Apr. 25 | 1427–1500 | D.C. | Ohio, Massachusetts | Solar eruption, 1428–1445. |
| Apr. 25 | 1653–1735 | D.C. | Ohio, Mass., D.C.* | Solar eruption, 1650–1724.<br>Ter. mag. pulse, 1650–1700.<br>L-f atmos. increase, 1658–1755. |
| Apr. 30 | 0940–1100 | Japan | Europe | |
| | 1000–1100 | France | Japan | |
| | 1000–1100 | Germany | Japan | |
| | 1000–1110 | England | Japan | |
| May 8 | 2020–2029–2037 | D.C. | Ohio, Massachusetts | Ter. mag. pulse, 2020–2035.<br>Earth-current pulse, 2020. |
| May 14 | 1755–1759 | New York | Europe, U.S.A. | |
| | 1750–1800–1817 | D.C. | Ohio | |
| May 15 | 0550–0730 | Japan | Philippines, Asia, Europe | Solar eruption, from before 0704 to 8030. |
| | 0550–0620 | Philippines | Japan | |
| | 0600–0620 | France | Japan | |
| May 25 | 1233–1240–1256 | D.C. | Ohio, Mass., D.C.* | Ter. mag. pulse, 1233–1250 |
| | 1232–1243–1257 | New York | (Numerous) | Earth-current pulse, 1233–1234–1236. |
| | 1238 | Florida | U.S.A. | L-f atmos. increase, 1228–1330 |
| | 1235–1300 | Holland | Canada, Japan, Java | |
| | 1232–1245 | France | U.S.A., S. America, Japan | |
| | 1237–1245 | England | Europe, S. America, Japan | |
| May 26 | 1130–1135 | New York | (Numerous) | Solar eruption, 1115–1203. |
| | 1130–1134 | D.C. | Ohio | L-f atmos. increase, 1128–1158. |
| | 1132–1139 | Holland | Hungary | |
| | 1131 | France | (Numerous) | |
| | 1130–1145 | England | (Numerous) | |
| May 27 | 0335–0430 | Holland | Japan, Java | |
| | 0355–0410 | California | Asia, Philippines, Java | |
| | 0350–0415 | Japan | Calif., Philip., Asia, Europe | |
| May 27 | 2345–2430 | Japan | N. & S. America | |
| | 2345–2430 | Argentina | Japan | |
| | 2345–2430 | California | Japan | |

* Disappearance or weakening of sky waves reflected vertically from ionosphere.

TABLE I—*Continued*

| Date | Time, G.M.T. | Reported observed in | Reported locations of transmitting stations | Reported solar and magnetic effects, etc. |
|---|---|---|---|---|
| 1936 | | | | |
| May 28 | 0345–0415 | California | Asia, Philippines, Java | |
| | 0340–0420 | Holland | Japan, Java | |
| | 0330–0420 | Japan | China, Philip., California | |
| May 28 | 0730–0745 | Philippines | Hawaii | Solar eruption, 0715–0800 |
| | 0728–0743 | California | Asia, Philippines, Java | Ter. mag. pulse, 0725–1738 |
| | 0730–0800 | Holland | Japan, Austria, Java | L-f atmos. increase, 0726–0800 |
| | 0728–0730 | France | (Numerous) | |
| | 0720–0745 | Japan | Europe, Philippines | |
| May 28 | 1403–1416–1430 | D.C. | Ohio, Massachusetts | L-f atmos. increase, 1400–1450. |
| | 1400–1409–1445 | New York | Europe, S. Amer., California | |
| | 1402–1430 | Holland | N. & S. America, Europe | |
| | 1405 | France | (Numerous) | |
| May 28 | 1759–1840–2000 | D.C. | Ohio, Massachusetts, Texas, Nebraska, Oklahoma | Ter. mag. pulse, 1800–1850. Earth-current pulse, 1758–1807. |
| | 1800–1808–1817 | New York | Europe, N. & S. America | L-f atmos. increase, 1758–1907. |
| | 1800–1823 | Oklahoma | (Numerous) | |
| | 1800–1823 | Texas | (Numerous) | |
| | 1800–1823 | Nebraska | (Numerous) | |
| | 1758–1815 | N. Dakota | (Numerous) | |
| | 1800–1815 | Illinois | (Numerous) | |
| | 1800–1815–1830 | British Columbia | (Numerous) | |
| | 1759–1820–1830 | Ohio | (Numerous) | |
| | 1800–1818–1828 | Arkansas | (Numerous) | |
| | 1800–1818–1828 | Kansas | (Numerous) | |
| | 1800–2000 | S. Carolina | (Numerous) | |
| May 28 | 1758–1815 | Missouri | (Numerous) | |
| | 1800–1816 | England | (Numerous) | |
| | 1800 | France | (Numerous) | |
| | 1755–1825 | Japan | California, Europe | |
| | 1800–1813–1840 | Holland | New York, Argentina | |
| May 29 | 1020–1030 | Holland | Java, Sweden, Austria | L-f atmos. increase, 1015–1115. |
| | 1020–1035 | Japan | Europe | |
| | 1025–1035 | England | (Numerous) | |
| | 1023 | France | (Numerous) | |
| | 1020–1027 | New York | (Numerous) | |
| May 30 | 1730–1800 | Florida | (Numerous) | Ter. mag. pulse, 1728–1750. |
| June 3 | 0045–0130 | Japan | Calif., Philip., Europe, N. & S. America, Asia | |
| | 0045–0130 | California | Japan | |
| | 0045–0130 | Buenos Aires | Japan | |
| | 0045–0130 | Philippines | Japan | |
| | 0100–0110 | S.S. *Gen. Pershing*, long. 154°52′W | (Numerous) | |
| June 3 | 1635–1655–1712 | D.C. | Ohio, Massachusetts | Solar eruption, 1629–1700. |
| | 1636–1640–1720 | New York | Europe, N. & S. America | Ter. mag. pulse, 1635–1700. |
| | 1637–1650 | Illinois | (Numerous) | L-f atmos. increase, 1635–1718. |
| | 1630 | Missouri | (Numerous) | |
| | 1630–1645–1700 | Pennsylvania | (Numerous) | |
| | 1640–1700 | Holland | U.S.A., Japan, Java | |
| | 1633–1650 | France | (Numerous) | |
| | 1635–1650 | England | (Numerous) | |
| June 3 | 1830–1835 | New York | Europe, S. America | Ter. mag. pulse, 1825 |
| | 1823–1841 | D.C. | Ohio, D.C.* | |
| June 4 | 0440–0500 | Japan | California, S. Amer., Asia | |
| | 0442–0455 | California | Asia, Philippines, Java | |
| | 0440–0505 | Holland | Java | |
| June 4 | 1154–1200–1210 | D.C. | Ohio, D.C.* | Ter. mag. pulse, 1153–1206 |
| | 1151–1206–1300 | New York | Europe, N. & S. America | L-f atmos. increase, 1152. |
| | 1155–1210 | France | (Numerous) | |
| | 1153–1209 | Holland | Japan, S. America, Europe | |
| | 1155–1205 | England | (Numerous) | |
| June 5 | 0235–0250 | California | Asia, Philippines, Java | |
| | 0236–0250 | Japan | California, S. Amer., Philip. | |

* Disappearance or weakening of sky waves reflected vertically from ionosphere.

TABLE I—*Continued*

| Date | Time, G.M.T. | Reported observed in | Reported locations of transmitting stations | Reported solar and magnetic effects, etc. |
|---|---|---|---|---|
| 1936 | | | | |
| June 9 | 0131–0150 | Japan | Asia | |
| | 0130–0155 | California | Asia, Philippines, Java | |
| June 9 | 1424–1451–1512 | D.C. | Ohio, Massachusetts | Solar eruption, 1424–1432. |
| | 1422–1441–1530 | New York | (Numerous) | L-f atmos. increase, 1425–1550. |
| | 1425 | France | (Numerous) | |
| | 1425–1440–1515 | England | Europe, N. & S. America | |
| | 1426–1440–1500 | Holland | U.S.A., Java, Europe | |
| June 9 | 1750–1845 | Holland | N. & S. America | Solar eruption, from before 1755 to after 1805.<br>Ter. mag. pulse, 1750–1805. |
| June 9 | 1859–1923–2023 | D.C. | Ohio, Mass., D.C.* | Ter. mag. pulse, 1900. |
| | 1900–1930 | Missouri | (Numerous) | L-f atmos. increase, 1900. |
| | 1900–2030 | Ohio | (Numerous) | |
| | 1906 | Illinois | (Numerous) | |
| | 1900–1915 | New York | Europe, N. & S. America | |
| | 1900–1920 | England | N. & S. America | |
| June 10 | 2056–2136–2159 | D.C. | Ohio, Mass., D.C.* | Ter. mag. pulse, 2055 |
| | 2105–2115–2150 | Oregon | (Numerous) | |
| | 2050 | Nebraska | (Numerous) | |
| | 2056–2120 | Illinois | (Numerous) | |
| | 2058–2103–2107 | Hawaii | California | |
| | 2058–2103–2107 | California | Hawaii | |
| | 2053–2200 | California | Asia, Philippines, Java | |
| | 2051–2146 | New York | (Numerous) | |
| | 2045–2129 | Guatemala | (Numerous) | |
| June 11 | 0625–0710 | California | Asia, Philippines, Java | L-f atmos. increase, 0620–0724. |
| | 0620–0700 | Holland | Japan, Java | |
| | 0625–0700 | Japan | California, S. America, Europe, Asia | |
| | 0625–0700 | Argentina | Japan | |
| | 0630–0640 | England | Japan, India | |
| | 0625 | France | (Numerous) | |
| June 11 | 1230–1250 | Holland | N. & S. America, Norway, Java | L-f atmos. increase, 1225–1330. |
| | 1228–1240 | England | Asia, N. & S. America | |
| | 1230–1243–1300 | D.C. | Ohio, Massachusetts | |
| | 1230 | France | (Numerous) | |
| June 16 | 1330–1400 | Holland | N. & S. America, Europe | Solar eruption, 1327–1348. |
| | 1330–1335–1400 | D.C. | Ohio, Massachusetts | |
| | 1330–1349 | New York | England, Spain | |
| | 1330–1337 | England | (Numerous) | |
| June 16 | 1713–1718–1733 | D.C. | Ohio, Massachusetts | L-f atmos. increase, 1715. |
| | 1715–1728–1745 | New York | S. America, California | |
| June 16 | 1803–1808–1820 | New York | S. America, California | Solar eruption, 1801–1809. |
| | 1800–1807 | D.C. | Ohio | Ter. mag. pulse, 1800.<br>L-f atmos. increase, 1802. |
| June 17 | 0723–0740 | Japan | S. America, Asia, Europe, Philippines | Solar eruption, 0727–0810<br>L-f atmos. increase, 0718 |
| | 0720 | France | (Numerous) | |
| June 17 | 0908–0925 | Japan | India, Holland, Norway | |
| | 0908–0925 | Holland | Japan | |
| | 0908–0925 | India | Japan | |
| June 17 | 1248–1254–1316 | D.C. | Ohio, Massachusetts | |
| | 1248–1254 | England | India, Italy | |
| | 1246–1256 | New York | (Numerous) | |
| June 19 | 0907–0910–1000 | Holland | Belgian Congo | Solar eruption, 0900–1100. |
| | 0910–0920 | England | India, Egypt, N. & S. America | L-f atmos. increase, 0905. |
| | 0910 | France | (Numerous) | |
| | 0910–0930 | Japan | Europe, India | |

* Disappearance or weakening of sky waves reflected vertically from ionosphere.

TABLE I—*Continued*

| Date | Time, G.M.T. | Reported observed in | Reported locations of transmitting stations | Reported solar and magnetic effects, etc. |
|---|---|---|---|---|
| 1936 | | | | |
| June 19 | 1633–1638 | D.C. | Ohio | Solar eruption, 1629–1637. |
| | 1610–1630 | France | (Numerous) | Ter. mag. pulse, 1630. |
| June 19 | 1730–1815 | Massachusetts | (Numerous) | Solar eruption, 1736–1800. |
| | 1733–1737 | D.C. | Ohio | |
| June 19 | 1936–1955–2115 | D.C. | Ohio | Solar eruption, 1938–1957 |
| | 1940–2000 | Idaho | (Numerous) | |
| | 1937–1945–2005 | New Jersey | England | |
| June 25 | 1030–1135 | Holland | Hungary, Norway | Solar eruption, 1051–1140. |
| | 1045 | France | (Numerous) | L-f atmos. increase, 1025. |
| | 1050–1100 | England | (Numerous) | |
| June 25 | 1115–1125 | England | (Numerous) | Solar eruption, 1110–1130. |
| July 1 | 0130–0150 | Japan | N. & S. America, Philippines, Java, China | |
| | 0133–0150 | California | Japan | |
| | 0135–0155 | China | Japan | |
| July 15 | 1327–1331 | New York | S. America, Europe | Solar eruption, from before 1330 to 1340. |
| | 1330 | France | (Numerous) | Ter. mag. pulse, 1325–1330. |
| | 1328–1342 | England | (Numerous) | L-f atmos. increase, 1328–1415. |
| | 1322–1332 | D.C. | Ohio | |
| July 30 | 1337–1347 | New York | (Numerous) | L-f atmos. increase, 1332–1432. |
| | 1340 | France | (Numerous) | |
| | 1342–1346–1400 | D.C. | Ohio | |
| July 31 | 0015–0035 | Japan | Europe, N. & S. America, Asia | Solar eruption, 0011–0030. |
| | 0016–0025 | England | (Numerous) | |
| | 0015–0020–0030 | California | (Numerous) | |
| Aug. 4 | 1727–1733–1746 | D.C. | Ohio, Massachusetts | Solar eruption, 1719–1723 Ter. mag. pulse, 1725. |
| Aug. 5 | 1609–1615–1630 | New York | West Indies, S. America, Europe | Solar eruption, 1603–1630. Ter. mag. pulse, 1605. |
| | 1606–1617–1621 | D.C. | Ohio, D.C.* | |
| Aug. 8 | 1725–1729–2000 | D.C. | Ohio, D.C.* | Solar eruption, 1716–1834 |
| | 1726–1730–1830 | New York | S. America | |
| Aug. 23 | 1130–1210 | England | (Numerous) | T r. mag. pulse, 1149. |
| Aug. 25 | 1829–1851–1930 | D.C. | Massachusetts | Solar eruption, from before 1858 to 1922. |
| | 1830–1850–1955 | New York | Europe, M. & S. America | Ter. Mag. pulse., 1825–1930. |
| | 1917–1945 | New Jersey | Bermuda | Earth-current pulse, 1825–1910. |
| | 1830–1905 | Ontario, Canada | (Numerous) | L-f atmos. increase, 1831. |
| | 1835–1850–1920 | France | N. & S. America | |
| | 1828–1854–1925 | California | (Numerous) | |
| | 1835–1908 | Japan | N. & S. America | |
| | 1840–1855 | England | U.S.A. | |
| | 1839–1855–1920 | Holland | N. & S. America | |
| | 1800–2000 | S. America | N. & S. America | |
| | 1800–2000 | British Columbia, Canada | Canada | |
| Aug. 26 | 0000–0020 | Japan | Europe, Asia, California | Solar eruption, 2357–0001. |
| Aug. 28 | 0930–1020 | Italy | (Numerous) | Solar eruption, 0920–1030. |
| | 0930 | France | (Numerous) | Ter. mag. pulse, 0920. |
| | 0930–0955–1020 | Holland | Japan, Java | L-f atmos. increase, 0923–1023. |
| | 0930–0955–1015 | England | (Numerous) | |
| | 0929–0945 | Japan | Europe | |
| Sept. 4 | 0147–0202–0230 | California | Asia, Philippines, Java | Solar eruption, 0140–0256 |
| | 0145–0215 | Java | (Numerous) | |
| | 0145–0200 | Philippines | (Numerous) | |
| | 0150–0200 | Argentina | Japan | |
| | 0146–0208 | Siam | (Numerous) | |
| | 0145–0210 | England | Japan, Australia | |
| | 0145–0215 | Japan | Asia, Java, Europe, N. & S. America | |

* Disappearance or weakening of sky waves reflected vertically from ionosphere.

TABLE I—*Continued*

| Date | Time, G.M.T. | Reported observed in | Reported locations of transmitting stations | Reported solar and magnetic effects, etc. |
|---|---|---|---|---|
| 1936 | | | | |
| Sept. 4 | 1238–1244–1252 | D.C. | Ohio, Mass., D.C.* | |
| | 1238–1250 | England | (Numerous) | |
| Sept. 4 | 1713–1732–1740 | D.C. | Ohio, Massachusetts | Ter. mag. pulse., 1714–1721. |
| | 1715–1720–1750 | New York | N. & S. America | Earth-current pulse, 1714. |
| | 1714–1723–1740 | California | U.S.A. | |
| Sept. 5 | 0902–0912–0932 | Holland | Japan, Java | Ter. mag. pulse, 0900. |
| | 0902–0915–0930 | England | (Numerous) | L-f atmos. increase, 0859. |
| | 0905 | France | (Numerous) | |
| | 0902–0930 | Japan | Europe | |
| Oct. 9 | 1424–1440–1517 | D.C. | Ohio, Massachusetts | Solar eruption, from before 1454 to after 1503. |
| | 1422–1542 | New York | (Numerous) | |
| | 1435 | France | (Numerous) | L-f atmos. increase, 1417–1554. |
| | 1430–1450 | England | (Numerous) | |
| Oct. 13 | 0342–0355 | Japan | Asia, Europe | Solar eruption, 0250–0430. |
| Oct. 16 | 1733–1752–1820 | D.C. | Ohio, Mass., D.C.* | Ter. mag. pulse, 1730. |
| | 1735–1750–1815 | New York | Europe, N. & S. America | |
| | 1740–1750 | California | (Numerous) | |
| | 1736–1754–1834 | Panama, C.Z. | N. America | |
| | 1736–1754–1834 | Florida | N. America | |
| | 1720–1820 | Japan | Europe | |
| Oct. 21 | 1535–1545–1600 | D.C. | U.S.A. Panama, Spain | Solar eruption, 1600 |
| | 1538–1550–1615 | New York | England, N. & S. America | Ter. mag. pulse, 1535–1550. |
| | 1536–1550–1555 | California | D.C., Panama, West Indies | Earth-current pulse, 1535. |
| | 1536–1550–1555 | Panama, C.Z. | D.C., California, West Indies | L-f atmos. increase, 1535–1645. |
| | 1538–1550 | England | (Numerous) | |
| Nov. 4 | 1701–1715–1720 | D.C. | Ohio | Solar eruption, beginning 1657. |
| Nov. 6 | 1610–1638–1700 | D.C. | Ohio, Mass., D.C.* | Solar eruption, from before 1624 to 1650. |
| | 1611–1630–1655 | New York | N. & S. America, Europe | |
| | 1609–1702 | Peru | Peru* | Ter. mag. pulse, 1610–1645. |
| | 1614–1630–1645 | California | U.S.A., Philippines, China, Japan | Earth-current pulse, 1606–1616–1636.– L-f atmos. increase, 1612–1658. |
| | 1610–1625–1640 | Massachusetts | (Numerous) | |
| | 1610–1625–1640 | Pennsylvania | (Numerous) | |
| | 1615–1650 | Illinois | (Numerous) | |
| | 1615 | Japan | N. & S. America | |
| | 1612–1626–1630 | Germany | N. & S. America | |
| | 1615–1625 | England | (Numerous) | |
| | 1613–1620 | Holland | (Numerous) | |
| | 1612–1645 | France | N. & S. America | |
| Nov. 7 | 0344–0410 | Japan | Asia, N. & S. America | |
| | 0345–0415 | Philippines | (Numerous) | |
| | 0347–0358 | California | (Japan) | |
| Nov. 7 | 1450–1523–1624 | D.C. | Ohio, Mass., D.C.* | Solar eruption, from before 1537 to 1600. |
| | 1452–1459–1620 | New York | N. & S. America, Europe | |
| | 1450–1505 | England | (Numerous) | L-f atmos. increase, 1451–1550. |
| | 1450–1530–1620 | Holland | S. America, Japan | |
| | 1450–1530 | France | S. America | |
| Nov. 8 | 1819–1827–1834 | D.C. | Ohio, Mass., D.C.* | Solar eruption, 1819–1827. |
| | 1812–1834 | California | Japan | Ter. mag. pulse, 1815–1825. |
| Nov. 16 | 1500–1545 | New York | N. & S. America, Europe | Solar eruption, from before 1530 to after 1700. |
| | 1457–1530 | D.C. | Ohio, Mass., D.C.* | L-f atmos. increase, 1450–1605. |
| Nov. 24 | 1710–1749–1820 | D.C. | Ohio, Mass., D.C.*, Panama, Porto Rico, California | |
| | 1720–1735–1800 | Holland | N. & S. America | |
| | 1712–1744–1810 | New York | N. & S. America, Europe | |
| Nov. 24 | 1915–1930 | Argentina | Holland | Solar eruption, 1908 to after 1944. |
| | 1913–1945–2010 | D.C. | Ohio, Mass., Calif., D.C.,* Panama, West Indies | Ter. mag. pulse, 1914–1940. |
| | 1915–1948 | W. Indies | (Numerous) | |
| | 1915–1940 | England | (Numerous) | |
| | 1914–1945–2015 | California | N.Y., Wash., Philippines | |

* Disappearance or weakening of sky waves reflected vertically from ionosphere.

TABLE I—*Continued*

| Date | Time, G.M.T. | Reported observed in | Reported locations of transmitting stations | Reported solar and magnetic effects, etc. |
|---|---|---|---|---|
| 1936 Nov. 24 | 1914–1935–2010 | New York | N. & S. America, Europe | |
| | 1845–1945 | Br. Col., Canada | Quebec | |
| | 1920–1940–2000 | Holland | S. America | |
| | 1915–2000 | France | S. America | |
| Nov. 26 | 0900–0930 | England | (Numerous) | L-f atmos. increase, 0857–1000. |
| | 0900–0920–0940 | Holland | (Numerous) | |
| | 0901–0925 | France | (Numerous) | |
| Nov. 26 | 1749–1835–1859 | D.C. | Ohio, Mass., D.C.,* Panama, W. Indies, Calif. | Solar eruption, 1749–1828. Ter. mag. pulse, 1750. |
| | 1750–1825–1840 | Br. Col., Canada | Canada | |
| | 1755–1820 | England | (Numerous) | |
| | 1753–1810–1900 | New York | N. & S. America, Europe | |
| | 1755–1815 | France | N. & S. America | |
| Nov. 27 | 1651–1659–1713 | D.C. | Ohio, D.C.* | Solar eruption, 1650–1658. |
| | 1650–1724 | New York | (Numerous) | Ter. mag. pulse, 1650. |
| | 1651–1654 | Peru | Peru* | Earth-current pulse, 1650. |
| | 1656–1715 | France | S. America | L-f atmos. increase, 1658. |
| Nov. 28 | 1500–1520 | D.C. | Ohio | L-f atmos. increase, 1507–1537. |
| | 1510–1545 | France | S. America | |
| Nov. 29 | 1547–1602–1640 | D.C. | Ohio, D.C.* | Solar eruption, from before 1555 to after 1637. |
| | 1546–1631 | New York | (Numerous) | |
| Nov. 30 | 1235–1315 | England | (Numerous) | L-f atmos. increase, 1230–1400. |
| | 1240–1300 | France | S. America | |
| Dec. 3 | 12?5–1330 | Holland | N. & S. America, Europe | Solar eruption, from before 1146 to after 1245. |
| | 1205–1245 | France | S. America, Japan | L-f atmos. increase, 1200–1302. |
| | 1205–1242 | England | (Numerous) | |
| | 1200–1320 | New York | (Numerous) | |
| Dec. 9 | 1337–1517 | New York | (Numerous) | L-f atmos. increase, 1300. |
| | 1320–1700 | Holland | S. America | |
| | 1315–1330 | France | S. America | |
| | 1310–1355 | England | (Numerous) | |
| Dec. 21 | 1817–1822–1828 | D.C. | Ohio | Ter. mag. pulse, 1815. |
| | 1825–1829 | California | Oregon, Wash., California | |
| Dec. 22 | 1305–1315 | France | (Numerous) | |
| | 1303 | Holland | (Numerous) | |
| Dec. 24 | 2202–2220 | California | Western U.S.A., Japan, China, Philippines | Solar eruption, 2200–2218. |
| Dec. 24 | 2348–2400 | California | Western U.S.A., Japan, China, Philippines | Solar eruption, 2349–2358. Ter. mag. pulse, 2348. |
| Dec. 26 | 1932–1958–2019 | D.C. | Ohio, Massachusetts | |
| | 1944–1954–2015 | New York | (Numerous) | |
| | 1939–2016 | California | U.S.A., Japan, China, Philippines | |
| Dec. 28 | 1055–1100 | England | (Numerous) | L-f atmos. increase, 1103–1145 |
| | 1100 | Holland | (Numerous) | |
| | 1100–1110 | France | (Numerous) | |
| Dec. 29 | 0820–0835 | France | Africa, Asia | |
| | 0820 | Holland | Java | |
| | 0848–0910 | England | (Numerous) | |
| Dec. 30 | 0852–0908 | France | Africa, Asia | L-f atmos. increase, 0848–0920. |
| Dec. 30 | 1031–1045 | England | (Numerous) | Solar eruption, from before 0944 to to 1056. L-f atmos. increase, 1030. |
| Dec. 30 | 1100–1120 | England | (Numerous) | Solar eruption, from before 1053 to 1217. L-f atmos. increase, 1053. |

* Disappearance or weakening of sky waves reflected vertically from ionosphere.

On account of the necessity of compressing the data into a table of reasonable length, the times given are in most cases averages. The individual times of beginning of the radio fade-out or other effect agree, however, in almost all cases within two or three minutes. For the radio fade-outs, the times of ending differed greatly. The times given are averages. (See Section III regarding the differences at different frequencies.)

The data on the radio fade-outs are based on: (a) experiences of operators receiving radio signals, (b) graphical records from field in-

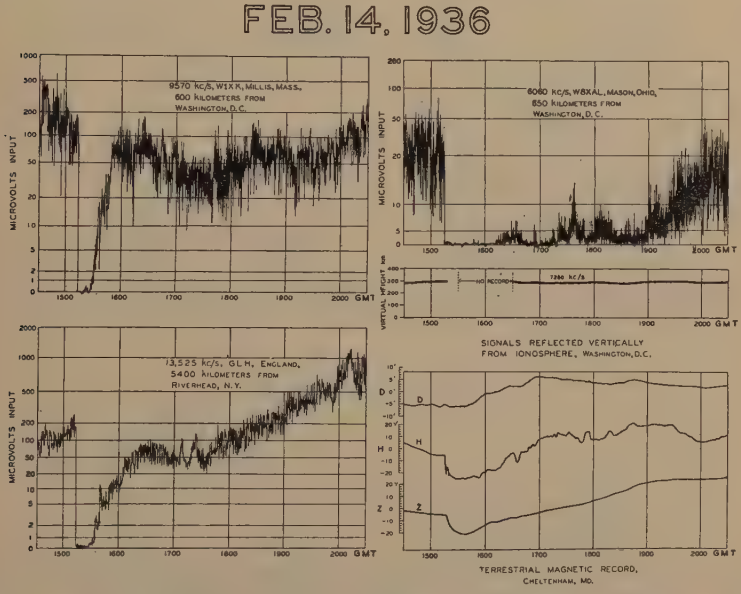
FEB. 14, 1936
9570 KC/S, WIXK, MILLIS, MASS., 600 KILOMETERS FROM WASHINGTON, D.C.
6060 KC/S, W8XAL, MASON, OHIO, 850 KILOMETERS FROM WASHINGTON, D.C.
MICROVOLTS INPUT
13,525 KC/S, GLH, ENGLAND, 5400 KILOMETERS FROM RIVERHEAD, N.Y.
SIGNALS REFLECTED VERTICALLY FROM IONOSPHERE, WASHINGTON, D.C.
TERRESTRIAL MAGNETIC RECORD, CHELTENHAM, MD.
GMT

Fig. 1—Sudden disturbance of the ionosphere on February 14, 1936, as revealed by radio fade-out and terrestrial magnetic perturbation.

tensity recorders, and (c) observations of echo signal pulses from the ionosphere. All the radio fade-outs which occurred at Washington, including practically all observable in the American hemisphere, after August, 1935, were recorded on automatic field intensity recorders maintained by the National Bureau of Standards at Meadows, Maryland, near Washington, D.C. These recorders made continuous records of the field intensities of certain high-frequency transmitting stations.

Typical fade-outs as recorded graphically are shown in Figs. 1 to 8. Note the sudden drop of intensity, and the subsequent gradual rise. As observed by a radio operator, a radio fade-out is simply the sudden disappearance of the signal from a distant high-frequency transmitting station. In most instances the intensity of the received signal was re-

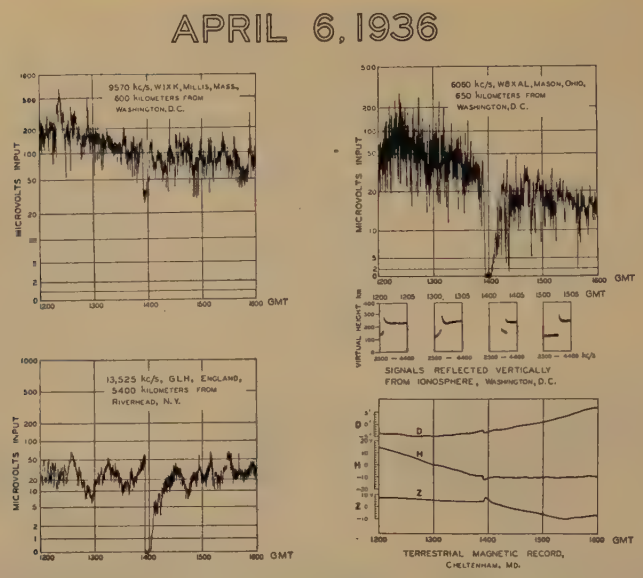
APRIL 6, 1936
9570 kc/s, WIXK, MILLIS, MASS., 600 KILOMETERS FROM WASHINGTON, D.C.
MICROVOLTS INPUT
GMT
6060 kc/s, WBXAL, MASON, OHIO, 650 KILOMETERS FROM WASHINGTON, D.C.
VIRTUAL HEIGHT km
SIGNALS REFLECTED VERTICALLY FROM IONOSPHERE, WASHINGTON, D.C.
13,525 kc/s, GLH, ENGLAND, 5400 KILOMETERS FROM RIVERHEAD, N.Y.
D
H
Z
TERRESTRIAL MAGNETIC RECORD, CHELTENHAM, MD.

Fig. 2—Sudden disturbance of the ionosphere on April 6, 1936, as revealed by radio fade-out and terrestrial magnetic perturbation.

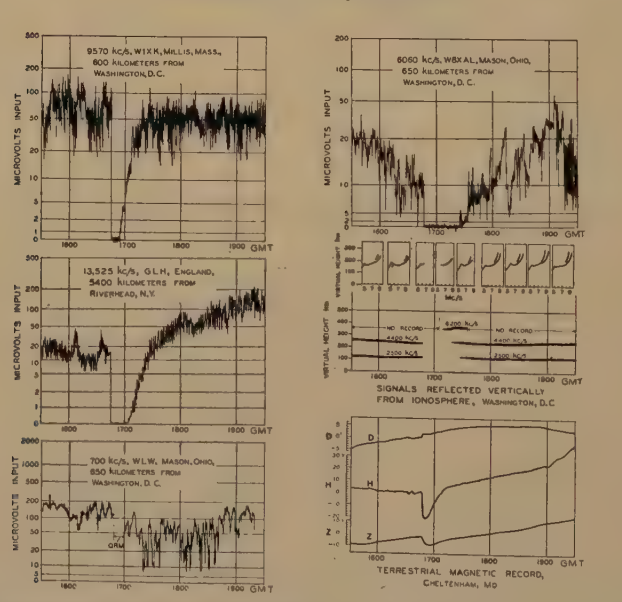
APRIL 8, 1936
9570 kc/s, WIXK, MILLIS, MASS., 600 KILOMETERS FROM WASHINGTON, D.C.
MICROVOLTS INPUT
GMT
6060 kc/s, WBXAL, MASON, OHIO, 650 KILOMETERS FROM WASHINGTON, D.C.
VIRTUAL HEIGHT km
SIGNALS REFLECTED VERTICALLY FROM IONOSPHERE, WASHINGTON, D.C
13,525 kc/s, GLH, ENGLAND, 5400 KILOMETERS FROM RIVERHEAD, N.Y.
700 kc/s, WLW, MASON, OHIO, 650 KILOMETERS FROM WASHINGTON, D.C.
D
H
Z
TERRESTRIAL MAGNETIC RECORD, CHELTENHAM, MD

Fig. 3—Sudden disturbance of the ionosphere on April 8, 1936, as revealed by radio fade-out and terrestrial magnetic perturbation.

duced to zero, in some it merely sank to an intensity so low as to be unreadable. Whenever echo signal pulses were being transmitted at the time of a fade-out in a given locality, the ionosphere echoes were weakened or disappeared. This is also illustrated in Figs. 1 to 8. The instances of these phenomena given in these eight figures are illustrative of many thousands of observations for which the author has data on file, which are in turn samples of the hundreds of thousands of observations on the 118 occasions listed.

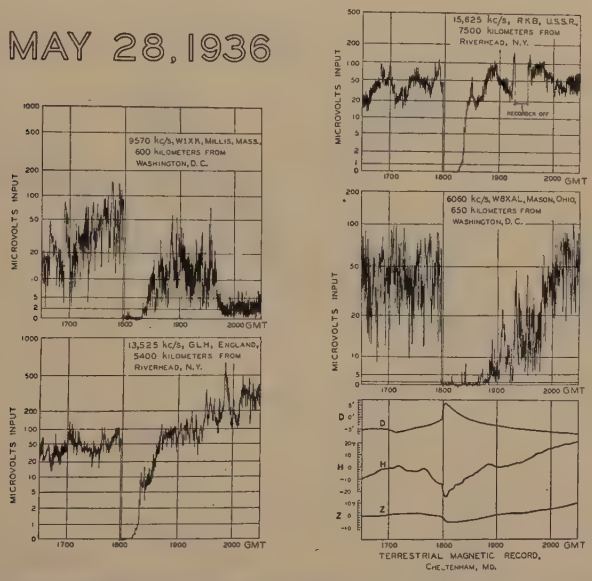


Fig. 4—Sudden disturbance of the ionosphere on May 28, 1936, as revealed by radio fade-out and terrestrial magnetic perturbation.

In the last column of Table I are numerous entries of increase of radio atmospherics at the same times as the other effects. These are all based on data published by R. Bureau of France. They refer to an increase in atmospherics as recorded on frequencies between twenty-seven and forty kilocycles per second, at observing points in France and Northern Africa.

The expression "ter. mag. pulse," in last column of Table I, means an abrupt change in one or more of the terrestrial magnetic elements, viz, horizontal intensity, vertical intensity, and declination, usually in all three. Some typical examples are shown in Figs. 1 to 8. Most of the data on terrestrial magnetic effects were obtained from the magnetograms of the Cheltenham Observatory of the U. S. Coast and Geodetic Survey, supplemented in some cases by information from other mag-

netic observatories, particularly the Mt. Wilson, California, Observatory of the Carnegie Institution of Washington. A comprehensive examination of the terrestrial magnetic and earth-current records from all observatories has not been made, so these data, like all the others, are decidedly incomplete.

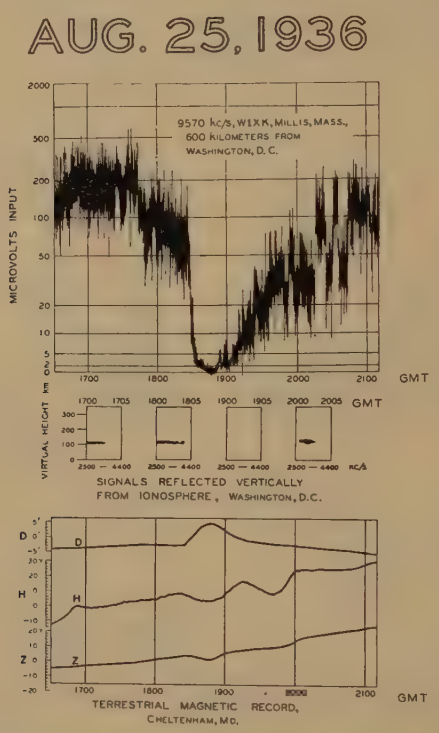


Fig. 5—Sudden disturbance of the ionosphere on August 25, 1936, as revealed by radio fade-out and terrestrial magnetic perturbation.

For the terrestrial magnetic and earth-current effects, the times of both beginning and ending as observed at different places are in almost all cases in agreement within about five minutes.

The information on the times of the solar eruptions coincident with the other effects was obtained from the "Bulletin for Character Figures of Solar Phenomena," published in Zurich, Switzerland, under the auspices of the International Astronomical Union, supplemented by data from R. S. Richardson of Mt. Wilson Observatory, from the Huancayo Observatory of the Carnegie Institution of Washington, and from R. R. McMath of Pontiac, Michigan.

## III. Characteristics of the Radio Transmission Effects

In this Section the known facts regarding the effects of the sudden ionosphere disturbances upon radio transmission are summarized. Explanation and theory are given in Section VI.

Radio transmission is subject to so many vagaries that it is not surprising that the existence of this particular type of vagary was not recognized until the present investigation. The various vagaries cause large fluctuations in the field intensity received at a distance. These

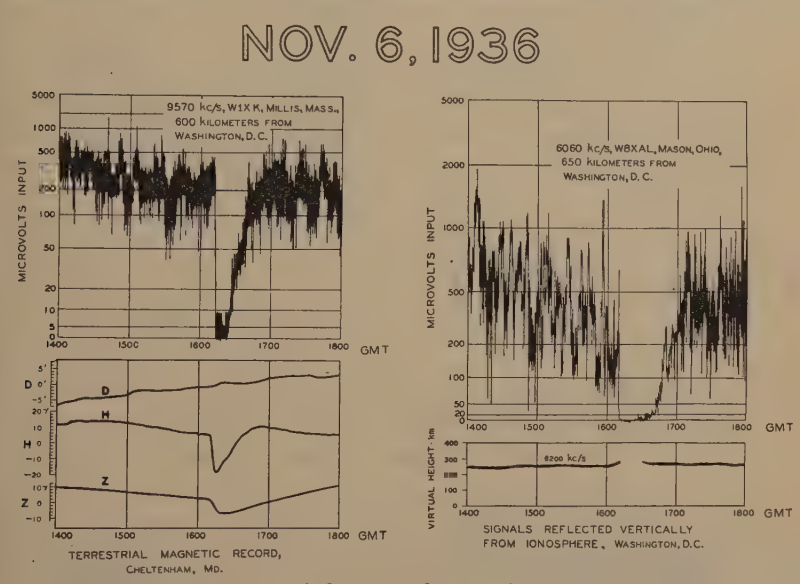


Fig. 6—Sudden disturbance of the ionosphere on November 6, 1936, as revealed by radio fade-out and terrestrial magnetic perturbation.

vagaries include such things as fading, abrupt change of general level of intensity due to change of transmission from one ionosphere layer to another, disappearance or appearance of signals because of change of critical frequency at sunrise or other time of day, change associated with magnetic storms, and "fade-outs." The term "fade-out" is here reserved for the relatively sudden radio effect of the type described in this paper. Each of these kinds of vagary may produce marked diminution of received intensity of radio waves, and in the past they have not been clearly differentiated. A major result of the present research is the demonstration that the fade-out has a number of characteristics which marks it off as a distinct phenomenon.

The data here presented have to do essentially with relatively high frequencies, i.e., above about 1500 kilocycles. The limited information

for frequencies below 1500 kilocycles is mentioned below under "Frequencies Affected." Ordinarily the intensities of the waves received from radio stations on frequencies below about 1500 kilocycles are not

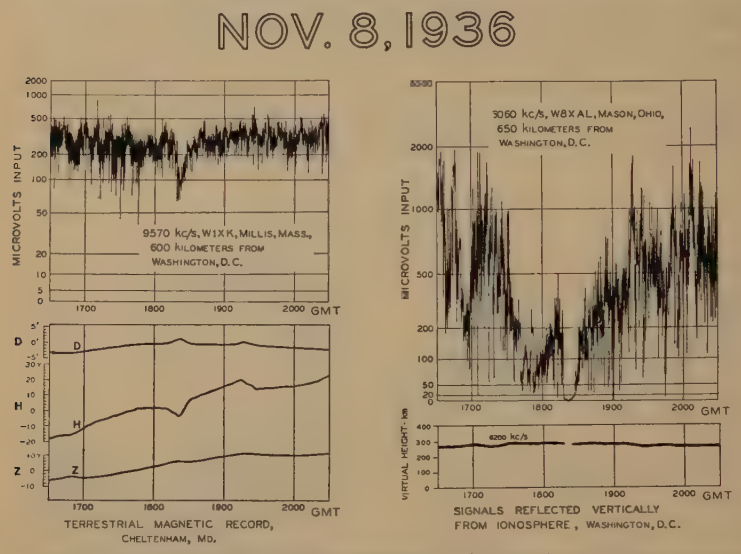


Fig. 7—Sudden disturbance of the ionosphere on November 8, 1936, as revealed by radio fade-out and terrestrial magnetic perturbation.

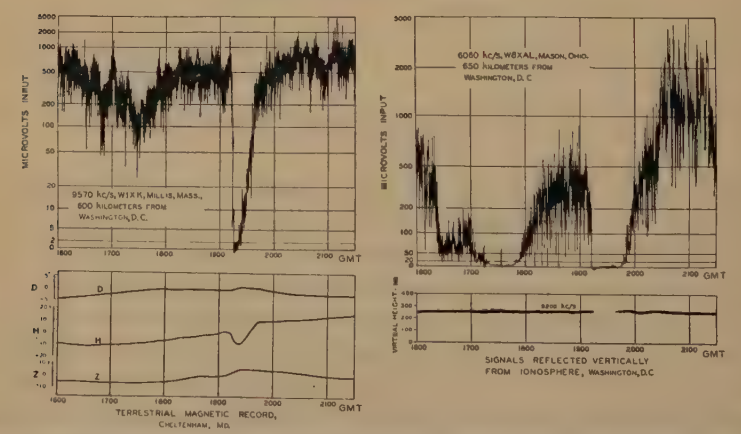
NOV. 24, 1936
MICROVOLTS INPUT
9570 kc/s, W1XK, MILLIS, MASS., 600 KILOMETERS FROM WASHINGTON, D.C.
GMT
D
H
Z
TERRESTRIAL MAGNETIC RECORD, CHELTENHAM, MD.
6060 kc/s, W8XAL, MASON, OHIO, 650 KILOMETERS FROM WASHINGTON, D.C
SIGNALS REFLECTED VERTICALLY FROM IONOSPHERE, WASHINGTON, D.C

Fig. 8—Sudden disturbance of the ionosphere on November 24, 1936, as revealed by radio fade-out and terrestrial magnetic perturbation.

perceptibly affected during a fade-out. The outstanding and definite effect of a sudden ionosphere disturbance on radio transmission is thus the fade-out observed on frequencies over about 1500 kilocycles.

The fade-outs are characterized by simultaneity of beginning at all places affected, suddenness, very great change of intensity, differing duration and intensity change on different frequencies and at different distances, maximum effect where the sun's radiation is perpendicular, and no effect for all-dark paths. Details of these characteristics follow.

*Geographic Simultaneity.* Leaving aside the question of simultaneity of the radio fade-outs with other phenomena (solar, etc.), a distinguishing characteristic of the radio fade-out is the simultaneity of its beginning at the various places where it is observed. As shown in Table I, the beginning of a fade-out is in nearly all cases simultaneous within a few minutes. Variations of more than ten minutes are reported in only seventeen of the 118 cases, and these are probably due to incompleteness or inaccuracies of observation. It is likely that every fade-out began simultaneously within three minutes everywhere, and in many cases the simultaneity was doubtless well within one minute.

The time of ending of a fade-out, on the other hand, is very different at different radio frequencies, at different distances, and in different parts of the earth; this is discussed further under "Frequencies Affected" and "Geographic Distribution" below.

*Suddenness.* The suddenness of the radio fade-outs has astonished many radio observers, operators, and amateurs. Radio signals being received at normal intensity suddenly begin to diminish and the intensity falls to zero, usually within a minute. The effect is on some occasions preceded by a short period of unusually violent fading, echoes, and noise (of a type different from atmospherics), but the effect usually comes without warning. There is sometimes also a period of violent fading, echoes, and noise (different from atmospherics) after as well as before a fade-out.

The suddenness of commencement of a fade-out is vividly illustrated by numerous reports in which the observer stated he thought that the power had gone off in the receiving station, or that a fuse had blown, or that the stations to which he was listening had stopped transmitting, or that his receiving apparatus had developed a sudden fault. Many an observer has dissected his receiving equipment on such occasions in the vain effort to determine why it suddenly went dead.

As may be seen from the examples in Figs. 1 to 8, the received radio wave intensity drops from full value to zero, in most cases, within a minute. In some of the more intense fade-outs, like that of February 14, 1936, shown in Fig. 1, the cutoff occurs within a few seconds. The duration of the effect is greater for the lower frequencies of the frequency range affected; this is discussed further below under "Frequencies Affected." Sometimes the drop to zero is not quite so sudden

for the higher frequencies as for the lower; this is illustrated in Fig. 6 (November 6, 1936) and Fig. 8 (November 24, 1936). In a few rare cases, such as the extra fade-out at 1715, November 24, 1936, shown in Fig. 8, the drop to zero was gradual, lasting ten minutes or so; such a case was not one of the more intense fade-outs, and was not accompanied by a terrestrial magnetic effect.

*Degree of Intensity Change.* The sudden change of intensity in a fade-out is very great. In most fade-outs there is a certain band of radio frequencies throughout which the intensity drops from normal value to zero. Sometimes the intensity does not drop all the way to zero for the higher frequencies; see for example Fig. 7 (November 8, 1936). There is evidence that there is often a frequency limit above which radio transmission is merely weakened rather than reduced to zero, and sometimes a still higher limit above which radio transmission intensity is not perceptibly reduced. Such is not always the case, however, for sometimes the sky wave intensity is reduced to zero throughout the entire high-frequency radio spectrum.

The sudden reduction of the intensity to zero when a fade-out occurs is an extraordinary experience. Not only does the radio station appear to stop transmitting, but in the more intense fade-outs even the background noise due to atmospherics ("static") disappears. The impression of the observer is that reception goes dead. This enhances the effect of the suddenness of the fade-out and further impels the observer to look for trouble in his receiving equipment.

*Frequencies Affected.* The data on radio fade-outs indicate that they occur on all the high frequencies used for long-distance radio work; i.e., from about 1500 to 30,000 kilocycles. Reports are available on radio reception at lower frequencies during many of the fade-outs, and in nearly all cases they indicate that reception was not affected. Some automatic records made by the National Bureau of Standards indicated that the sky wave, at broadcast frequencies, was weakened during a fade-out. As the ground wave plays a large part in daytime transmission at broadcast and lower frequencies, and the ground wave is unaffected by ionosphere phenomena, fade-out effects would not be prominent and would tend to escape notice. In a very few cases there have been reports of a changed character of fading on broadcast or lower frequencies, or of an increase of intensity on the lower frequencies. R. Bureau of France (see Bibliography) has found that recorders of atmospherics on frequencies between twenty-seven and forty kilocycles show an increase in numbers of atmospheric pulses recorded during many of the fade-outs; the times of such occurrences are given in Table I.

For the frequency range in which fade-out effects are conspicuous, i.e., from about 1500 to 30,000 kilocycles, the effects are greater on the lower frequencies. This is true in regard to the duration of the effects and the degree of intensity change. The variation of intensity change with frequency is described in the Section just above on "Degree of Intensity Change." The variation of the duration of a fade-out with frequency is illustrated in Figs. 1 to 8.

As shown in the figures, the beginning of a fade-out is simultaneous on all frequencies. This simultaneity is exact in most cases, and where not exact the times of beginning seldom differ more than two or three minutes and the effect occurs first on the lower frequencies. As also shown conspicuously in the figures, the duration or time of ending of a fade-out is very different on different frequencies. The time during which the received intensity is zero, and the time of recovery to normal intensity, are both greater the lower the frequency, other factors being the same. Interpretation of the variation of the effect with frequency in particular cases is complicated by the variation of the effect (discussed in next section below) with geographic location of the radio transmission paths affected, and also by the variation with distance of transmission. Since in long-distance transmission the waves travel a much longer path through the lower ionosphere the effects are greater for long distances than for short distances. Thus, a fade-out for a long-distance transmission path, on a given frequency, will have a greater reduction of intensity and a greater duration than for a short-distance transmission path. Expressed otherwise, the fade-out effects for a long-distance path correspond to those at a lower frequency for a short-distance path. Bearing this in mind, the variation of fade-out effects with frequency is consistent in the figures and in all known fade-outs. H. A. G. Hess reported that during the intense fade-out of November 6, 1936, which happened to occur during a time when long-distance transmission on 40,000 kilocycles was possible, there was no diminution in transatlantic reception on about that frequency. This fade-out was not as intense as some others. It is believed that during the most intense fade-outs all high-frequency sky waves fail.

It is found, and it is consistent with the foregoing conclusion, that fade-outs which last longer are usually observed up to higher frequencies than those of shorter duration; where the duration is short, the higher frequencies are less affected. This is illustrated by a comparison of Fig. 1 and Fig. 7.

*Geographic Distribution.* All of the fade-outs known to date, listed in Table I, have the characteristic discovered by the author in 1935 for the fade-outs then known, that they occur throughout the hemi-

sphere illuminated by the sun and not in the dark hemisphere. More precisely stated, whenever a radio fade-out occurs some part of the radio transmission path is in the daylight hemisphere. The continuous automatic recorders of the National Bureau of Standards, recording the field intensities of domestic stations, and the normal incidence ionosphere reflections have detected no fade-outs between sunset and sunrise. Since many other observers throughout the world have been watching for the effects, the lack of any reports whatever of disturbances on all-dark paths may be taken as proof of their nonoccurrence. For many of the times when radio fade-outs were reported, there have also been specific reports from the dark hemisphere that radio transmission was unaffected. Sometimes a fade-out is reported as observed at a place where it is dark, but in every such case the fade-out occurs only on radio transmission paths which are partly in the hemisphere illuminated by the sun. Thus, fade-outs have in a few cases been observed at midnight in certain places, without violating this principle. Conspicuous examples are: Argentina, 0400, April 2, 1936; California, 0728, May 28, 1936; England, 0016, July 31, 1936.

A study has been made to determine more specifically the variation of intensity of the effect with latitude, longitude, and direction. It is found that the effects are most pronounced in localities where the sun's radiation is perpendicular to the earth's surface. Thus, they are most intense in the equatorial regions and diminish with increasing latitude. Similarly, they are most intense at longitudes where it is noon and diminish in both directions toward longitudes where it is night. These relations are true in respect to the suddenness of beginning of the radio fade-out, the time it lasts, the upper limit of frequency affected, and the degree of reduction of field intensity. A fade-out which, at the place where the sun's radiation is perpendicular, may be very intense and prolonged, may, for the same frequency, be a mere brief reduction of field intensity near the boundary of the illuminated hemisphere.

Variations with direction have not been completely analyzed, but they appear to be consistent with the foregoing relations. For example, at receiving points in the United States, reception from stations in the southern hemisphere usually exhibit greater effects than reception from other directions (because of passing the equatorial regions). Similarly, a disturbance occurring in the morning usually exhibits greater effects in reception from the east than from the west, and vice versa for the afternoon (because of passing the region where it is noon).

Interpretation of particular cases is complicated by the variation of the effect with the radio frequency and distance.

## IV. Characteristics of the Terrestrial Magnetic and Earth-Current Effects

In this Section the known facts regarding the effects of the sudden ionosphere disturbances upon terrestrial magnetism and earth currents are summarized. The phenomena are explained in Section VI.

In many respects the terrestrial magnetic and earth-current effects have the same characteristics as the radio transmission effects. These similar characteristics include geographic simultaneity, suddenness, limitation of occurrence to the illuminated hemisphere, and the same variation of intensity of effect with latitude and longitude. They are similar also in being only one among the many types of vagaries of terrestrial magnetism and earth currents, such as diurnal and seasonal variations, irregular fluctuations, and magnetic storms. Also, as in radio, the effects due to the sudden ionosphere disturbances have in the past not been recognized as something different from the other classes of vagaries; this study has shown that they have characteristics which mark them off as a distinct and separate type of magnetic perturbation.

*Limitation to Illuminated Hemisphere.* The data on terrestrial magnetism in Table I are based principally on the magnetograms of the Cheltenham Observatory of the U. S. Coast and Geodetic Survey. These magnetograms were examined for the times of all the radio fade-outs. In a few cases data were available from the records of other observatories. In the more intense fade-outs, magnetic effects occurred simultaneously everywhere throughout the sun-illuminated hemisphere. In none of them did effects occur in the dark hemisphere.

The data on earth currents are highly fragmentary, as no systematic examination of earth-current records was made. The few entries of earth-current effects in Table I are based on occasional reports to the author by various collaborators. The phenomena of earth currents and terrestrial magnetism are so closely interrelated that very probably earth-current effects occurred whenever there were perturbations of terrestrial magnetism.

*Simultaneity with Radio Fade-outs.* Typical examples of the terrestrial magnetic effects are shown in Figs. 1 to 8, in which a few Cheltenham magnetograms are reproduced. The magnetic pulses, when they occur, are simultaneous with the radio effects, indicating that both are manifestations of an ionosphere change. As indicated in the table, the magnetic pulses occurred during many of the radio fade-outs but not all. The suddenness and the duration of the pulses may be judged from the figures.

*Geographic Distribution.* The geographic distribution of intensity of the terrestrial magnetic effects is, so far as the limited data indicate, the same as for the radio fade-outs. That is, they are most pronounced in the vicinity of that region of the earth's surface to which the sun's radiation is perpendicular, and diminish to zero at the boundary of the illuminated hemisphere. Thus the effects are greatest at low latitudes, and at longitudes where it is noon. They do not occur in the night hemisphere.

*Comparison with Magnetic Storms.* The geographic distribution of intensity of the effects is strikingly different from that of terrestrial magnetic and earth-current effects hitherto known. For example, a world-wide magnetic storm is characterized by a "sudden commencement," a pulse which is simultaneous over the whole earth. The magnetic storms and their sudden commencements thus differ markedly from the magnetic effects associated with sudden ionosphere disturbances in respect to distribution in longitude, since the latter occur only in the sun-illuminated hemisphere.

The two phenomena differ even more extraordinarily in respect to their distribution in latitude. Magnetic storms have minimum effects at the equator and maximum effects near the magnetic poles, just the opposite of the effects of sudden ionosphere disturbances. An interesting consequence of this is that the magnetic and earth-current pulses due to the sudden ionosphere disturbances are much more striking when observed in equatorial regions then in high latitudes. They may be of the same order of magnitude as the fluctuations due to magnetic storms in equatorial regions, relatively small in middle latitudes, and negligible in high latitudes.

Besides these differences in the geographic distribution of the effects magnetic storms and the sudden ionosphere disturbances differ in duration, the former lasting hours or days instead of the brief period of the latter.

A study has been made to determine whether there is any relation between times of occurrence of magnetic storms and the sudden ionosphere disturbances. It is concluded that there is none, and the occurrence of each is quite random with respect to the other. Sudden ionosphere disturbances usually occur during magnetically quiet times, but some have occurred during magnetic storms. In studying this subject, caution should be observed to consider the results observed at a number of different locations in order to be sure that an apparent effect of the sudden type really is one. Observations of the effect at a single location are often hard to distinguish from other types of vagaries.

One of the major results of this research is the discovery of a separate type of terrestrial magnetic disturbance, with remarkable charac-

teristics which clearly differentiate it from magnetic storms or any previously known types of magnetic perturbations. This is analogous to the discovery of the fade-out as a distinct type of radio vagary.

## V. Solar Phenomena Associated with Sudden Ionosphere Disturbances

In this Section the known facts regarding solar phenomena having a bearing on the sudden ionosphere effects are summarized. Explanation and discussion follow in Section VI.

*Exactness of Simultaneity.* The times of the solar eruptions known to have occurred at the times of the sudden ionosphere disturbances are given in the last column of Table I. They were simultaneous in the sense that the reported time of the solar eruption overlapped the time of the sudden ionosphere disturbance.

The times stated for the solar eruptions are in most cases uncertain by many minutes. This is because of difficulties in their observation. They are sometimes seen with difficulty, and the observing astronomer cannot be sure when a solar disturbance begins or ends. They are often obtained by photographs which may be taken at intervals of fifteen minutes or more, so that the time of a phenomenon indicated by a difference between two successive photographs may be uncertain.

Because of the uncertainties of their observational material, different astronomers adopt different criteria. The conditions of seeing (presence of haze, etc.) are also different at different observatories at any one time. It results that different solar observers differ considerably in the times they report for the beginning and end of solar eruptions. For example, the solar eruption of August 5 listed in the table was reported by Mt. Wilson Observatory as ending at 1613 and by Zurich Observatory as ending at 1648. As another example, the eruption listed for August 28 was reported by Zurich Observatory as ending at 1030, and was reported by Greenwich Observatory as still in progress at 1130. Likewise, an eruption was reported by Zurich Observatory as having begun on July 4, 1936, at 1655, and the same eruption was reported by Mt. Wilson Observatory as having begun at 1707. These cases were all major eruptions, more easily visible than most solar eruptions. It is evidently impossible to determine the times of solar changes within a small number of minutes.

The lack of precision of the solar data thus makes it impossible to say how close is the correspondence of times of the solar eruptions and the terrestrial effects. All of the cases listed in Table I may reasonably be described as simultaneous occurrences within the limits of our knowledge.

*Proportionate Number of Simultaneous Occurrences.* Of the 118 ionosphere disturbances listed in Table I, fifty-nine (exactly half) are shown to have been coincident in time with solar eruptions. There may have been a much larger proportion than shown. The sun is not under continuous observation and hence it is not known whether a visible solar eruption occurred or not at the time of any ionosphere disturbance for which no solar eruption is reported. Most solar observatories have in the past carried on observations for not more than an hour each day. An arrangement is in effect by which observatories in different parts of the world stagger their times of observation with a view to a continuous watch on the sun. Cloudy weather and other conditions, however, prevent the full attainment of this program.

On the other hand, however, when we examine the solar records (in the "Bulletin for Character Figures of Solar Phenomena"), we find that many solar eruptions occur when no ionosphere disturbances are known to have occurred. For example, from January to June, 1936, the above-mentioned Bulletin lists 302 solar eruptions, and only twenty-nine of these were simultaneous with known disturbances of the ionosphere. A larger proportion of coincidences is found if we consider only the more intense solar eruptions (those of arbitrary intensities two or three); there were in the same period sixty-nine of these listed, of which seventeen were simultaneous with known disturbances of the ionosphere. It is probable that many of the visible solar eruptions were not accompanied by detectable ionosphere disturbances, although the converse may not be true. Many of these eruptions may rise high enough in the solar atmosphere to permit the escape of visible light but not high enough to permit the escape of the ultraviolet radiation responsible for the sudden bursts of ionization in the earth's atmosphere. The use of automatic radio and magnetic recorders continuously has assured knowledge of the occurrence of practically all ionosphere disturbances in the western hemisphere.

*Character of Eruptions.* The eruptions here discussed are bright chromosphere eruptions. They are visible as sudden increases of brightness of large bright patches on the sun's surface, and when occurring at the limb of the sun are seen as eruptive prominences. An eruption usually, but not always, takes place near an active sunspot group. Most of the eruptions simultaneous with sudden disturbances of the ionosphere are much brighter than the average.

*Location of Eruptions on Sun.* It is of interest to know whether the eruptions causing sudden ionosphere disturbances occur wholly or predominantly at any particular location on the sun's surface. It might be thought, for instance, that the radiation would be effective only when projected radially from the sun to the earth; i.e., when the erup-

tive area is in the center of the sun's disk. The solar locality of all the visually observed eruptions simultaneous with sudden ionosphere disturbances is known, and has been examined in this connection. It is found to be random, which means that the eruptions send out their radiations in all directions from the sun's surface; the terrestrial effects occur regardless of where the eruption takes place, near the sun's limb, at or near the center of the disk, or anywhere between.

The locations of the eruptive areas on the sun have also been examined to find out whether particular areas give rise to repeated effects, and especially whether such effects are repeated after one or more rotations of the sun. On a number of occasions, successive eruptions from a given solar area, accompanying sudden ionosphere disturbances, have occurred in the course of a day or two. Little evidence however has been found of any repetition of eruptions from a particular area after one or more rotations of the sun.

*Recurrence Tendency.* A possible periodic tendency in the times of occurrence of the sudden ionosphere disturbance was suggested by the occurrence of the ones first known to the author, and listed first in Table I, at intervals of approximately fifty-five days. This is shown graphically in Fig. 9, in which all the occurrences are plotted. The intensity of each occurrence was weighted on an arbitrary basis, having regard to the duration and magnitude of the effect, the number of places from which reported, etc. The intensities thus weighted by two persons independently agreed very well and were plotted as ordinates on an arbitrary scale in Fig. 9. The abscissas are time, each horizontal line being an interval of fifty-five days. In Fig. 10 is plotted an average curve for all the 55-day periods. The existence of a 55-day recurrence tendency is indicated. This should not be taken as proved, as two years is not considered to be a sufficient time to establish such a tendency with certainty. It may be mentioned that the 55-day recurrence tendency remains very marked even if the first seven cycles, in which it is so pronounced, be disregarded. Further analysis has indicated that the recurrence tendency averages slightly less than fifty-five days, but is closer to fifty-five than fifty-four.

It is of interest that there is no indication of a recurrence tendency of the order of twenty-seven days. The sun rotates on its axis in a remarkable way, rotating faster at the equator than elsewhere. The rotation period is about twenty-four days at the sun's equator and about thirty-six days near its poles. The average rotation period of the portion of the sun in which the eruptions take place, and also incidentally the period for which terrestrial magnetic disturbances show a recurrence tendency (presumably dependent upon some unidentified type of solar eruptions), is between twenty-seven and twenty-eight

days. Thus the tendency to a recurrence period of fifty-five days, of the ionosphere disturbances, is twice the well-known solar period of approximately twenty-seven days. Again, caution should be observed in any conclusions from this, since data are available for only two years.

*Relation to Sunspots.* In a general way, solar eruptions tend to be more prevalent in years when sunspots are more numerous, and thus

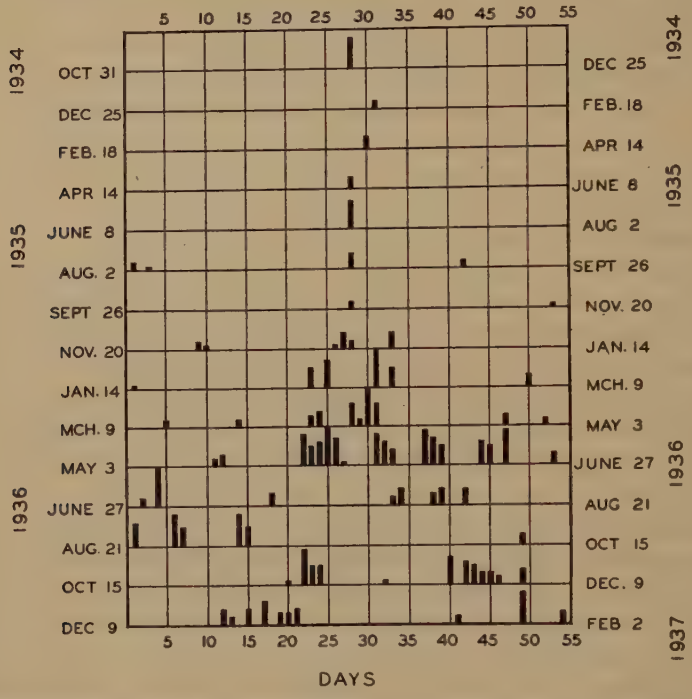


Fig. 9—Recurrence diagram of sudden ionosphere disturbances, arranged in 55-day periods; intensity of disturbance is approximately indicated by ordinate. (NOTE: By error, the first six days in each line are displaced one line too high. This error in drawing does not affect the accuracy of Fig. 10.)

their number may be expected to wax and wane in an 11-year cycle with the sunspots. There is no evidence, however, of any short-time correlation with sunspot numbers of the sudden ionosphere disturbances or the particular solar eruptions accompanying them. The number of sudden ionosphere disturbances certainly does not vary from day to day, or from month to month, in accordance with the sunspot numbers. Data are not available over a long enough time to permit a conclusion as to whether there is any correlation of yearly averages.

## VI. Discussion and Explanation

The foregoing facts clearly outline a phenomenon which is some type of sudden change somewhere in the ionosphere. Whenever the phenomenon occurs, it is most intense in that region of the earth where the sun's radiation is perpendicular and diminishes to zero at the outer edge of the illuminated hemisphere. Its onset usually occurs within a minute, and is simultaneous throughout the hemisphere affected. Its various effects begin simultaneously, and last from about ten minutes

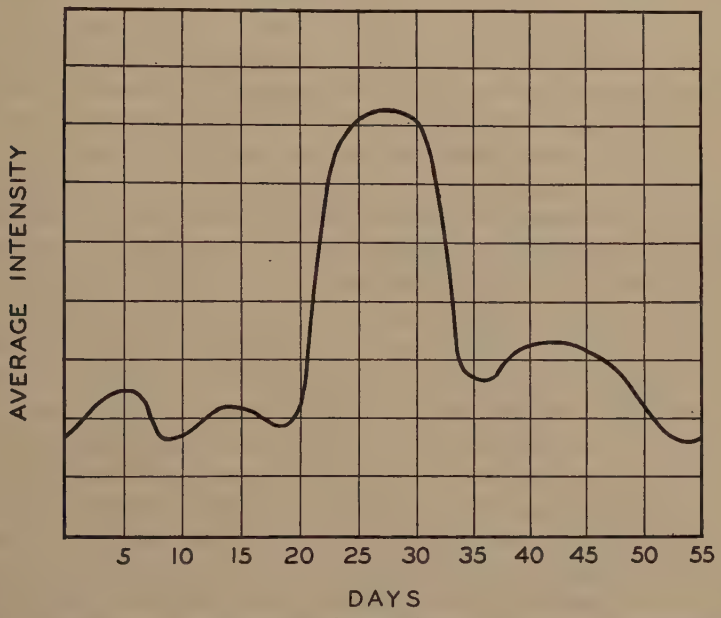


Fig. 10—The 55-day recurrence tendency, shown by smoothed average of disturbance intensity for all periods.

to several hours, the occurrences of greater intensity in general producing effects of longer duration. The effects include the sudden blotting out of high-frequency radio sky-wave transmission, sudden changes in low-frequency atmospherics, sudden changes in terrestrial magnetic intensities, and sudden changes in earth currents. The effects are markedly different from other types of changes in these quantities. They are more intense where it is noon than where it is other times of day, and are more intense in equatorial regions than in higher latitudes. The radio effects are very large, indicating that the ionosphere changes producing them are intense ones.

*Seat of the Disturbances Deduced from Radio Effects.* The various characteristics of the effects summarized in the preceding paragraph

and detailed earlier in the paper indicate them to be due to an ionosphere phenomenon; and the nature of that phenomenon is more particularly elucidated by a consideration of the radio effects.

Long-distance radio transmission takes place by means of so-called sky waves which are reflected back to earth from the ionosphere or the ionized upper portion of the atmosphere. The ionization is stratified in the daytime into a number of layers, of which three principal layers are well recognized: the E layer, $F_1$ layer, and $F_2$ layer. The E and $F_1$ layers are respectively about 120 and 220 kilometers above the earth's surface, and the $F_2$ layer is at a height varying from about 250 to 400 kilometers at different times. The maximum ionization density is progressively greater from the E to the $F_2$ layer. The presence of ionized particles of air makes the layers reflect radio waves which reach them. For a given maximum ionization density and angle of incidence, all radio waves up to a certain frequency are reflected and waves of higher frequency pass through to higher layers. For example, at a given time and distance, all radio frequencies up to 9000 kilocycles might be reflected by the E layer, those from 9000 to 30,000 kilocycles be reflected from the $F_2$ layer, and no frequencies above 30,000 kilocycles be reflected at all (i.e., no frequencies above this limit could be received over the distance considered).

An increase in the maximum ionization density of a layer raises the upper limit of frequency of radio waves which it can reflect. During a number of the sudden ionosphere disturbances measurements or recordings were in progress to determine this upper limit of frequency for the several layers, E, $F_1$, and $F_2$. In no case was an appreciable change observed during or just after the disturbance. (It is possible to speak of radio observations being in progress during a fade-out because there were usually some frequencies, distances, or locations for which radio transmission continued while for others the radio transmission was annihilated. See Section III.) It may be concluded that the sudden ionosphere disturbances do not change the maximum ionization density of the E, $F_1$, or $F_2$ layers, either not at all or very slightly.

On the other hand, ionosphere studies have amply proved that an increase in the ionization density of a region *through* which radio waves pass on the way to being reflected by a higher layer causes an increase in absorption of the radio waves' energy and results in a diminution of the received wave intensity. This is exactly what happens, and indeed to a striking degree, during one of the sudden disturbances. On some occasions an increase of virtual height of one of the ionosphere layers has been observed. (See Fig. 6.)

It may, therefore, be concluded that these sudden disturbances

involve a sudden great increase of ionization in some region through which radio waves pass on the way to being reflected by a higher region. Since the fade-out occurs in radio waves reflected by the E as well as the higher layers, the absorbing medium must be below the E layer.

The seat of the sudden large increase of ionization is thus below the E layer; i.e., lower than 120 kilometers above the earth's surface. The E layer is thus not the lowest part of the ionosphere. This is in harmony with some other facts which have been discovered recently. It is now known that waves of broadcast and lower frequencies are propagated in the daytime at certain seasons by reflection from a layer lower than the E layer. This was discovered by Smith and Kirby,[4] by observation of the changes in the characteristics of received waves near sunset and sunrise, showing a change from E layer at night to a lower layer in the daytime and back to the E layer at night.

This low layer may perhaps be called the D layer, but not enough is yet known about it to be sure that this designation is appropriate. There may be several layers acting, whose combined effect we observe, or one or another of them may predominate at different times. Or the effective layer may more or less merge into the E layer. With our present limited knowledge it is perhaps as well to think tentatively of a single low layer or region in which low-frequency transmission takes place, and in which the sudden ionosphere disturbances occur.

For low frequencies (below about 1500 kilocycles), a sudden ionosphere disturbance does not produce as complete a fade-out as at higher frequencies, because radio waves tend to be reflected by, instead of passing through, the layer in which the sudden increase of ionization occurs. Indeed, the sudden increase of ionization may even tend to increase rather than decrease the very low-frequency radio wave intensity; this is in harmony with the results of R. Bureau on low-frequency atmospherics (30 to 40 kilocycles).

For frequencies above about 1500 kilocycles, the ionization of the low layer is ordinarily not great enough to reflect the waves. They pass through and are reflected from the E or higher layers where the ionization density is greater. When the sudden increase of ionization in the low layer occurs, however, the ionization suddenly becomes great enough to produce large absorption of the radio wave energy and a fade-out occurs. There is less interchange of energy between the ions and the radio waves, the higher the frequency, and therefore for very high frequencies the fade-out effects are less pronounced; this is in accordance with experience, as described in Section III and illustrated in Figs.

[4] "Critical frequencies of low ionosphere layers," *Phys. Rev.*, vol. 51, p. 890; May 15, (1937).

2 to 8. It is also clear from this conception why the effects on a given frequency for normal-incidence transmission are the same as the effects on a much higher frequency for grazing incidence transmission: the waves at grazing incidence travel a much longer path through the abnormally ionized layer and thus experience an added amount of energy interchange with the ions, thus compensating for their higher frequency.

The source of the sudden ionization changes must be outside the earth, and therefore has to come through the E, $F_1$, and $F_2$ layers. It must have a character, therefore, distinctly different from the source of ionization of those layers. It produces its effect at a level where the air density is great enough to insure numerous collisions of moving ions and hence rapid absorption of the radio wave energy. The radiation producing this effect is therefore of a type which can penetrate the better known higher layers and produce ionization where the mean free path is shorter than at the higher levels. The effect must be produced by a very sudden burst of very penetrating radiation, which reaches and ionizes a level of the atmosphere where the air density is great enough to insure rapid recombination of the ions as well as rapid absorption of the energy of radio waves reaching such region. This explains the great reduction of the radio wave intensity and the short duration of the effect, as well as the suddenness of the drop of radio intensity.

The recombination proceeds so fast that the ionization and the ionizing energy are very nearly in equilibrium at all times. As the ionizing radiation from the sun dies out, in accordance with the disappearance of the solar eruption, the intense ionization in the lower ionosphere wanes, and the highest radio frequencies affected are soon freed of its effects. As the ionization diminishes, lower and lower frequencies recover from the effects. The duration of a fade-out at a given frequency is thus dependent not only on the intensity of the burst of ionizing energy but also on the duration of the solar eruption.

*Magnetic Effects.* The occurrence of the sudden ionization being thus inferred and explained from the radio effects, it is clear why simultaneous changes are sometimes observed in terrestrial magnetism and earth currents. Both of the latter phenomena are due in part to the motion or drift of ions in the earth's atmosphere, constituting in the aggregate vast currents whose associated magnetic field constitutes a portion of the earth's magnetism and whose fluctuations account for the variations in terrestrial magnetism and earth currents. When a sudden ionosphere disturbance of the type here considered takes place, the sudden increase in ionization permits a simultaneous sudden change in net

current flowing and thus perturbations in terrestrial magnetism and earth currents. It is to be noted that such perturbations do not depend entirely on the amount of the ionization, as do the radio effects, but involve also drift or motion of the ions. The radio effects are therefore not always accompanied by magnetic and earth-current perturbations. Whether the latter become observable or not depends on the complicated circumstances of the earth's magnetism at various places and times. When observed, they share the characteristics of the radio effects and the acting cause in the ionosphere; i.e., simultaneity throughout the portion of the earth affected, absence in the dark hemisphere, suddenness, and maximum intensity where the sun's radiation is perpendicular.

As previously stated, this type of perturbation of terrestrial magnetism and earth currents is strikingly different from the perturbations associated with "magnetic storms." Radio effects have shown that during magnetic storms the ionization density of the highest layer of the ionosphere ($F_2$ layer) is reduced and the ionization is diffused rather than sharply stratified. These effects thus prove that at least part of the phenomena of magnetic storms have their seat in the $F_2$ layer.[5]

It has here been shown, on the other hand, that the sudden ionosphere disturbances have their seat below the E layer, and the phenomena causing the terrestrial-magnetic and earth-current perturbations associated therewith must therefore also have their seat below the E layer.

Thus the two kinds of magnetic phenomena arise in entirely different portions of the ionosphere, in entirely different ways, and are probably due to two different kinds of ionizing agent. We thus have a new tool for analysis of the characteristics of terrestrial magnetism and for determination of their causes. There has hitherto been little known as to the locations of the vast ionosphere current systems which cause the fluctuations of terrestrial magnetism. The new possibility of localizing the levels in which different types of perturbations originate will aid in deciding between rival theories of terrestrial magnetism and should do much to bring to light the hitherto unknown mechanisms of terrestrial magnetic variations.

*Solar Source.* The sun is in an extremely turbulent state, and on it

[5] S. S. Kirby, T. R. Gilliland, E. B. Judson, and N. Smith, "The ionosphere, sunspots, and magnetic storms, *Phys. Rev.* vol. 48, p. 849, (1935).
S. S. Kirby, T. R. Gilliland, N. Smith, and S. E. Reymer, "The ionosphere, solar eclipse, and magnetic storm," *Phys. Rev.* vol. 50, p. 258, (1936).
S. S. Kirby, N. Smith, T. R. Gilliland, and S. E. Reymer, "The ionosphere and magnetic storms," *Phys. Rev.* vol. 51, (1937).

occur frequent eruptions from which are emitted radiations having a great range of wave lengths. There is no reason to doubt that some of the radiations from some of these eruptions are the sudden bursts which cause the sudden disturbances of the ionosphere of this planet. This is strongly indicated by the numerous observations of such eruptions and ionosphere disturbances coinciding in time.

The lack of occurrence of an ionosphere disturbance during every visible solar eruption does not at all vitiate the idea of a causal relation, because many different kinds of radiation are emitted in solar eruptions and visible radiation is not the kind which affects the ionosphere. The existence of visible solar effects during the solar cataclysms which cause the ionosphere disturbances is fortuitous. The simultaneous occurrence of an ionosphere disturbance and the flare of light which makes the solar eruption visible indicates that the radiation causing the ionosphere disturbance travels to earth with the velocity of light. As shown above, the radiation which causes the sudden large increase of ionization of a low region of the ionosphere is of a very penetrating type; it is therefore electromagnetic radiation of frequency far above visible light.

This doubtless gives the explanation why not all visible solar eruptions cause ionosphere disturbances. Evidently some eruptions emit the particular types of radiation which penetrates to the region below the E layer and ionizes it, and some do not.

The ionosphere disturbances and their associated effects are the only known means of detecting the causative solar radiation, because this radiation cannot penetrate the relatively dense lower atmosphere and reach the earth's surface and thus can not be directly detected by any instrumental means. We have thus come into possession of a means of studying a new class of invisible solar radiation, not hitherto accessible to detection or measurement.

The results of this research prove conclusively that ultraviolet radiation from the sun can cause terrestrial magnetic fluctuations. E. O. Hulburt has advocated similar ideas in numerous papers during the past ten years.

Ionosphere phenomena should be of very great value in increasing our knowledge of the sun. The ionization phenomena of the $F_2$ layer are decidedly different from those of the E layer, and there may thus be differences in the causative radiations for the two layers. Certain effects in the $F_2$ layer, associated with magnetic storms, may be due to a different type of radiation. As we have seen, the radiation causing the sudden ionosphere disturbances is of still different character. All of these classes of radiation can be studied only by their ionosphere ef-

fects, as they do not penetrate down to the earth's surface. Ionosphere phenomena, as detected by radio, terrestrial-magnetic, and earth-current effects thus become the unique means by which we can study various classes of radiation from the sun.

The physical nature of the sun is extremely interesting, and presents many mysteries. One of the chief mysteries is the eruptions. Little is known about the precise relation of the eruptions to sunspots or about the cause of either. The sun is a rotating sphere of very hot gas, and a sunspot is a vortex resulting from a great cataclysmic change in a portion of the sun. A sunspot lasts from a few days to a few months. The sudden eruptions, usually lasting only a few minutes, commonly occur during the early stages of a neighboring sunspot group; they may be connected with the process which gives birth to sunspots. This process is thought by astronomers to be the sudden formation of vast quantities of helium from hydrogen by the combination of four hydrogen atoms to form one of helium, with great energy liberation. Determination of the wave lengths of the radiation accompanying sudden pulses which occur during this process should aid in further identifying its nature and the obscure cause within the sun. Such determination is among the possibilities of future study of the sudden ionosphere disturbances. The duration of some of the phenomena during eruptions may also be learned through this study.

Another aspect of the sudden ionosphere disturbances which is worthy of study in connection with solar phenomena is the time grouping of the disturbances. As shown in Fig. 9, the major disturbances showed a very marked 55-day recurrence tendency from November, 1934, to May, 1936; then in May and June, 1936, there was an extraordinary outburst of them, after which there were relatively few of them for several months.

A study of the solar circumstances of the eruptions accompanying such disturbances, and the possible future determination of the wave lengths of the solar radiation associated with them, may eventually elucidate the nature of the eruptive processes within the sun and the causes of sunspots.

## VII. Acknowledgment

The work here reported has been in large measure a world-wide co-operative study. Many individuals and organizations have sent me reports of their observations of various aspects of the sudden disturbances of the ionosphere as they occurred.

The most consistent source of data has been the continuous records of field intensity of high-frequency stations, and the records of iono-

sphere phenomena, made by my colleagues in the National Bureau of Standards, Messrs. S. S. Kirby, N. Smith, T. R. Gilliland, and S. E. Reymer.

Dr. R. Jouaust of the Laboratoire Central de Radio-electricite, France, and the author have regularly interchanged data during this study. Dr. Jouaust has compiled and distributed comprehensive bulletins of data on the radio fade-outs, principally as observed in Europe. These were forwarded from the French National Committee to the other national committees of the International Scientific Radio Union, and this service is being continued.

The Carnegie Institution of Washington has collaborated in the supplying of solar and terrestrial magnetic data. In particular, Dr. R. S. Richardson, of the Mt. Wilson Observatory, California, has cooperated with the author through the supplying of information monthly on solar eruptions.

The Coast and Geodetic Survey has assisted by supplying copies of its daily magnetograms made at its terrestrial magnetic observatory at Cheltenham, Maryland.

Regular reports on radio fade-outs as observed during the handling of radio communication traffic have been furnished by:

H. H. Beverage, Chief Research Engineer, R.C.A. Communications, Inc.

H. Pratt, Chief Engineer, Mackay Radio and Telegraph Company.

L. Espenschied, Bell Telephone Laboratories, Inc.

N. Koomans, Chief, Staatsberdreijf der P.T.T., Holland.

T. Nakagami, Chief Engineer, Kokusai-Denwa Kaisha Ltd., Japan.

Reports have been furnished on particular radio fade-outs and related phenomena by many others, including:

Chief Signal Officer, War Dept., U.S.A.

Naval Communication Service, U.S.A.

Aeronautical Radio Inc., U.S.A.

British Broadcasting Corporation, England.

W. Calloway, Office of Posts and Telegraphs, Kuala Lumpur, Malaya.

J. H. McMullin, Commissioner of Police, British Col., Canada.

C. P. Edwards, Department of Transport, Ottawa, Canada.

Reports on numerous radio fade-outs have been supplied by many radio amateurs, forwarded through the American Radio Relay League. Of these, the reports of Mr. F. D. Jenkins, of Atlanta, Ga., have been particularly helpful.

## Bibliography

J. H. Dellinger, "A new cosmic phenomenon," *Science*, vol. 82, 351; October 11, (1935).

J. H. Dellinger, "A new radio transmission phenomenon," *Phys. Rev.*, vol. 48, p. 705; October 15, (1935).

J. H. Dellinger, "Confirmation of cosmic phenomenon," *Science*, vol. 82, p. 548; December 6, (1935).

J. H. Dellinger, "New radio transmission phenomenon," *QST*, vol. 19, p. 21 of December, (1935).

J. H. Dellinger, "A new solar radio disturbance," *Electronics*, vol. 9, p. 25; January, (1936).

R. S. Richardson, "The hydrogen outburst on the sun and radio fading," *Science*, vol. 83, 6 Supp., January 10, (1936).

J. H. Dellinger, "New cosmic phenomenon," *QST*, vol. 20, p. 8 of January, (1936).

R. S. Richardson, "Sunspot activity and radio transmission fade-outs," *Trans. Amer. Geophys. Union*, Part I, p. 172, (1936).

J. H. Dellinger, "High-frequency radio fade-outs continue," *QST*, vol. 20, p. 37 of June, (1936).

R. S. Richardson, "The bright hydrogen eruption and radio fade-out of April 8, 1936," *Ter. Mag. and Atmos. Elec.*, vol. 41, p. 197; June, (1936).

O. W. Torreson, W. E. Scott, H. E. Stanton, "A conspicuous solar eruption on April 8, 1936, and simultaneous disturbances on magnetic, ionospheric, and earth-current records at Huancayo magnetic observatory," *Ter. Mag. and Atmos. Elec.*, vol. 41, p. 199; June, (1936).

G. Leithäuser, "On abnormal upper atmospheric ionization on February 14, 1936," *Funktech. Monats.*, vol. 2, p. 241; July, (1936).

D. Arakawa, "Abnormal attenuation in short radio wave propagation," *Report of Radio Research in Japan*, vol. 6, p. 31, (1936).

Ohno, Nakagami, and Miya, "On the fall of short-wave intensity of short duration," (In Japanese), *J.I.E.E.* (Japan), p. 938; August, (1936).

A. M. Braaten, "Fade-out observations at Riverhead, N. Y." *T. and R. Bull.*, vol. 12, p. 111; September, (1936).

M. Waldmeier, "The great solar eruption of August 28, 1936," *Naturwiss*, vol. 24, p. 638; October 2, (1936).

R. S. Richardson, "The bright eruption and radio fade-out of August 25, 1936," *Pub. Astr. Soc. Pacific*, vol. 48, p. 278; October, (1936).

"The ionosphere; the Dellinger wipe-out," *T. and R. Bull.*, vol. 12, p. 214; November, (1936).

R. Bureau and J. Maire, "Ionospheric anomalies of sudden onset," *Compt. Rend.*, vol. 203, p. 1275; December 7, (1936).

H. W. Newton, "Radio fadings and bright solar eruptions," *Nature*, vol. 138, p. 1017; December 12, (1936).

J. H. Dellinger, "Direct effects of particular solar eruptions on terrestrial phenomena, *Phys. Rev.*, vol. 50, p. 1189; December 15, (1936).

R. Jouaust, R. Bureau, and L. Eble, "The probable causes of sudden fade-outs of short radio waves and their relation to magnetic phenomena," *Compt. Rend.* vol. 203, p. 1534; December 28, (1936).

J. A. Fleming, "Notes on radio fade-outs of August 25, 1936," *Ter. Mag. and Atmos. Elec.*, vol. 41, p. 404; December, (1936).

O. W. Torreson, W. E. Scott, F. T. Davies, and H. E. Stanton, "A solar eruption on November 6, 1936, and disturbances in earth's magnetism, earth-currents, and the ionospheric regions," *Ter. Mag. and Atmos. Elec.*, vol. 41, p. 409; December, (1936).

D. Arakawa, "Abnormal attenuation in short radio wave propagation," (Second Report), *Report of Radio Research in Japan*, vol. 6, p. 169 (1936).

"Solar eruptions and radio fade-outs," *Nature*, vol. 139, p. 61; January 9, (1937).

R. Bureau, "Abnormalities of the ionosphere and bright solar eruptions," *Nature*, vol. 139, p. 110; January 16, (1937).

J. H. Dellinger, "Radio fade-outs through 1936," *QST*, vol. 21, p. 35 of February, (1937).

A. G. McNish, "Magnetic effects associated with bright solar eruptions and radio fade-outs," *Nature*, vol. 139, p. 244; February 6, (1937).

J. H. Dellinger, "Sudden ionospheric disturbances," *Ter. Mag. and Atmos. Elec.*, vol. 42, p. 49; March, (1937).

F. T. Davies, O. W. Torreson, W. E. Scott, and H. E. Stanton "A solar eruption of November 27, 1936, and simultaneous disturbances in earth's magnetism, earth-currents, and the ionospheric regions," *Ter. Mag. and Atmos. Elec.*, vol. 42, p. 93; March, (1937).

H. A. G. Hess, "Observations on the Dellinger-effect on Nov. 6, 1936," *Funktech. Monats.*, vol. 3, p. 74; March, (1937).

*Proceedings of the Institute of Radio Engineers*
*Volume 25, Number 10* *October, 1937*

# FIELD STRENGTH OBSERVATIONS OF TRANSATLANTIC SIGNALS, 40 TO 45 MEGACYCLES*

By

H. O. Peterson and D. R. Goddard

(R.C.A. Communications, Inc., Riverhead, L.I., N. Y.)

***Summary***—*The results of daily observations at Riverhead, L.I., N. Y., since the middle of January, 1937, are reported. Some of the schedules of London and Berlin television transmissions are reported as being heard and measurements of field strengths are summarized. The vertical angle of arrival was measured, and by means of a reversible directive antenna it was determined that the signal at times arrives from a direction other than that of the great-circle path through London and Riverhead.*

THIS paper will report briefly on the results of a series of observations started at Riverhead, L. I., N. Y., January 11, 1937, on the frequencies of the television transmitters at Alexandra Palace, London, and which later also included the frequencies of the television transmitters at Berlin.

London was understood to have a sound channel on 41.5 megacycles with a power rating of 3 kilowatts and a vision channel on 45 megacycles with a rating of 5 kilowatts. The Berlin transmissions consisted of a sound channel on 42.5 megacycles and a vision channel on 44.3 megacycles. The transmitting antennas were vertically polarized. The distances involved were 3400 miles for London and 3900 miles for Berlin.

Most of the observations took place between 1000 and 1100 E.S.T. Observations were, however, also made at other hours between 600 and 1700 E.S.T. The observations were at first made at the Frequency Measuring Laboratory of the Riverhead Station. They were later extended to another site where special antennas could be erected.

To facilitate the design of an antenna some measurements of the vertical angle of arrival were made. For these measurements, three horizontal dipoles were erected at 16.7 feet, 27.3 feet and 50 feet above ground. Fig. 1 shows how these antennas were arranged. By comparing the strengths of the signals picked up on each of these dipoles the vertical arrival angle was determined, according to the method described by Friis, Feldman, and Sharpless.[1] In order not to introduce errors due

* Decimal classification: R270. Original manuscript received by the Institute, May 19, 1937. Presented before joint U.R.S.I.-I.R.E. meeting, Washington, D. C., April 30, 1937.

[1] H. T. Friis, C. B. Feldman, and W. M. Sharpless, "The determination of the direction of arrival of short radio waves," Proc. I.R.E., vol. 22, pp. 47–78; January, (1934).

to transmission line losses and standing wave patterns the transmission lines from the dipoles were made of equal lengths. A receiver was mounted in the survey car shown, which could be parked near the antennas. The three transmission lines passed to the receiver through a plug and jack arrangement providing rapid change from one antenna to another.

A number of measurements made showed that the vertical arrival

Fig. 1—Three horizontal dipoles and survey car containing receiver used for vertical arrival angle measurements.

angle of the signals heard was close to 7.5 degrees. A horizontal rhombic antenna was then constructed so as to have its maximum lobe towards England at this angle. Its effective height was about eight meters.

As the observations made at the Frequency Measuring Laboratory indicated that possibly the signal was arriving along paths other than the shorter arc of the great circle from England to Riverhead it was decided to arrange the rhombic antenna in such a fashion that its direction of reception could be reversed. This was done by installing at each end of the antenna remotely controlled double-pole double-throw switches. From the blades of these switches transmission lines of equal

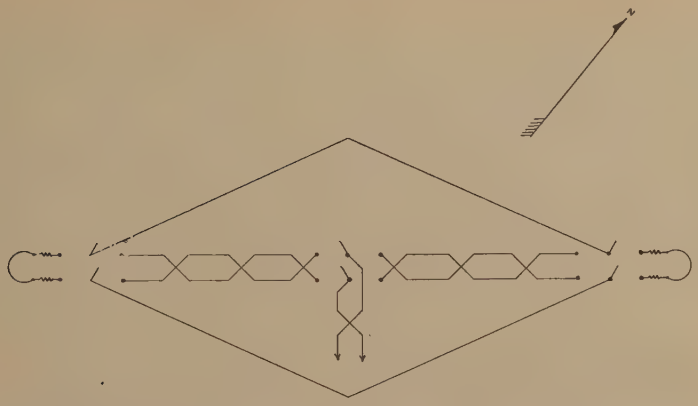

Fig. 2—41.5-megacycle horizontal rhombic antenna fitted with remotely controlled switches to reverse directivity.

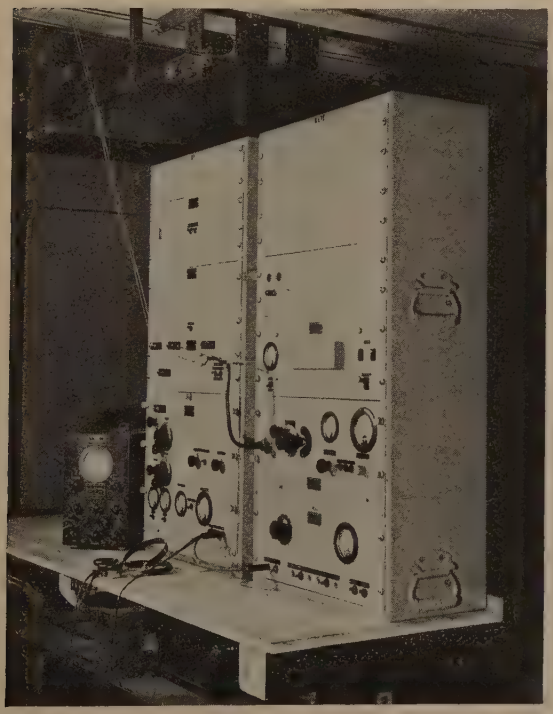

Fig. 3—Ultra-high-frequency receiver and signal generator used for field strength measurements.

length were run to another remotely controlled double-pole double-throw switch and from the blades of this latter switch a transmission line was run to a receiver. Fig. 2 shows a diagram of the antenna and the way in which these switches were connected. The control circuits of the switches were connected so that by operating a toggle switch at the receiver it was possible to connect the receiver to either end of the antenna and simultaneously connect a damping network to the other end. This made it possible to "listen" in either a northeasterly or southwesterly direction. It was found that the damping network re-

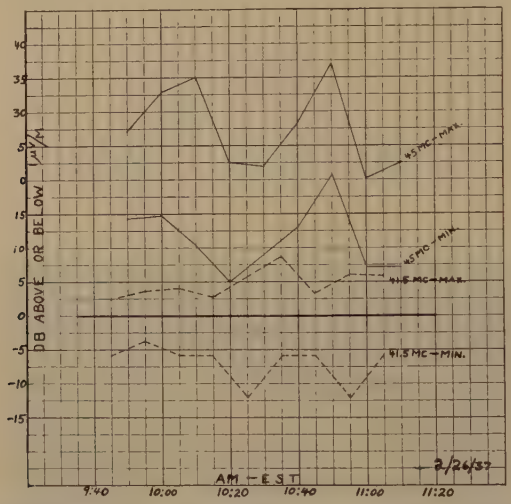


Fig. 4—London television. Plot of single day's observation of the two transmitters at Alexandra Palace showing maximum and minimum values for each.

duced the back-end signal sensitivity about 28 decibels. Fig. 3 shows the receiver and measuring equipment used.

The measurements were made by dividing the observations into five-minute periods and alternately measuring the 41.5- and 45-megacycle emissions. During each period maximum and minimum signal strengths were recorded.

Fig. 4 shows the results of one day's measurements. The solid lines indicate the maximum and minimum values obtained on the London 45-megacycle channel. The broken lines indicate the maximum and minimum values obtained from the 41.5-megacycle channel. It shows the maximum signal received at the terminals of the receiver to have reached a peak value of about 700 microvolts on the 45-megacycle channel. It is also evident that there is a fairly constant ratio of fading of about 25 to 30 decibels on this channel. This phenomenon was ob-

served on several occasions but was not evident on the 41.5-megacycle signal.

Fig. 5 gives a summary of all daily observations made on 41.5 and 45 megacycles between 1000 and 1100, E.S.T. The solid lines represent the daily ranges of the 41.5-megacycle field strength and the dotted lines represent the same for the 45-megacycle channel. Dates on which no observations were made are indicated by "X". It will be noted that the signals were first heard January 21. Conditions for this form of propagation seemed to be at their best during February, falling off

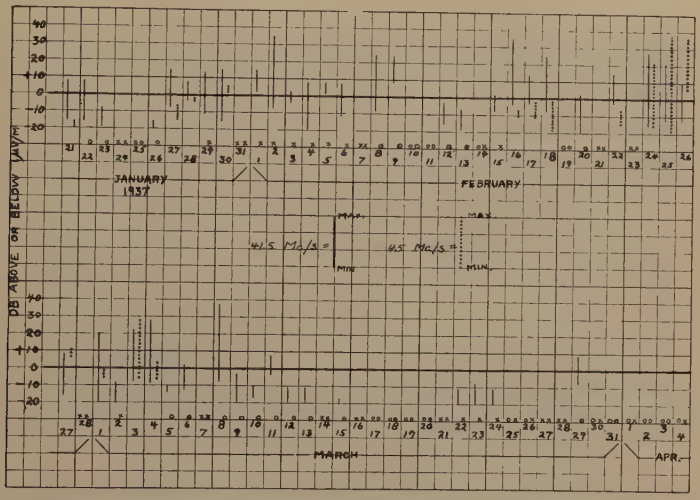


Fig. 5—Daily maximum and minimum field strengths. "X's" indicate no observation made. "0's" indicate signal unheard.

badly in March. Whilst the data have not been plotted for the Berlin signals, these were also heard on a number of occasions in February.

Since a possible explanation for long-distance propagation at these frequencies is that perhaps they are reflected by the $F_2$ layer, an examination of the $F_2$ critical frequencies for vertical incidence is of interest. Fig. 6 shows a plot of monthly averages of the $F_2$ critical frequency for noon, Eastern Standard Time, as measured at Washington, D. C., by the National Bureau of Standards[2] over a period of years. It will be noted that the tendency has been toward higher values of $F_2$ critical frequency. It seems this tendency is in phase with the increase of

[2] T. R. Gilliland, S. S. Kirby, N. Smith, and S. E. Reymer, "Averages of critical frequencies and virtual heights of the ionosphere, observed by the National Bureau of Standards, Washington, D. C., 1934–1936," *Terr. Mag. and Atmos. Elec.*, vol. 41, pp. 379–392; December, (1936).

sunspot numbers on the present eleven-year cycle of solar disturbances, which is due to reach a maximum about 1939.

Fig. 7 shows $F_2$ critical frequencies as measured at Washington, D. C. by the Bureau of Standards,[3] each Wednesday between the hours of 1000 and 1600 E.S.T. plotted along the data relative to conditions observed on the 41.5-megacycles and 45-megacycle channels on the same days. It is noted that the correlation is not perfect. Perhaps better correlation could be had if data were used for critical frequency measurements made more nearly on the path of propagation. Such data however, were not available at the time.

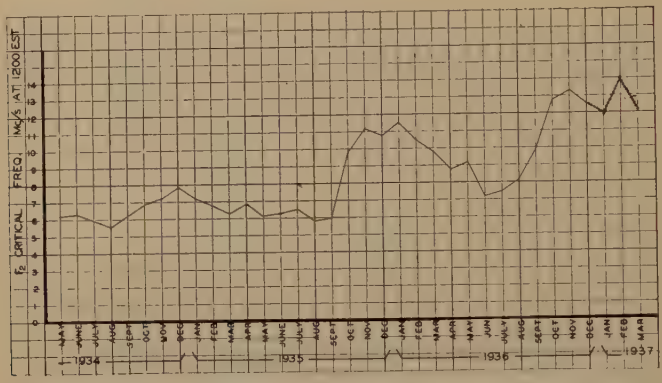


Fig. 6—Monthly averages of $F_2$ critical frequency, noon, E.S.T., at Washington, D. C.

The type of fading observed on the 41.5- and 45-megacycle channels differed greatly. Usually the 41.5-megacycle channel faded rapidly and deeply while the 45-megacycle channel was quite steady for several minutes at a time and would then slowly fade to a new signal level or pass through a shallow dip. The maximum field strength observed on the 45-megacycle channel was about thirty-seven decibels above one microvolt per meter.

Normally the schedule of operation of the English transmitters was from 9:45 A.M. to 11:00 A.M. and again from 4:00 to 5:00 P.M., Eastern Standard Time. The 4:00 to 5:00 P.M. schedule so far has not definitely been heard at Riverhead.

For the week of February 8 the 41.5-megacycle transmitter was kept in operation until noon, Eastern Standard Time, but no definite improvement in field strength was observed during the additional hour. On March 31 the 41.5-megacycle transmitter was operated continu-

[3] The critical frequency data for January, February, and March of 1937 were kindly furnished by Dr. J. H. Dellinger of the Bureau of Standards.

ously from 6:30 A.M. until 1:00 P.M., Eastern Standard Time, but during this run the signal was unheard at Riverhead.

Observations were made simultaneously at LeRoy, Indiana, from March 3 to March 31 inclusive. The 41.5-megacycle channel was heard on four occasions at LeRoy. On these four occasions, the signal was also heard at Riverhead, the field strength being somewhat higher at River-

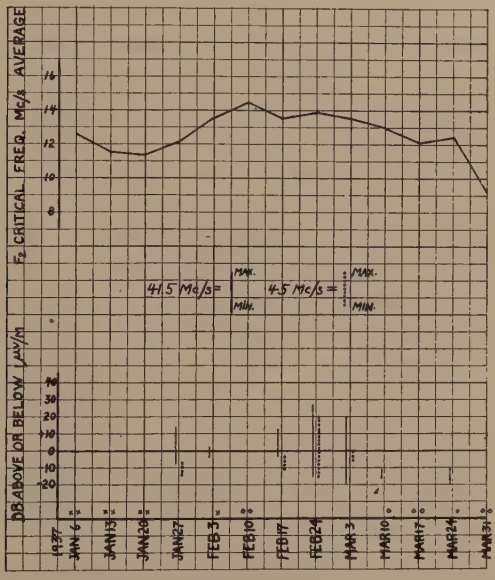


Fig. 7—Average $F_2$ critical frequency 10:00 A.M. to 4:00 P.M., E.S.T., each Wednesday at Washington, D. C., plotted with field strength ranges on same days. "X's" indicate no observation made. "0's" indicate signal unheard.

head. Apparently conditions favorable to transmission affect large areas at the same time.

The measurements made at the Frequency Measuring Laboratory consisted in observing both the 41.5- and 45-megacycle signals on various antennas. There were available several short-wave fishbone antennas directed toward Europe, South America, the west coast, etc. All of these were tried and it was frequently noted that when the signal was weak, best reception could be obtained by using an antenna directed toward the west coast. On several occasions the signal was inaudible on antennas directed toward Europe but of reasonable strength on the west coast antenna. However, during periods of strong signal the European antennas gave the best results. In general the reversible rhombic antenna gave similar results except that at no time did this

antenna show an improved signal from the southwesterly direction. Usually during periods of weak signal the normal direction gave from six to twelve decibels better signal than the reverse direction. However, on two occasions for a period of several minutes each, the signals from both directions were of equal strength.

A possible explanation for the failure of the reversible rhombic antenna to show a good signal from the reverse direction is that the signal may have been coming to Riverhead over some path other than the great-circle one. If this had been the case the rhombic antenna, being rather sharply directive, would show a good back-end response from the southwest only, whereas the Frequency Measuring Laboratory reported best reception either from the northeast or west.

Towards the end of the observations the front-to-back ratio arrangement was dismantled and the remotely controlled antenna switches were arranged to transfer the receiver to either the rhombic antenna directed toward England or a sloping wire antenna designed to receive vertically polarized waves arriving at a vertical angle of $7\frac{1}{2}$ degrees also directed toward England. The few times that it was possible to compare this new antenna with the rhombic indicated no instances of better results with the vertically polarized receiving antenna. The fact of the polarization of the received signal being independent of the polarization of the transmitting antenna supports the conclusion that propagation was by refraction phenomena in the ionosphere much the same as in the case of frequencies on the order of ten to twenty megacycles.

Some additional vertical arrival angle measurements were made in the 29-megacycle amateur band. Table I shows a table of the amateurs

TABLE I

LAYER HEIGHT DETERMINATIONS AT RIVERHEAD, L. I., N. Y.
29-MEGACYCLE AMATEURS

| Call | Location | Distance km | Arrival Angle Degrees | Layer Height km |
|---|---|---|---|---|
| W5FHJ | Ruleville, Miss. | 1800 | 17.2 | 360 |
| | Dallas, Tex. | 2340 | 8.9 | 282 |
| W9YUD | Fremont, Neb. | 2040 | 14.1 | 378 |
| W9DHO | Wisner, Neb. | 2090 | 13.7 | 358 |
| W5CZZ | Terrill, Tex. | 2280 | 11.7 | 357 |
| W5EYV | Refugio, Tex. | 2600 | 9.0 | 357 |
| W9JWI | Independence, Mo. | 1960 | 17.2 | 402 |
| W6LUL | Los Angeles, Calif. | 4050 | 11.6 | 302 |
| W9GND | Grand Falls, N.D. | 2070 | 12.6 | 331 |
| W9DHQ | Wishek, N.D. | 2200 | 9.5 | 290 |
| W5FNH | Kerrville, Tex. | 2720 | 8.1 | 353 |
| W5CZZ | Terrill, Tex. | 2280 | 10.6 | 332 |
| | Kansas City, Mo. | 1950 | 16.2 | 378 |
| W7CKZ | Aberdeen, Wash. | 4050 | 12.4 | 318 |
| W9LKD | Wichita, Kan. | 2180 | 10.9 | 332 |

Mean Layer Height—346 km.

Layer height and vertical arrival angle determinations made with setup shown in Fig. 3.

observed on March 4, 1937. The vertical arrival angle together with the distance between Riverhead and the transmitter location allows a figure for the reflecting layer height to be computed if an assumption is made as to the number of reflections. In the calculations made to determine the column on the right a single reflection was assumed in all but two cases, in which two reflections were assumed. The average apparent layer height derived by this method on these assumptions was 346 kilometers. The average minimum $F_2$ layer height as measured by the Bureau of Standards at Washington, D.C., on March 3 during approximately the same time of day was 240 kilometers. This large difference may be due to lack of knowledge of the region of the $F_2$ layer causing these frequencies to reflect. Repeated determinations on the London signal gave about 340 kilometers as the $F_2$ layer height.

## Acknowledgment

In concluding, the authors wish to express their appreciation for the special schedules of transmission arranged by the British Broadcasting Company and for the ionosphere data supplied by the National Bureau of Standards.[3]

*Proceedings of the Institute of Radio Engineers*
*Volume 25, Number 10* *October, 1937*

# A TRANSFORMATION FOR CALCULATING THE CONSTANTS OF VACUUM TUBES WITH CYLINDRICAL ELEMENTS*

By
W. van B. Roberts
(Radio Corporation of America, New York City)

***Summary***—*By the method of conjugate functions formulas are derived for the amplification constant of a relatively long tube structure comprising a small cylinder concentric with the axis of the structure, a number of wires parallel to the axis and located on a circle concentric with and outside the first cylinder, and a second cylinder also concentric with the axis and surrounding the wires. Several cases are considered, according to which of these elements are taken as cathode, anode, and control electrode. The calculation of tube capacitances by means of the same transformation is illustrated and the basis for setting up transformations for other cylindrical structures is indicated.*

THERE are shown in Fig. 1 $n$ points equally spaced on a circle of radius $a$ drawn about the origin of the complex plane. The positions of these points are $ae^{j(2\pi/n)}$, $ae^{j(4\pi/n)}$, $\cdots$, $ae^{j(n2\pi/n)}$. Let us consider the function

$$f(z) = -q\log z + \log(z - ae^{j(2\pi/n)}) + \log(z - ae^{j(4\pi/n)}) + \cdots + \log(z - ae^{j(n2\pi/n)}). \tag{1}$$

Since $z$ is a complex quantity, $f(z)$ consists of a real part and an imaginary part so we may set $f(z) = U + jV$. Replacing $z$ by $\rho e^{j\theta}$, (1) becomes

$$e^{U+jV} = \rho^{-q}e^{-jq\theta}\rho^n e^{jn\theta}\prod_{t=1}^{t=n}\left(1 - \frac{a}{\rho}e^{j(2\pi t/n)-j\theta}\right). \tag{2}$$

As shown in the Appendix (2) may be reduced to

$$e^{U+jV} = \rho^{n-q}\left[e^{j(n-q)\theta} - \left(\frac{a}{\rho}\right)^n e^{-jq\theta}\right] \tag{3}$$

whence,

$$e^U\cos V = \rho^{n-q}\left[\cos(n-q)\theta - \left(\frac{a}{\rho}\right)^n\cos q\theta\right] \tag{4}$$

$$e^U\sin V = \rho^{n-q}\left[\sin(n-q)\theta + \left(\frac{a}{\rho}\right)^n\sin q\theta\right]. \tag{5}$$

Squaring (4) and (5) and adding we obtain

$$e^{2U} = \rho^{2(n-q)}\left[1 - 2\left(\frac{a}{\rho}\right)^n\cos n\theta + \left(\frac{a}{\rho}\right)^{2n}\right]. \tag{6}$$

* Decimal classification: R131. Original manuscript received by the Institute, October 2, 1936; revised manuscript received by the Institute, June 16, 1937.

Dividing (5) by (4) we have

$$\tan V = \frac{\sin (n-q)\theta + \left(\frac{a}{\rho}\right)^n \sin q\theta}{\cos (n-q)\theta - \left(\frac{a}{\rho}\right)^n \cos q\theta}. \tag{7}$$

It is a fundamental property of the method of conjugate functions[1] that if $U$ is held constant in (6) the equation defines an equipotential surface in two dimensions (that is, the cross section of a long equipotential surface extending perpendicular to the plane of the complex plane) whose potential may be taken numerically equal to $U$. By choosing successively different values of $U$ we obtain the equations of the entire family of equipotentials corresponding to the transformation (1). Fig. 2 shows, qualitatively only, the result of plotting (6) for three different values of $U$.

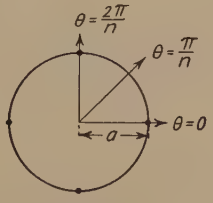


Fig. 1.

In similar fashion (7) gives the field of electric force. That is, for every value of $V$, (7) defines a line of force.

It may be seen from the symmetry of Figs. 1 and 2 about the directions $\theta=0$ and $\theta=\pi/n$ that the electric force along these lines is the negative rate of change of $U$ with respect to $\rho$. Setting $\theta=0$ in (6) we find

$$\frac{dU}{d\rho} = \mp \frac{(n-q)\rho^n + qa^n}{\rho^{q+1}e^v} \tag{8}$$

where the minus sign is used when $\rho<a$ and the plus sign when $\rho>a$ and along the line $\theta=\pi/n$

$$\frac{dU}{d\rho} = \frac{(n-q)\rho^n - qa^n}{\rho^{q+1}e^v}. \tag{9}$$

From these equations it is evident that if we wish the electric force to vanish at a desired distance, say $\rho_1$ along the line $\theta=0$ we must

[1] J. H. Jeans, "Mathematical Theory of Electricity and Magnetism," p. 261.

choose the heretofore undetermined quantity $q$ of the equations to satisfy

$$q = \frac{n\rho_1^n}{\rho_1^n - a^n}. \tag{10}$$

Similarly for the force to vanish at the point $\rho_1$ along the line $\theta = \pi/n$ we must have

$$q = \frac{n\rho_1^n}{\rho_1^n + a^n}. \tag{11}$$

Equations (6), (10), and (11) are all that is needed to proceed with the calculation of the amplification constant of the vacuum tube structure whose electrode shapes conform sufficiently closely to equipotentials defined by (6). Let us define the amplification constant, $\mu$, of a vacuum tube as the ratio of plate voltage to grid voltage when emission is just cut off from all parts of the cathode. When the voltages are in this ratio the electric field at the surface of the cathode is zero at the point on the cathode from which emission first starts as the plate voltage is raised. This seems a more useful definition than the ratio of voltages that just begins to cut off emission from any part of the cathode.

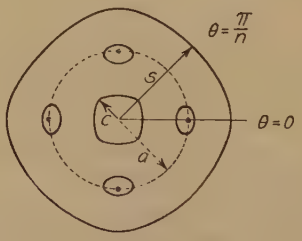


Fig. 2.

*Case I*—Inner electrode acting as cathode, outer electrode as plate.

It is obvious that emission will start first at the point where the cathode is cut by the line $\theta = \pi/n$ or by the line $\theta = 3\pi/n$, etc. To reduce the field to zero at these points we must have, by (11),

$$q = \frac{nc^n}{c^n + a^n} \tag{12}$$

where $c$ is the distance from the origin to the cathode along the line $\theta = \pi/n$. Putting this value of $q$ into (6) we have

$$e^v = \left| \rho^{na^n/(c^n+a^n)} \left[ 1 \mp \left( \frac{a}{\rho} \right)^n \right] \right| \tag{13}$$

where the minus sign is used for points along $\theta=0$ and the plus sign is used for points along $\theta=\pi/n$.

Using the plus sign and putting $\rho=c$ in (13) we have

$$\text{cathode potential} = \log \left| c^{na^n/(c^n+a^n)} \left[ 1 + \left(\frac{a}{c}\right)^n \right] \right|. \tag{14}$$

Using the minus sign and taking the distance to the nearest part of the grid wire as $(a-r)$ we have

$$\text{grid potential} = \log \left| (a-r)^{na^n/(c^n+a^n)} \left[ \left(\frac{a}{a-r}\right)^n - 1 \right] \right|. \tag{15}$$

Using the plus sign and letting $s$ be the distance to the anode along $\theta=\pi/n$ we have

$$\text{anode potential} = \log \left| s^{na^n/(c^n+a^n)} \left[ 1 + \left(\frac{a}{s}\right)^n \right] \right|. \tag{16}$$

From (14), (15), and (16) the ratio of potential difference between cathode and anode to the potential difference between grid and cathode which, in accordance with the definition adopted is the amplification constant, is

$$\mu = \frac{\dfrac{na^n}{c^n+a^n} \log \dfrac{c}{s} + \log \left[ 1 + \left(\dfrac{a}{c}\right)^n \right] - \log \left[ 1 + \left(\dfrac{a}{s}\right)^n \right]}{\dfrac{na^n}{c^n+a^n} \log \dfrac{a-r}{c} + \log \left[ \left(\dfrac{a}{a-r}\right)^n - 1 \right] - \log \left[ 1 + \left(\dfrac{a}{c}\right)^n \right]}. \tag{17}$$

In ordinary structures where $r/a$, $(c/a)^n$, and $(a/s)^n$ are each small compared to unity, the above expression becomes approximately

$$\mu = n \frac{\log \dfrac{s}{a}}{\dfrac{nr}{a} - \log \dfrac{nr}{a}}. \tag{18}$$

By repeating the process of calculating the amplification but starting by making the electric force vanish at the point where the cathode is cut by the line $\theta=0$, which is equivalent to adopting the alternative definition of $\mu$ mentioned above, it will be found that the resulting expression differs from (17) only by a change of the sign of the quantity $c^n$ in the first term of both numerator and denominator. Since this quantity was neglected in obtaining the approximate formula (18) however,

it is seen that the approximate formula is the same regardless of which definition was chosen for $\mu$.

*Case II*—Outer surface used as cathode and inner surface as anode.

The electric field is made zero where the cathode is cut by the line $\theta=\pi/n$ by giving $q$ the value determined by (11) with $\rho_1$ taken as $s$. Using this value of $q$ in (6) we have

$$e^v = \left| \rho^{na^n/(s^n+a^n)} \left[ 1 \mp \left(\frac{a}{\rho}\right)^n \right] \right| \tag{19}$$

the signs being as described in Case I. Using (19) to obtain the potentials of the three electrodes we arrive at the formula

$$\mu = \frac{\dfrac{na^n}{s^n+a^n} \log \dfrac{s}{c} + \log\left[1+\left(\dfrac{a}{s}\right)^n\right] - \log\left[1+\left(\dfrac{a}{c}\right)^n\right]}{\dfrac{na^n}{s^n+a^n} \log \dfrac{a-r}{s} + \log\left[\left(\dfrac{a}{a-r}\right)^n - 1\right] - \log\left[1+\left(\dfrac{a}{s}\right)^n\right]} \tag{20}$$

which becomes approximately

$$\mu = \frac{n \log \dfrac{c}{a}}{\log \dfrac{nr}{a}} \tag{21}$$

if $r/a$ and $(c/a)^n$ are small compared to unity and $(s/a)^n$ is large compared to $n$.

*Case III*—Inner surface the anode, outer surface the grid.

In this case we make the field vanish at the point on the cathode nearest to the anode. By (10) this requires

$$q = \frac{n(a-r)^n}{(a-r)^n - a^n} \tag{22}$$

or, if we assume $r/a \ll 1$ to simplify matters,

$$n - q = a/r. \tag{23}$$

Combining (23) with (6) we have

$$e^v = \left| \rho^{a/r} \left[ 1 \mp \left(\frac{a}{\rho}\right)^n \right] \right| \tag{24}$$

with the same convention as to signs as before. Proceeding as before,

$$\mu=\frac{\frac{a}{r}\log\frac{a-r}{c}+\log\left[\left(\frac{a}{a-r}\right)^n-1\right]-\log\left[1+\left(\frac{a}{c}\right)^n\right]}{\frac{a}{r}\log\frac{s}{a-r}+\log\left[1+\left(\frac{a}{s}\right)^n\right]-\log\left[\left(\frac{a}{a-r}\right)^n-1\right]} \tag{25}$$

or, if $r/a$, $(a/s)^n$, and $(c/a)^n$ are all small compared to unity, we have approximately

$$\mu=\frac{\left(\frac{a}{r}-n\right)\log\frac{a}{c}+\left(\log\frac{nr}{a}-1\right)}{\frac{a}{r}\log\frac{s}{a}-\left(\log\frac{nr}{a}-1\right)}. \tag{26}$$

*Case IV*—Inner surface the grid, outer surface the anode.

Call the distance to the point on the cathode nearest to the anode $a+R$ and making the field vanish at this point we have $n-q=-a/R$ approximately, so that

$$e^v=\left|\rho^{-a/R}\left[1\mp\left(\frac{a}{\rho}\right)^n\right]\right| \tag{27}$$

whence in the same manner as in previous cases we obtain

$$\mu=\frac{-\frac{a}{R}\log\frac{a+R}{s}+\log\left[1-\left(\frac{a}{a+R}\right)^n\right]-\log\left[1+\left(\frac{a}{s}\right)^n\right]}{-\frac{a}{R}\log\frac{c}{a+R}+\log\left[1+\left(\frac{a}{c}\right)^n\right]-\log\left[1-\left(\frac{a}{a+R}\right)^n\right]} \tag{28}$$

or, if $R/a$, $(c/a)^n$, and $(a/s)^n$ are all small compared with unity,

$$\mu=\frac{\frac{a}{R}\log\frac{s}{a}+\left(\log\frac{nR}{a}-1\right)}{\left(\frac{a}{R}+n\right)\log\frac{a}{c}-\left(\log\frac{nR}{a}-1\right)}. \tag{29}$$

It must be emphasized that these formulas for $\mu$ are not so much to be considered as approximate formulas for tube structures having circular electrodes as they are exact formulas (except for the approximate value taken for $q$ in Cases III and IV) for structures having shapes defined by (6). These shapes are sufficiently similar to ordinary tube structures in many cases however to make the formulas applicable. For example, in Case I, by using (13) it can be shown that the anode is almost exactly circular if $(1/n)(a/s)^n$ is negligible in compari-

son with unity. However when we calculate the distance to the cathode along the line $\theta=0$ we find it less than $c$ in the ratio $n/(n+1)$. Thus the cathode surface is slightly "corrugated" no matter how small it is.

This corrugated shape is shown in Fig. 3 which is a plot of three equipotential surfaces calculated from (6) to illustrate Case 1, together with the assumption of particular values as follows: $c=1$, $a=e$ (the base of natural logarithms), and $n=20$. The curves are drawn for the condition of complete cutoff, that is, by using (12). The solid curve is the cathode, the dotted curve is a surface whose potential is very

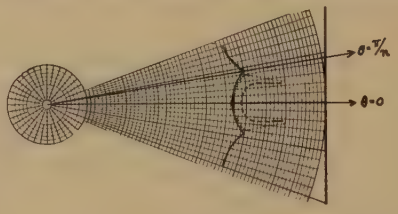


Fig. 3

nearly the same as that of the cathode, and the dashed line curve is a surface differing in potential from the cathode by ten times as much as the dotted curve differs. The line $\theta=0$ is the direction toward one grid wire, and the line $\theta=\pi/n$ (in this case nine degrees) is the direction halfway between grid wires where emission is just cut off.

Similarly in Case III the cathode wires, no matter how small $r$ is taken, are found to be considerably flattened on the grid side as well as squeezed out along the circle on which the wires are located. This squeezing out should by its shielding effect make the expression of (25) and (26) a trifle less than the amplification constant of a tube having circular wires of radius $r$. Thus it would be advisable to plot enough of (6) to determine in any particular case in which any doubt exists, whether the surfaces defined by the equation are reasonably similar to the electrodes of the tube being investigated.

While the foregoing formulas have been derived for wires parallel to the axis, it has been generally assumed by various writers and borne out by experiment that formulas for such an arrangement apply almost equally well to the more common structure having a spiral of wire of equal spacing between two cylinders, at least in cases where the wire spacing is small compared to the distance to the other elements.

## Calculation of Interelectrode Capacitances

The conjugate function method is commonly used for the calculation of capacitances. In the present case let us calculate the grid-cathode and the plate-cathode capacitances per unit length of a struc-

ture such as Fig. 2 when the inner surface is taken as the cathode and the outer surface as the anode. By definition the grid-cathode capacitance $C_{gc}$ is the charge on the cathode divided by the difference of potential between grid and cathode when the plate potential is made the same as that of the cathode so that all the lines of force leaving the cathode must terminate on the grid. Substituting the known co-ordinates of cathode and plate into (6) and equating the resulting potentials we obtain an equation determining $q$

$$c^{n-q}\left[1+\left(\frac{a}{c}\right)^n\right] = s^{n-q}\left[1+\left(\frac{a}{s}\right)^n\right] \tag{30}$$

whence,

$$q = n - \frac{\log\left[1+\left(\frac{a}{c}\right)^n\right] - \log\left[1+\left(\frac{a}{s}\right)^n\right]}{\log\frac{s}{c}}. \tag{31}$$

Now it is a basic property of the method of conjugate functions that if $U$ is taken as the potential, the total charge on a conductor occupying an equipotential surface is $1/4\pi$ times the total change in the value of $V$ that occurs in traveling around the conductor. Let us suppose for the moment that the cathode is very small so that $a/c$ is very great. Then (7) becomes approximately $V = -q\theta$ and the total change in $V$ that occurs in going around the cathode is $-q2\pi$ whence the charge on the cathode is numerically equal to $q/2$. Although the cathode was assumed very small to simplify the calculation of charge, the same result would necessarily have been reached with any larger cathode as all the lines of force coming out of a small cathode must also pass through the successive surrounding equipotentials.

Putting the value of $q$ given by (31) into (6) and using the known co-ordinates of the cathode and the nearest point on the grid we may write the cathode and grid potentials. The required capacitance is then $q/2$ divided by the difference of these potentials, or

$$C_{gc} = \frac{1}{2}\left|\frac{n\log\frac{s}{c} - \log\left[1+\left(\frac{a}{c}\right)^n\right] + \log\left[1+\left(\frac{a}{s}\right)^n\right]}{\left\{\log\left[1+\left(\frac{a}{c}\right)^n\right] - \log\left[1+\left(\frac{a}{s}\right)^n\right]\right\}\log\frac{a-r}{c} + \left\{\log\left[\left(\frac{a}{a-r}\right)^n - 1\right] - \log\left[1+\left(\frac{a}{c}\right)^n\right]\right\}\log\frac{s}{c}}\right|. \tag{32}$$

In similar fashion, by choosing $q$ to make the cathode and grid potentials equal and dividing $q/2$ by the resulting difference of potential between cathode and plate we have the cathode-plate capacitance

$$C_{cp}=\frac{1}{2}\left|\frac{n\log\frac{a-r}{c}-\log\left[1+\left(\frac{a}{c}\right)^n\right]+\log\left[\left(\frac{a}{a-r}\right)^n-1\right]}{\text{(Same denominator as in (32))}}\right|. \quad (33)$$

At this point it is of interest to compare the ratio $C_{gc}/C_{cp}$ with the value of $\mu$ calculated in Case I above since this capacitance ratio has been stated by von Laue[2] to be the amplification constant of a tube. It is easily seen that this ratio differs from (17) only by the absence in the ratio of the quantity $c^n$ appearing in the first term of both numerator and denominator of (17). Since we already noted that the sign of this quantity was reversed if we altered our definition of the amplification constant it appears that the capacitance ratio gives a value of $\mu$ intermediate to the values calculated according to the two definitions considered. In some cases the discrepancy may be important, for example if the cathode consists of broad flat ribbons between plane grid and plate electrodes one would expect a very great difference between the grid bias at which emission from the grid side of the ribbon is cut off and the bias at which complete cutoff occurs.

In conclusion, a word of explanation seems desirable to indicate how the transformation (1) was arrived at, especially since the reasoning involved is applicable to other cases than the one here treated. First of all it is well known that the potential due to a line charge involves the amount of charge per unit length and the logarithm of the distance from the line, and that in the immediate vicinity of a finite magnitude of charge the equipotentials are approximately circular cylinders around it. Thus to represent the $n$ wires it was natural to try writing the sum of the logarithms of the differences between the point $z$ and the locations of the wires, and to add $\log(z)$ to take care of the inner surface. The coefficient $-q$ was included to represent an undetermined charge of opposite sign from the charges on the wires. It thus appears that any arrangement of cylinders that are small in comparison with their distances apart will be given by the transformation $f(z)=A\log(z-a)+B\log(z-b)+C\log(z-c)$, etc., where $A$, $B$, $C$, etc., are proportional to the charges at the points represented by the complex quantities $a$, $b$, $c$, etc., which points are the locations of the centers of the desired small cylinders. The values of the charges may be deter-

[2] *Ann. der Phys.*, vol. 59, (1919).

mined later just as the value of $q$ was chosen in the present transformation to fulfill various requirements.

## Appendix

The product indicated by $\Pi$ in (2) is of the form $(1-ke^{j(2\pi/n)})(1-ke^{2j(2\pi/n)})\cdots(1-ke^{nj(2\pi/n)})$ where $k$ stands for $(a/\rho)e^{-j\theta}$.

Multiplying out and collecting terms in similar powers of $k$ we obtain

$$\begin{aligned} &1 \\ &-k\left\{e^{j(2\pi/n)}+e^{2j(2\pi/n)}+e^{3j(2\pi/n)}+\cdots+e^{nj(2\pi/n)}\right\} \\ &+k^2\left\{e^{j(2\pi/n)}e^{2j(2\pi/n)}+\cdots\right\} \\ &-k^3\left\{e^{j(2\pi/n)}e^{2j(2\pi/n)}e^{3j(2\pi/n)}+\cdots\right\} \qquad (1) \\ &\cdots\cdots\cdots\cdots\cdots \\ &\pm k^n\left\{e^{j(2\pi/n)}e^{2j(2\pi/n)}\cdots e^{nj(2\pi/n)}\right\}. \end{aligned}$$

By symmetry, everything vanishes except the first and last term. For the coefficient of $k$ is simply the sum of $n$ evenly spaced unit vectors, which of course add up to zero. The coefficient of $k^2$ is the sum of all the possible products taken two at a time among these same vectors. By symmetry these products are also unit vectors equally spaced. The coefficient of $k^3$ is the sum of the products taken three at a time and also vanishes for the same reasons.

The coefficient of $k^n$ however does not vanish because it is a single vector. Writing it in the form $e^{j(2\pi/n)(1+2+\cdots+n)}$ it is easily reduced to $e^{j\pi(n+1)}$ which is merely $\pm 1$ according as $n$ is odd or even. But the sign in front of $k^n$ is minus or plus according as $n$ is odd or even. Hence the last term is $-k^n$ in any case, and the expansion reduces to the simple form $(1-k^n)$. Replacing $k$ by $(a/\rho)e^{-j\theta}$ and substituting for the $\Pi$ term of (2), (3) follows at once.

*Proceedings of the Institute of Radio Engineers*
*Volume 25, Number 10* *October, 1937*

# SIMPLE METHOD FOR OBSERVING CURRENT AMPLITUDE AND PHASE RELATIONS IN ANTENNA ARRAYS*

By
John F. Morrison
(Bell Telephone Laboratories, Inc., New York City)

***Summary***—*The paper describes a simple apparatus arrangement for observing the relative amplitudes and phases of the currents in the elements of a multi-element radiating system. The process of adjusting the array is greatly facilitated, much less time and skill being required than when each step in the process is checked by field intensity measurements. Using the method described, these measurements need only be used as a final verification of the adjustment. Field experience with a commercial application is described.*

*The arrangement is also suitable for use by operating personnel in making routine checks to verify the maintenance of the desired amplitude and phase relations or to indicate the direction and magnitude of changes if they have occurred.*

## Introduction

TO obtain a desired distribution of the radiated field about an array of antenna elements, the design engineer must specify, in addition to the spacing and arrangement of the elements, definite relations as to the amplitude and phase of the currents in the elements. With these relations established the field intensity pattern may be computed by a vector summation of the fields contributed by each element of the array.[1] The field contributed by each element is directly proportional to the amplitude of the element current and the relative phases of the fields are directly related to the phase of the corresponding element currents.

Heretofore, field intensity measurements offered the only evidence of the phase relations obtained in practice. This has been accomplished by measuring the field intensity at many points about an array and plotting the data thus collected to obtain the field intensity distribution pattern. The phase relations of the element currents have then been estimated from the shape of the measured pattern.

The device described by this paper permits a more direct observation of the relative phases of the currents in the antenna elements. Furthermore, it may be located at a convenient place in the transmitter building thereby greatly facilitating the "tuning-up" operation and providing a rapid means for periodic checks upon the array performance.

* Decimal classification: R242. Original manuscript received by the Institute, July 1, 1937. Presented before Silver Anniversary Convention, New York City, May 10, 1937.

[1] Ronald M. Foster, *Bell Sys. Tech. Jour.*, vol. 5, pp. 292–307; April, (1926).

## Element Interaction and Its Effect Upon the Adjustment of an Array

The interaction between the elements of an antenna array is briefly discussed here in order to point out certain complexities in the adjustment of an array. The subject of element interaction has been treated

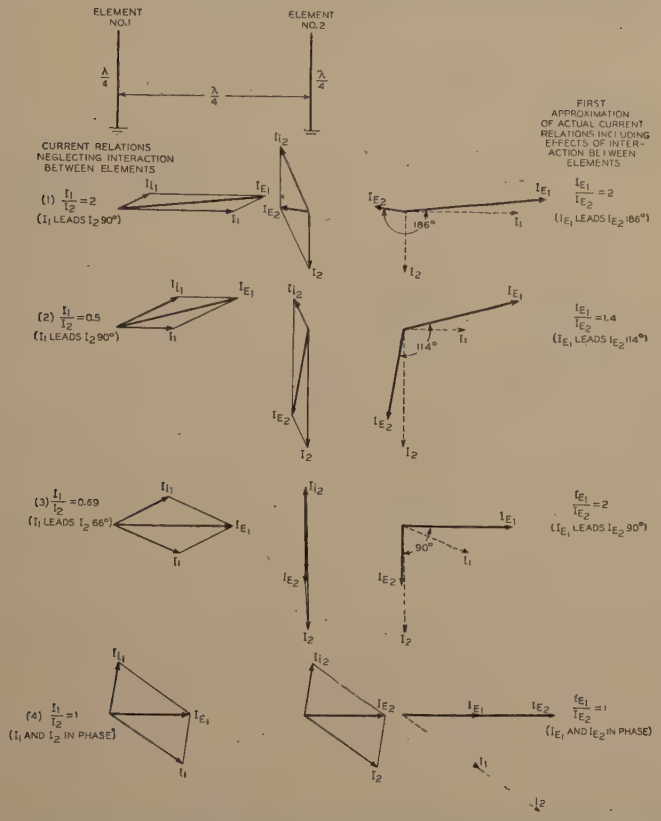


Fig. 1—Vector diagram of current relations in an array of two identical elements spaced one-quarter wave length.

by other authors[2,3] and reference may be made to those publications for a mathematical treatment of the problem. However, for this purpose the interaction effects can be clearly illustrated by a vector representation of the currents in the elements. For simplicity of illustration a first approximation of the effects which occur in an array of

[2] P. S. Carter, "Circuit relations in radiating systems and applications to antenna problems," Proc. I.R.E., vol. 20, pp. 1004–1041; June, (1932).

[3] E. J. Sterba, "Theoretical and practical aspects of directional transmitting systems," Proc. I.R.E., vol. 19, pp. 1184–1215; July, (1931).

two identical elements spaced one-fourth wave length is shown in Fig. 1. Successive approximations converge rapidly from the first so that the first approximation is sufficiently close for illustration.

It has been assumed that the pattern to be produced by this array calls for a current amplitude relation of 2:1 and the current in element 1 to lead the current in element 2 by 90 degrees. $I_1$ and $I_2$ represent, respectively, the current components produced in elements 1 and 2 by an applied generator voltage. If there were no interaction between the elements, $I_1$ and $I_2$ would be the actual element currents; i.e., they represent the current which would flow if the transmission lines feeding the elements were terminated in resistances not mutually coupled. However, when these same currents are allowed to flow in the mutually related elements they will each induce a voltage in the adjacent element causing the currents $I_{i_1}$ and $I_{i_2}$ to flow. The amplitudes of $I_{i_1}$ and $I_{i_2}$ are each proportional to the current in the adjacent element and their phase relation depends upon the element spacing as well as the phase of the adjacent element current. $I_{E_1}$ and $I_{E_2}$ are the vector resultant of the currents produced by the generator and induced voltages and represent closely the actual element currents.

When computing the field intensity pattern about an array of two identical elements each excited with currents that differ in amplitude, the large current can be assigned to either element and the computed pattern will have the same shape. Accordingly in the example considered $I_{E_1}/I_{E_2}$ could equal either 2 or 0.5 without changing the pattern. It is, however, clearly shown by the first two sets of vector diagrams that the interaction between the elements is quite different for the two cases. For this reason, the choice as to which element carries the larger current should be dictated solely by the design of the element coupling apparatus.

It will be seen from the third set of vector diagrams that in order to obtain the desired element current relations, $I_{E_1}/I_{E_2}=2$, $I_{E_1}$ leads $I_{E_2}$ 90 degrees, the currents produced by the generator voltage must bear approximately the following relation: $I_1/I_2=0.69$, $I_1$ leads $I_2$ 66 degrees.

In the adjustment of an array it is desirable to make the necessary corrections in the phases of the applied voltages by adjustments in the apparatus used for coupling between the elements and the transmission lines, thereby minimizing or avoiding the occurrence of standing waves on the transmission lines. These phase correcting adjustments can also be made to a degree in the line branching and phase shifting networks, provided that no excess voltages develop because of standing waves on the transmission lines. At high frequencies a standing wave condition

may also increase the losses in the transmission lines to an objectionable amount.

The fourth set of vector diagrams represents the case where the two elements are to be excited in phase and unity current ratio to effect maximum signal broadside to the array. It will be seen that only in this special case do the resultant element currents bear the same relative relation to each other as the currents resulting from the applied generator voltages. This accounts for the comparative simplicity of adjustment afforded by the use of broadside arrays.

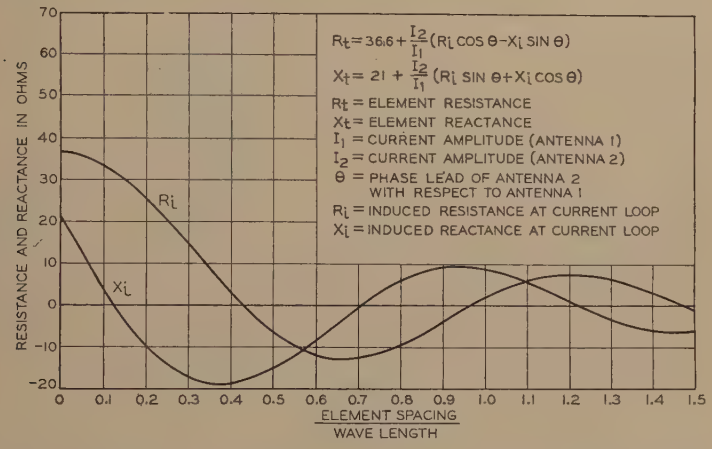


FIG. 2—Impedance interaction between quarter-wave-length elements.

By the use of the superposition theorem the interaction effects between the elements of an array can, for convenience, be considered from the viewpoint of impedance relations. Fig. 2 shows the resistance and reactance introduced at the base of a vertical quarter-wave-length element, erected perpendicular to a perfect ground, by an adjacent vertical quarter-wave-length element excited with currents of the same magnitude and phase. The spacing of the elements expressed in wave lengths is the abscissa of this figure. If the currents in the adjacent element are not of the same phase or amplitude, the base impedance of each element may be computed from the formula which is also shown on Fig. 2. $R_I$ in the formula is obtained from the curve for the element spacing under consideration. If more than two elements are to be considered, the effects of each may be computed separately from the formula, giving due regard to the spacing, current amplitude, and phase relations in each case. These effects may then be added to obtain the total effect.

Fig. 3 shows similar information for vertical half-wave-length elements. The values shown apply to the current loop which is not at the base of the antenna in this case. A knowledge of the element characteristic impedance,[4] which depends largely upon the conductor diameter, is necessary before the interaction effects at the base of a half-wave-length element can be estimated.

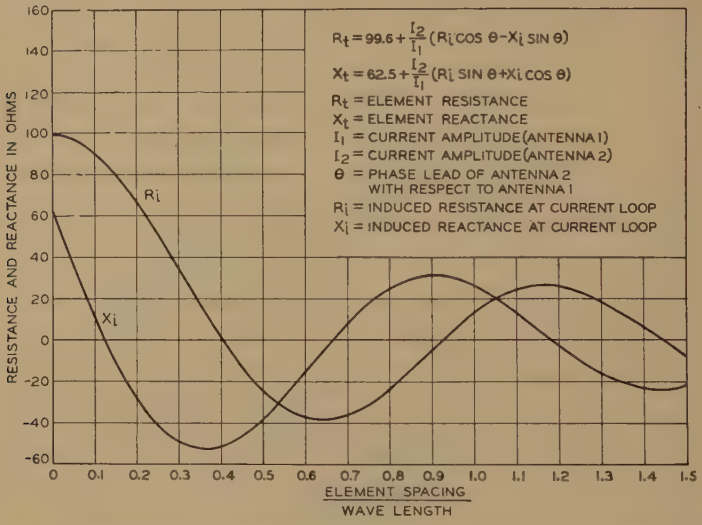
$R_t = 99.6 + \frac{I_2}{I_1}(R_i \cos\theta - X_i \sin\theta)$
$X_t = 62.5 + \frac{I_2}{I_1}(R_i \sin\theta + X_i \cos\theta)$
$R_t$ = ELEMENT RESISTANCE
$X_t$ = ELEMENT REACTANCE
$I_1$ = CURRENT AMPLITUDE (ANTENNA 1)
$I_2$ = CURRENT AMPLITUDE (ANTENNA 2)
$\theta$ = PHASE LEAD OF ANTENNA 2 WITH RESPECT TO ANTENNA 1
$R_i$ = INDUCED RESISTANCE AT CURRENT LOOP
$X_i$ = INDUCED REACTANCE AT CURRENT LOOP
RESISTANCE AND REACTANCE IN OHMS
160
140
120
100
80
60
40
20
0
-20
-40
-60
$R_i$
$X_i$
0 0.1 0.2 0.3 0.4 0.5 0.6 0.7 0.8 0.9 1.0 1.1 1.2 1.3 1.4 1.5
ELEMENT SPACING / WAVE LENGTH

Fig. 3—Impedance interaction between half-wave-length elements.

From an inspection of these curves and the accompanying formula, it will be seen that the impedance of the elements may assume almost any value, depending upon the several factors: element spacing, element height, current amplitude, and phase relations. The resistance component of the impedance of one or more of the elements may in some cases become negative, or in other words, the power flow may be toward, rather than from, the generator. An actual observation of this condition will be discussed later in the paper.

Since an array is excited by one generator at a common connection point in the system, it is not possible to measure the impedance at the driving point of each element with any present standard means for impedance measurement. The insertion of an impedance measuring instrument would upset the performance of the whole system and alter the impedance at all points in the system. The impedance being unknown, the current at the driving point of each element cannot be used for power determination, but the relative values of the currents

[4] J. F. Morrison and P. H. Smith, "The shunt-excited antenna," Proc. I.R.E., vol. 25, pp. 673–696; June, (1937).

as measured at the several points in the system are useful as a check upon the constancy of an array adjustment.

In actual practice, where the conditions of ideal element configuration and perfect ground are not fully realized, the rigorous treatment of the interaction problem illustrated in Figs. 2 and 3 serves only as an approximation of the actual conditions. Therefore, it has been necessary for the engineer to adjust an array by a series of approximations and each time measuring the field intensity pattern to check his results. This approach to the problem is not only laborious but may require considerable time.

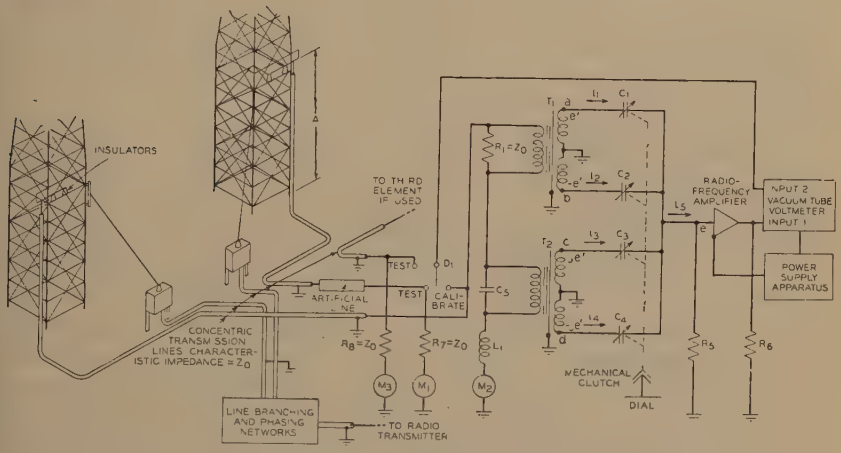


Fig. 4—Current amplitude and phase measuring circuit.

## A Method of Observing Current Amplitude and Phase Relations

Another and more straightforward approach to the problem of antenna array adjustment is to provide a simple means whereby the amplitude and phase relations of the element currents can be quickly and accurately observed at the transmitter location. This may be done by the method illustrated in Fig. 4.

There is placed on each shunt-excited element[4] at the height $A$ above ground a rigid single turn loop which may be constructed of angle iron. The dimension $A$ is chosen so that the loop is placed just above the connecting point of the inclined conductor of the antenna element. The dimensions of the loops as well as their location on the elements must be the same at each element of a particular array. The top of the loop is directly connected to the tower, while the bottom is insulated from the tower and connected to the center conductor of a concentric type transmission line.

Transmission lines having essentially identical characteristics are run from the loop on each element to a common convenient point, such as in the transmitter building. It is important that each line be terminated by an impedance which is equal to its characteristic impedance, $Z_0$. Furthermore, the lines must be made the same length, or in cases where this is not practicable, the shorter ones may be built out to the same equivalent length by artificial lines.

This arrangement of measuring loops and transmission lines makes available at a convenient location samples of the currents in each element. Symmetry of measuring loops and transmission lines is essential if the amplitude and phase relationships between current samples are to be the same as the corresponding relationships between the currents in the radiating elements but in practice it is not difficult to establish this symmetry with the required accuracy.

The amplitudes of the sample currents are read on the milliammeters $M_1$ and $M_2$ (Fig. 4) which are connected in series with the line terminating impedances.

The phase relation of the sample currents is determined as follows: The voltage developed across the terminating impedance of one transmission line is applied to the input of a continuously variable calibrated phase shifting network. The voltage at the output of the phase shifting network is amplified by a radio-frequency amplifier which compensates for the losses through the network. The voltage developed across the terminating impedance $R_6$ of the amplifier is applied to input No. 1 of the vacuum tube voltmeter. The voltage applied at the input of the phase shifter is at the same time applied to input No. 2 of the vacuum tube voltmeter when the switch, $D_1$, is in the CALIBRATE position. The continuously variable phase shifter is then adjusted until a null is observed on the vacuum tube voltmeter which indicates that the voltage at the input of the phase shifter is in phase with the voltage at the output of the amplifier. In other words, the phase shift through the combined phase shifter and amplifier is zero.

A mechanical clutch arranged between the shaft of the variable phase shifter and the calibrated dial is then released in order to permit rotation of the dial without disturbing the phase shifter adjustment. The dial is rotated until the zero marking on it coincides with the dial indicator and the clutch is then re-engaged.

By operating switch $D_1$, input No. 2 of the vacuum tube voltmeter is disconnected from the phase shifter and connected to the terminating impedance of a transmission line fed by another element of the array. The phase shifter is again adjusted until a null is observed

on the vacuum tube voltmeter and the phase relation of the currents in the two elements is then read directly on the phase shifter dial.

If the array consists of more than two elements, the phase relation of the current in each element can be observed by switching the vacuum tube voltmeter input No. 2 to the several transmission line terminating impedances, each time adjusting the phase shifter for a null indication on the vacuum tube voltmeter.

While this method of observing current amplitude and phase relations is relatively simple and straightforward, it is apparent that care must be exercised in the design and installation of the apparatus in order to obtain reasonably accurate results. In the first place, the measuring loops and transmission lines must be electrically identical. The terminating resistors of these lines should have as nearly as possible zero phase angle and be capable of maintaining their resistance value for an indefinite period, while dissipating approximately one watt of radio-frequency energy. The variable phase shifter must have practically constant loss with phase variation. Furthermore, it must be capable of maintaining its calibration under slight changes in circuit characteristics or permit of easy calibration in the field.

## A Continuously Variable Phase Shifter

A continuously variable phase shifter which makes use of variable condensers[5] in place of the usual rotating magnetic field and pickup coil was found more suitable for the purpose.

A circuit diagram of this phase shifter is also shown on Fig. 4. The resistor $R_1$ and condenser $C_5$ are connected in series and are related by the expression:

$$R_1 = \left| \frac{1}{\omega C_5} \right| = |Z_0|.$$

The transformers $T_1$ and $T_2$ are alike and their primaries are connected across the resistor $R_1$ and condenser $C_5$, respectively. The center of each transformer secondary is connected to ground.

The purpose of this part of the circuit is to produce at the points $a$, $b$, $c$, and $d$ four potentials of equal amplitude but unlike phase. If well-designed transformers are used the relative phases of the potentials at $a$, $b$, $c$, and $d$ are respectively 0, 180, 90, and 270 degrees.

The four variable condensers have a maximum capacitance small compared to $C_5$ so that they have a negligible effect upon the potentials at $a$, $b$, $c$, and $d$. The rotors of these condensers are connected together both mechanically and electrically.

[5] L. A. Meacham, Patent No. 2,004,613, June 11, 1935.

If we represent the variable condensers by generalized impedances such as $C_1=Z_1$, $C_2=Z_2$, $C_3=Z_3$, $C_4=Z_4$ and the resistance $R_5=Z_5$ the equations for this generalized circuit may be written as follows:

$$i_1 = \frac{e' - e}{Z_1} = Y_1(e' - e)$$

$$i_2 = \frac{-e' - e}{Z_2} = Y_2(-e' - e)$$

$$i_3 = \frac{je' - e}{Z_3} = Y_3(je' - e)$$

$$i_4 = \frac{-je' - e}{Z_4} = Y_4(-je' - e)$$

$$i_1 + i_2 + i_3 + i_4 = i_5 \frac{e}{Z_5} = Y_5 e.$$

Therefore,

$$Y_1(e' - e) + Y_2(-e' - e) + Y_3(je' - e) + Y_4(-je' - e) = Y_5 e.$$

This expression solved for $e$, gives

$$e = \frac{e'(Y_1 - Y_2)}{\Sigma Y_n} + \frac{je'(Y_3 - Y_4)}{\Sigma Y_n}. \tag{1}$$

It is desired that the phase of $e$ be advanced with respect to $e'$ uniformly as the condenser shaft is rotated, the amplitude of $e$ remaining constant.

This may be accomplished by letting

$$Y_1 = A + B \sin\theta$$
$$Y_2 = A - B \sin\theta$$
$$Y_3 = A + B \cos\theta$$
$$Y_4 = A - B \cos\theta$$
and $Y_5 = K$, a constant.

These values substituted in (1) give

$$e = e'(\sin\theta + j\cos\theta)\frac{(2B)}{(4A + K)}. \tag{2}$$

Since the absolute value of $(\sin\theta + j\cos\theta)$ is unity, the amplitude of $e$ is constant, and is given by

$$|e| = e'\frac{(2B)}{(4A + K)}.$$

The phase relation between $e$ and $e'$ is expressed by the term $(\sin\theta+j\cos\theta)$.

Since $Y=1/Z=2\pi fc$ the requirements on the variation of the admittances are met with variable condensers having characteristics as follows:

$$C_1=a+b\sin(\theta+0°),$$
$$C_2=a+b\sin(\theta+180°),$$
$$C_3=a+b\sin(\theta+90°),$$
$$C_4=a+b\sin(\theta+270°),$$

when $\theta$ represents the angular position of the rotor shaft.

It follows that these four condensers are similar and their rotors may be mounted on a common shaft.

The nature or magnitude of the impedance $Z_5$ does not affect the constancy of the output or the linearity of the phase shift with respect to the angular position of the rotor, if this output impedance is constant. This follows from (2) in which $1/Z_5=K$. If this output impedance should for any reason change in nature or magnitude because of changes in vacuum tubes or circuit characteristics, the effects upon phase shift are automatically corrected by the zero calibration adjustment of the phase indicator as explained in a foregoing paragraph.

The operation of the phase shifter is illustrated pictorially in Fig. 5. The four quadrature potentials are shown vectorially and designated $e'$, $-e'$, $je'$, $-je'$. The stator plates of the condensers are shown in the same relative position as the vector potentials applied to them. These stator plates are repeatedly drawn to show the respective location of the two rotors, which are connected by a common shaft, for five settings of the calibrated dial. The curves of Fig. 5 show the variation of capacitance with change in angular position of the rotor for the four condensers I, II, III, and IV. It will be noted that the resultant vector, shown at the bottom of the figure rotates in the same direction as the rotor plates of the condensers. It will also be noted that a clockwise rotation of the rotor plates rotates the resultant vector in the same direction, or vice versa for a counterclockwise rotation of the plates.

This feature is particularly valuable for the following reasons: If we have say two vector potentials $V_1$ and $V_2$ and assume that $V_1$ leads $V_2$ by 30 degrees; then if $V_2$ is applied to the input of the phase shifter and $V_1$ to the voltmeter input No. 2, a null will be observed on the voltmeter when the calibrated dial is rotated 30 degrees in a counterclockwise direction. If, on the other hand, we apply $V_1$ to the input of the phase shifter and $V_2$ to the voltmeter input No. 2 a null will be observed on the voltmeter when the dial is rotated 30 degrees in a clock-

wise direction. Therefore, we not only have an indication of relative phase but also the quadrature relations of the vector potentials. This provides for the determination of the lead or lag relations of the element currents.

The experimental model of the complete apparatus was tested by laboratory instruments on a frequency of 780 kilocycles and the results

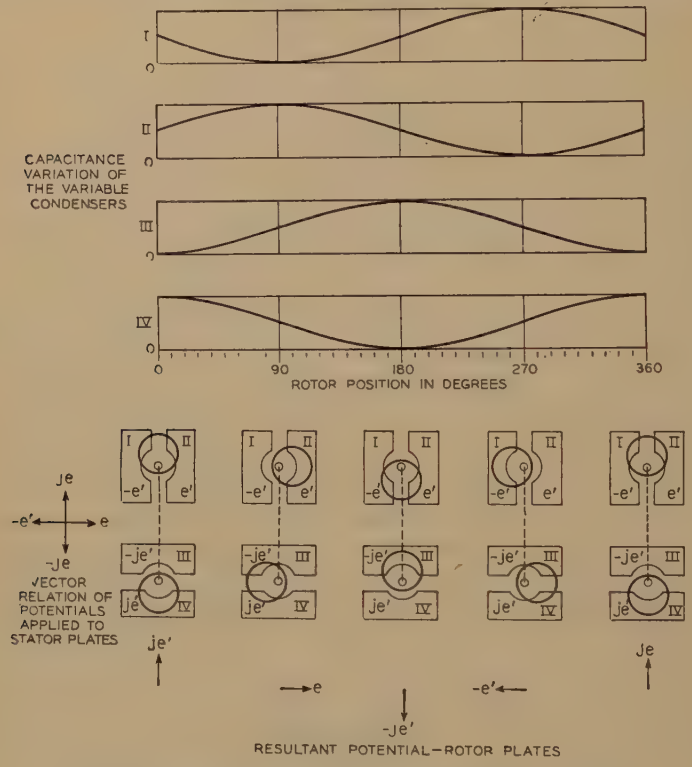


Fig. 5—Pictorial illustration of phase shifter operation.

are shown on Fig. 6. The ordinates of this figure represent the phase relations of two known voltages and the abscissas are the dial readings of the phase indicator when these voltages of known phase relation were applied to the indicator. Later developments have shown that the slight departure from linearity can be reduced in future design.

The photograph, Fig. 7, is a front view of an experimental model of the current amplitude and phase indicating equipment. The two meters which may be seen on the left side of the equipment indicate the current amplitude relations. The switch located between these meters, is designated as $D_1$ in Fig. 4. The switching of the phase indicator

between the calibrate and test positions is accomplished by operation of this switch. The meter located on the right side of the equipment is connected in the vacuum tube voltmeter circuit and the null indications are observed on this meter. When pressed, the push button located immediately underneath this meter, greatly increases the sensitivity of the meter. This feature prevents damage to the meter which might be caused by excessive voltages during the initial adjustments of the phase shifter. The calibrated phase indicator dial is viewed through the window at the top center of the panel and it is rotated by the lower left

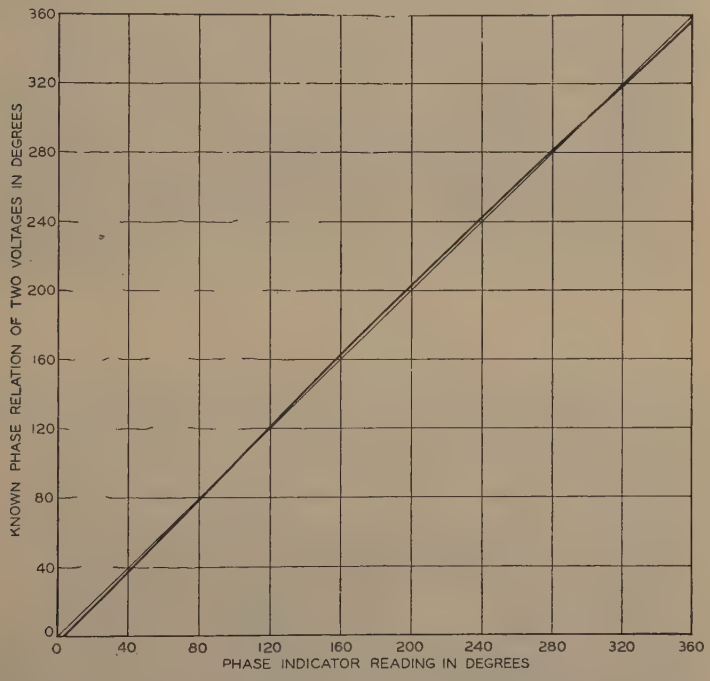


Fig. 6—Calibration curve of phase indicator.

knob which is a vernier control. The mechanical clutch referred to in a foregoing paragraph is located in the center of the panel. The remaining controls located along the bottom of the panel are amplifier gain control, meter balancing potentiometer, and alternating-current power switch.

The photograph, Fig. 8, is a rear view of the equipment. The apparatus on the left is power apparatus which supplies all necessary voltages for the operation of the amplifier and voltmeter. The special variable condenser may be seen at the center of the unit as well as the

radio-frequency transformers and amplifier tube shields. Two concentric transmission line jacks are located at the extreme right. These jacks are especially designed for use with concentric transmission lines. Ceramic insulation and German silver contacts are used in their construction.

Fig. 7—Front view of current amplitude and phase indicating apparatus.

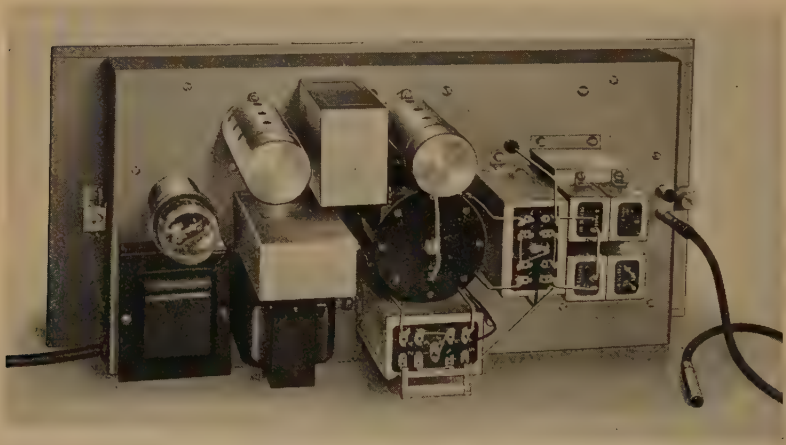

Fig. 8—Rear view of current amplitude and phase indicating apparatus.

## A Practical Application of the Current Amplitude and Phase Indicating Equipment

This apparatus was first used in November, 1936, in connection with the adjustment of the two-element directive antenna array of the Yankee Network station WEAN at Providence, R.I.

The antenna array at that station was designed by Paul deMars, consulting engineer for the Yankee Network. It consists of two quarter-wave-length shunt-excited elements spaced one eighth of a wave length apart. The desired pattern called for a 2.12:1 amplitude ratio of the element currents and a phase difference of 150 degrees. From the information shown on Figs. 2 and 3 it was estimated that the impedance of two base-insulated elements under the same conditions of spacing, current amplitude, and phase relations would be as follows:

Element No. 1 $-22.5+j56$

Element No. 2 $23.6+j14.4$

The negative resistance of element No. 1 indicates that the power flow is from the element toward the generator. From these impedance

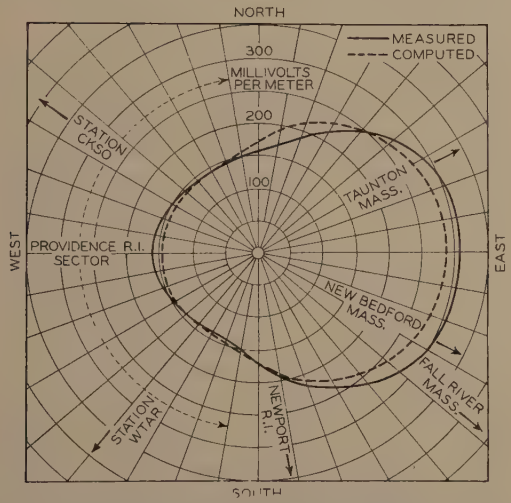


Fig. 9—Measured and computed field intensity pattern of the two-element antenna array at station WEAN.

relations it was estimated that the power from a 1000-watt transmitter would be distributed in the following manner: 1270 watts would flow toward element 2 and 270 watts would flow from element 1 toward the transmitter, the difference of the two powers being equal to 1000 watts.

Since the elements in the WEAN array are the shunt-excited type the impedance at the base of the inclined conductor of these elements depends largely upon the tap position and dimensions of the inclined conductor. Therefore, the means for tuning this array consisted in providing for adjusting the position of the connection of the inclined conductors to the radiating elements, for adjusting the reactance at the base of the inclined conductor, and for adjusting the phase shifting

and line branching networks which control the amplitude and phase relations of the currents fed to the individual radiating elements.

The current amplitude and phase indicating equipment proved to be a most valuable tool during the adjustment of the WEAN array. It provided at all times during the tuning adjustments an indication

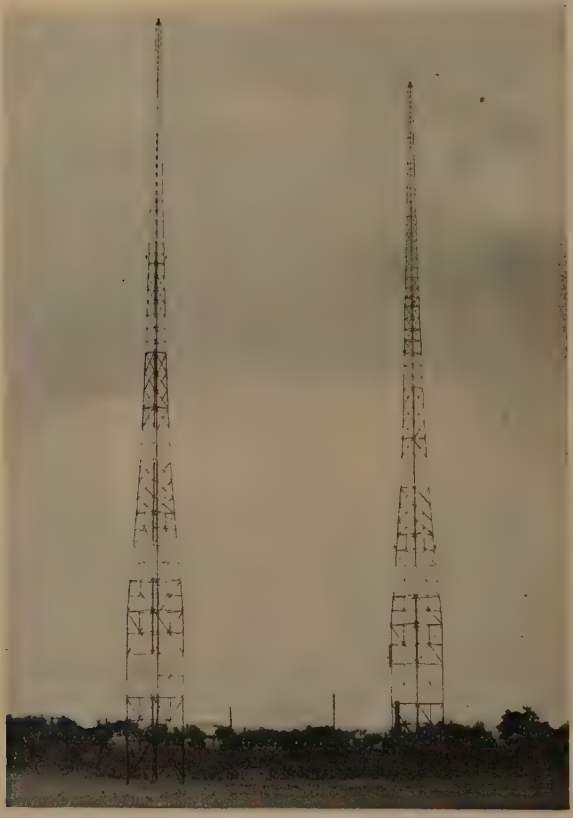

Fig. 10—The two-element antenna array at station WEAN.

of the element current relations. When the desired current amplitude and phase relations were obtained, as observed by this device, there remained only two things to be done. First, to establish by measurement that there were no excessive voltages present on the transmission lines or at the coupling equipment. This may be done by measuring with a suitable high impedance voltmeter[6] the standing wave on the

[6] E. J. Sterba and C. B. Feldman, "Transmission lines for short-wave radio systems," Proc. I.R.E., vol. 20, pp. 1163–1202; July, (1932).

transmission lines. Second, to make field intensity measurements to determine the element efficiency and the pattern produced by the array. The measured pattern is shown by the solid curve on Fig. 9. The dotted curve of this figure is the pattern estimated by deMars in the preliminary computations of the expected performance of the array.

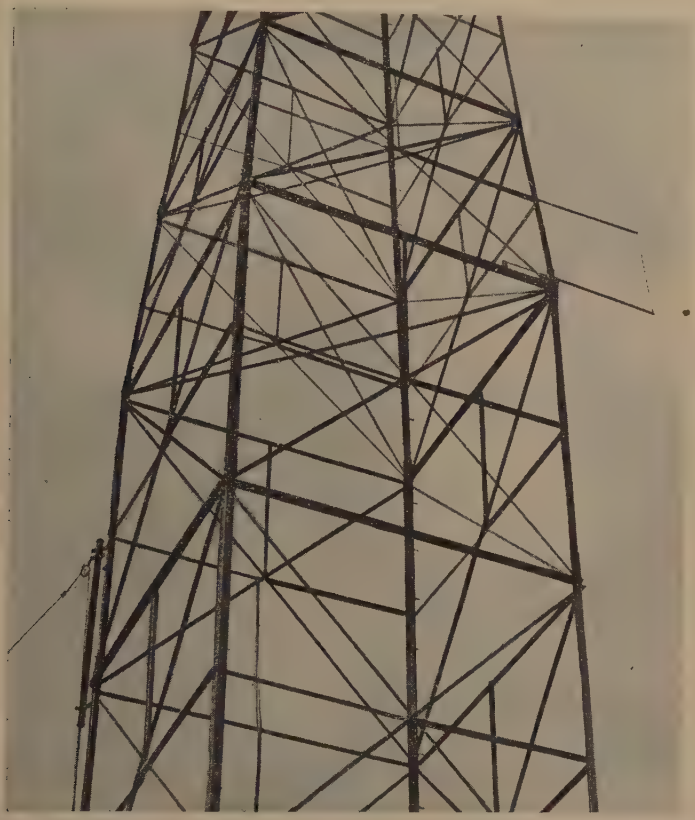

Fig. 11—Angle-iron loop on an element of the WEAN antenna array used in connection with the current sampling circuit.

The efficiency of the individual elements was found to be slightly greater than originally anticipated which accounts for the somewhat greater measured field in the front and back directions from the array. Because of this greater element efficiency it was necessary to change slightly the current ratio from the value first specified in order to reduce the field in the directions of stations CKSO and WTAR to the values allotted by the Federal Communications Commission. The solid curve

shown in this figure is an average of well over 100 field measurements collected by the technical staff of the Yankee Network.

Fig. 10 is a photograph of the WEAN two-element, shunt-excited array.

Fig. 11 is a close-up photograph of the measuring loop used to obtain the sampling current from one of the array elements.

## Acknowledgment

The author is indebted to his colleagues Messrs. R. H. Lindsay and W. L. Tierney for their encouragement during the development work and to the members of technical staff of the Yankee Network for their assistance in the collection of the data.

*Proceedings of the Institute of Radio Engineers*
*Volume 25, Number 10* *October, 1937*

# RADIATION FROM RHOMBIC ANTENNAS*

By
Donald Foster
(Boonton, New Jersey)

***Summary***—*A direct theoretical determination of the transmitting properties of the horizontal rhombic antenna and of the closely related inverted V structure has been made. Expressions are given for the intensity of the radiation, the polarization, the radiation resistance, and the gain.*

*The intrinsic simplicity of the radiation distribution functions is revealed by graphical representation. Stereographic representation also supplements the analysis and provides clear insight into the effects available through variations of design, and enables the essential features of a specific design to be obtained for all directions with a very small amount of labor.*

*Methods of diminishing the relative intensity of radiation from subordinate lobes are considered.*

## I. General

THE inverted V and the horizontal rhombus as receiving antennas have been discussed by Bruce.[1] The horizontal rhombic receiving antenna was recently treated in more detail by Bruce, Beck, and Lowry.[2] In order to obtain a formula for the current in the receiver in terms of the direction of arrival of the incoming wave, the authors assumed a polarization that is independent of the orientation of the ray with respect to the antenna.

Their equation is limited to the case of waves polarized with the electric vector normal to the plane of incidence. But the antenna is also sensitive to waves polarized parallel to the plane of incidence and in general such parallel components exist both when receiving and when transmitting. Because of this fact the directional properties in transmitting, and the receiving properties in the general case, cannot be obtained from their formula.

When the antenna is used for transmitting, the polarization of the radiation depends on the direction in which it is emitted. Consequently the directional properties of the antenna as a radiator cannot be inferred from the properties of the same antenna as a receiver of waves of fixed polarization, as may be done in the case of certain other antennas. Direct attack on the radiation problem is therefore necessary. The equations so obtained will yield not only the directional pattern but

* Decimal classification: R120. Original manuscript received by the Institute, June 18, 1937. Presented before joint I.R.E.-U.R.S.I. meeting, Washington, D. C., April 30, 1937.

[1] E. Bruce, Proc. I.R.E., vol. 19, pp. 1406–1433; August, (1931).

[2] E. Bruce, A. C. Beck, and L. R. Lowry, Proc. I.R.E., vol. 23, pp. 24–46; January, (1935).

also expressions for the radiation resistance, the gain, and the polarization. By means of the reciprocation theorem the generalized receiving properties may be deduced.

In order to calculate the electromotive and magnetomotive intensities of the wave, we start with an expression for the simultaneous complex magnetic vector potential in the form

$$\overline{A} = \frac{e^{-i\beta r}}{4\pi r} \int I(s,t) e^{i\beta r' \cos\psi} \, d\bar{s} \equiv \frac{e^{-i\beta r}}{4\pi r} \overline{F} \tag{1}$$

where $r$ is the distance from the origin (assumed large compared with the wave length and the dimensions of the antenna), $\beta$ is $2\pi$ divided by the wave length, $r'$ is the distance between the origin and the element of antenna $d\bar{s}$, and $\psi$ is the angle between the radius to this element and the direction of the ray. The complex current, $I$, is a function of distance $s$ along the antenna. This expression for $\overline{A}$ is derived by transforming the well-known element of retarded vector potential[3]

$$d\overline{A}_{\text{ret}} = \frac{I\left(s, t - \frac{r}{c}\right) d\bar{s}}{4\pi r} \tag{2}$$

into the simultaneous form referred to a common origin, and then integrating over the extent of the antenna. The expression, (1), for $\overline{A}$ consists of two factors, one of which depends only on the distance and the other only on the orientation of the ray. The latter factor is a characteristic of the antenna which we call the radiation vector $\overline{F}$.

At a sufficient distance from the antenna, the spherical components of the complex electromotive and magnetomotive intensities of the radiation are given by

$$E_\theta = -120\pi i\beta A_\theta; \quad E_\phi = -120\pi i\beta A_\phi; \quad E_r = 0. \tag{3}$$

$$H_\theta = i\beta A_\phi; \quad H_\phi = -i\beta A_\theta; \quad H_r = 0. \tag{4}$$

The time average of the rate of flow of energy per unit area normal to the ray is equal to one half the real part of the complex Poynting vector. Thus[4]

$$\bar{Q} = \text{real part of } \tfrac{1}{2}\overline{E} \times \overline{H}^*. \tag{5}$$

This is a vector in the radial direction whose magnitude is

$$Q = \text{real part of } \tfrac{1}{2}(E_\theta H_\phi^* - E_\phi H_\theta^*) \tag{6}$$

[3] The practical system of units is used throughout.

[4] $\overline{H}^*$ means the conjugate of $\overline{H}$.

which after substituting the values of the intensities in terms of the vector potential becomes[5]

$$Q = \frac{15\pi}{\lambda^2 r^2}(F_\theta F_\theta^* + F_\phi F_\phi^*) \tag{7}$$

where $(F_\theta F_\theta^* + F_\phi F_\phi^*) \equiv K^2$ is a factor in the intensity that depends on the direction and not on the distance from the source.

## II. Calculation of the Radiation Functions

The cartesian co-ordinates are chosen with the origin at the apex at which the power enters the antenna from the generator. The op-

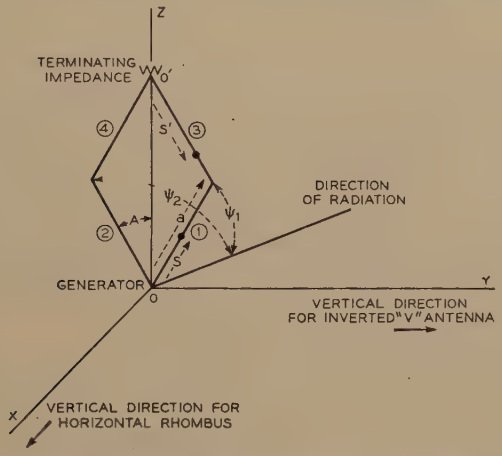


Fig. 1—The rhombic antenna, or the inverted V antenna and its image.

posite apex, where the terminating impedance is located, lies on the $Z$ axis; and the plane of the antenna coincides with the plane $X=0$. The angle between the principal axis and an arm of the antenna is called $A$. The length of a side of the rhombus is designed by $a$. Various sets of co-ordinate angles expressing direction relative to the rectangular frame will be used, the choice depending on whether we are considering a horizontal rhombic antenna or an inverted V antenna.

With the proper terminating impedances, and assuming uniformly distributed inductance and capacitance the current in the right-hand branch is[6]

[5] This expression for the average Poynting flux in terms of the complex vector potential is due to S. A. Schelkunoff, (private communication).

[6] This assumed current distribution is of course not strictly true, owing to mutual coupling and radiation. Nevertheless it appears to be justified as a first approximation by the agreement between the calculated positions of null points and those found experimentally by Bruce. The analysis would be greatly lengthened by a refinement in the description of the current distribution.

$$i = I_0 e^{-i2\pi(s-ct)/\lambda} = Ie^{-i\beta s}; \quad [I \equiv I_0 e^{i\omega t}] \tag{8}$$

where $s$ is the distance from 0 along the antenna, (Fig. 1). In the left-hand branch the current is the same function of $s$ measured away from 0 along that side, if the positive direction for current is reckoned one way, say counterclockwise, around the rhombus. In sections III and IV it is convenient to express the current in terms of the distance $s'$ measured from $0'$. Thus,

$$i = Ie^{-i\beta s} = Ie^{-i\beta(2a-s')} = Ie^{-i2a\beta} \cdot e^{i\beta s'}. \tag{9}$$

The relations between the components of current in the various branches (when $s$ and $t$ are constant) are

$$I_{y_1} = I_{y_2}; \quad I_{y_3} = I_{y_4}; \quad I_{z_1} = -I_{z_2}; \quad I_{z_3} = -I_{z_4} \tag{10}$$

and the components are given by

$$I_{y_1} = I \sin A \cdot e^{-i\beta s}; \quad I_{y_3} = -I \sin A \cdot e^{-i2a\beta} \cdot e^{i\beta s'} \tag{11}$$

$$I_{z_1} = I \cos A \cdot e^{-i\beta s}; \quad I_{z_3} = I \cos A \cdot e^{-i2a\beta} \cdot e^{i\beta s'}. \tag{12}$$

The radiation vectors of Sections I and II will be calculated with respect to 0 as origin, and Sections III and IV will be calculated with respect to $0'$. Then all will be referred to 0, and the resultant will be found.

The radiation vectors for the four sections are

$$\begin{aligned} \bar{F}_1 &= \int_0^a \bar{I}_1 e^{-i\beta s} \cdot e^{i\beta s \cos\psi_1} \, ds \\ &= \bar{I}_1 \frac{e^{i(a\beta/2)(\cos\psi_1 - 1)}}{\frac{\beta}{2}(\cos\psi_1 - 1)} \cdot \sin\frac{a\beta}{2}(\cos\psi_1 - 1) \end{aligned} \tag{13}$$

$$\begin{aligned} \bar{F}_2 &= \int_0^a \bar{I}_2 e^{-i\beta s} \cdot e^{i\beta s \cos\psi_2} \, ds \\ &= \bar{I}_2 \frac{e^{i(a\beta/2)(\cos\psi_2 - 1)}}{\frac{\beta}{2}(\cos\psi_2 - 1)} \cdot \sin\frac{a\beta}{2}(\cos\psi_2 - 1) \end{aligned} \tag{14}$$

$$\begin{aligned} \bar{F}_3' &= \int_0^a \bar{I}_3 e^{-i2a\beta} \cdot e^{i\beta s'} \cdot e^{i\beta s' \cos(\pi - \psi_2)} \, ds' \\ &= \bar{I}_3 \frac{e^{i(a\beta/2)(1-\cos\psi_2) - i2a\beta}}{\frac{\beta}{2}(1 - \cos\psi_2)} \sin\frac{a\beta}{2}(1 - \cos\psi_2) \end{aligned} \tag{15}$$

$$\overline{F}_4' = \int_0^a \bar{I}_4 e^{-i2a\beta} \cdot e^{i\beta s'} \cdot e^{i\beta s' \cos(\pi-\psi_1)}\, ds'$$

$$= \bar{I}_4 \frac{e^{i(a\beta/2)(1-\cos\psi_1)-i2a\beta}}{\frac{\beta}{2}(1-\cos\psi_1)} \sin\frac{a\beta}{2}(1-\cos\psi_1). \tag{16}$$

The primed vectors $\overline{F}_3'$, $\overline{F}_4'$ are referred to 0′ as origin. The vector currents $\bar{I}_1$, $\bar{I}_2$, etc., have the magnitude $I$ and the directions of the $s$ or $s'$ appropriate to the section.

Transformation from 0′ to 0 as origin is effected by means of the relations

$$\overline{F}_3 = \overline{F}_3' e^{i\beta(2a\cos A)\cos\theta}; \quad \overline{F}_4 = \overline{F}_4' e^{i\beta(2a\cos A)\cos\theta}, \tag{17}$$

the angle $\theta$ being the polar distance of the direction of radiation with respect to the $Z$ axis. The corresponding longitude, $\phi$, will be measured in the clockwise direction around the positive $Z$ axis with the positive $X$ axis as the initial line.

Relative to 0 the components of $F$ are

$$F_{y_1} = I\sin A \cdot \frac{e^{-i(a\beta/2)(1-\cos\psi_1)}}{\frac{\beta}{2}(1-\cos\psi_1)} \sin\frac{a\beta}{2}(1-\cos\psi_1) \tag{18}$$

$$F_{y_2} = I\sin A \cdot \frac{e^{-i(a\beta/2)(1-\cos\psi_2)}}{\frac{\beta}{2}(1-\cos\psi_2)} \sin\frac{a\beta}{2}(1-\cos\psi_2) \tag{19}$$

$$F_{y_3} = -I\sin A \cdot e^{i2a\beta(\cos A\cos\theta-1)} \frac{e^{i(a\beta/2)(1-\cos\psi_2)}}{\frac{\beta}{2}(1-\cos\psi_2)} \cdot \sin\frac{a\beta}{2}(1-\cos\psi_2) \tag{20}$$

$$F_{y_4} = -I\sin A \cdot e^{i2a\beta(\cos A\cos\theta-1)} \frac{e^{i(a\beta/2)(1-\cos\psi_1)}}{\frac{\beta}{2}(1-\cos\psi_1)} \cdot \sin\frac{a\beta}{2}(1-\cos\psi_1) \tag{21}$$

$$F_{z_1} = I\cos A \cdot \frac{e^{-i(a\beta/2)(1-\cos\psi_1)}}{\frac{\beta}{2}(1-\cos\psi_1)} \sin\frac{a\beta}{2}(1-\cos\psi_1) \tag{22}$$

$$F_{z_2} = -I \cos A \cdot \frac{e^{-i(a\beta/2)(1-\cos\psi_2)}}{\frac{\beta}{2}(1-\cos\psi_2)} \sin\frac{a\beta}{2}(1-\cos\psi_2) \tag{23}$$

$$F_{z_3} = I \cos A \cdot e^{i2a\beta(\cos A \cos\theta - 1)} \frac{e^{i(a\beta/2)(1-\cos\psi_2)}}{\frac{\beta}{2}(1-\cos\psi_2)} \cdot \sin\frac{a\beta}{2}(1-\cos\psi_2) \tag{24}$$

$$F_{z_4} = -I \cos A \cdot e^{i2a\beta(\cos A \cos\theta - 1)} \frac{e^{i(a\beta/2)(1-\cos\psi_1)}}{\frac{\beta}{2}(1-\cos\psi_1)} \cdot \sin\frac{a\beta}{2}(1-\cos\psi_1). \tag{25}$$

Adding the components, 1 to 4,

$$F_y = I \sin A \left[ \frac{\sin\frac{a\beta}{2}(1-\cos\psi_1)}{\frac{\beta}{2}(1-\cos\psi_1)} \left( e^{-i(a\beta/2)(1-\cos\psi_1)} - e^{i(a\beta/2)(1-\cos\psi_1)+i2a\beta(\cos A\cos\theta-1)} \right) + \frac{\sin\frac{a\beta}{2}(1-\cos\psi_2)}{\frac{\beta}{2}(1-\cos\psi_2)} \left( e^{-i(a\beta/2)(1-\cos\psi_2)} - e^{i(a\beta/2)(1-\cos\psi_2)+i2a\beta(\cos A\cos\theta-1)} \right) \right]. \tag{26}$$

By means of the relation

$$2 \cos A \cos\theta = \cos\psi_1 + \cos\psi_2 \tag{27}$$

the expression for $F_y$ may be transformed into

$$F_y = 2i e^{i(a\beta/2)(\cos\psi_1+\cos\psi_2-2)} I \sin A \cdot \sin\frac{a\beta}{2}(1-\cos\psi_1) \cdot \sin\frac{a\beta}{2}(1-\cos\psi_2) \cdot \left( \frac{1}{\frac{\beta}{2}(1-\cos\psi_1)} + \frac{1}{\frac{\beta}{2}(1-\cos\psi_2)} \right). \tag{28}$$

Similarly,

$$F_z = 2ie^{i(a\beta/2)(\cos\psi_1+\cos\psi_2-2)}\, I \cos A \cdot \sin\frac{a\beta}{2}(1-\cos\psi_1) \cdot \sin\frac{a\beta}{2}(1-\cos\psi_2)\cdot\left(\frac{1}{\frac{\beta}{2}(1-\cos\psi_1)} - \frac{1}{\frac{\beta}{2}(1-\cos\psi_2)}\right). \tag{29}$$

The spherical components of $F$ are

$$\begin{aligned} F_\theta &= F_y \cos\theta \sin\phi - F_z \sin\theta \\ &= 2ie^{i(a\beta/2)(\cos\psi_1+\cos\psi_2-2)}\, I \cos A \cdot \sin(a\beta/2)(1-\cos\psi_1)\cdot\sin\frac{a\beta}{2}(1-\cos\psi_2) \\ &\cdot\left[\left(\frac{1}{\frac{\beta}{2}(1-\cos\psi_1)} + \frac{1}{\frac{\beta}{2}(1-\cos\psi_2)}\right)\sin A \cos\theta \sin\phi \right. \\ &\left. - \left(\frac{1}{\frac{\beta}{2}(1-\cos\psi_1)} - \frac{1}{\frac{\beta}{2}(1-\cos\psi_2)}\right)\cos A \sin\theta\right] \end{aligned} \tag{30}$$

$$F_\phi = F_y \cos\phi = 2ie^{i(a\beta/2)(\cos\psi_1+\cos\psi_2-2)}\, I \sin\frac{a\beta}{2}(1-\cos\psi_1) \cdot \sin\frac{a\beta}{2}(1-\cos\psi_2)\cdot\left(\frac{1}{\frac{\beta}{2}(1-\cos\psi_1)} + \frac{1}{\frac{\beta}{2}(1-\cos\psi_2)}\right)\sin A \cos\phi. \tag{31}$$

The radiation function is

$$K^2 = F_\theta F_\theta^* + F_\phi F_\phi^* = 4I_0^2 \sin^2\frac{a\beta}{2}(1-\cos\psi_1)\cdot\sin^2\frac{a\beta}{2}(1-\cos\psi_2)\cdot \left[\left(\frac{1}{\frac{\beta}{2}(1-\cos\psi_1)} + \frac{1}{\frac{\beta}{2}(1-\cos\psi_2)}\right)\sin A \cos\theta \sin\phi - \left(\frac{1}{\frac{\beta}{2}(1-\cos\psi_1)} - \frac{1}{\frac{\beta}{2}(1-\cos\psi_2)}\right)\cos A \sin\theta\right]^2$$

$$+\left(\frac{1}{\frac{\beta}{2}(1-\cos\psi_1)}+\frac{1}{\frac{\beta}{2}(1-\cos\psi_2)}\right)^2\sin^2 A\cos^2\phi$$

$$=16\frac{I_0^2}{\beta^2}\frac{\sin^2\frac{a\beta}{2}(1-\cos\psi_1)\cdot\sin^2\frac{a\beta}{2}(1-\cos\psi_2)}{(1-\cos\psi_1)^2(1-\cos\psi_2)^2}$$

$$\cdot\Big[\Big((2-\cos\psi_1-\cos\psi_2)\sin A\cos\theta\sin\phi$$

$$-(\cos\psi_1-\cos\psi_2)\cos A\sin\theta\Big)^2$$

$$+(2-\cos\psi_1-\cos\psi_2)^2\sin^2 A\cos^2\phi\Big]. \tag{32}$$

Using the relations

$$\begin{aligned}\cos\psi_1&=\cos A\cos\theta+\sin A\sin\theta\sin\phi\\ \cos\psi_2&=\cos A\cos\theta-\sin A\sin\theta\sin\phi\\ \cos\psi_1+\cos\psi_2&=2\cos A\cos\theta\\ \cos\psi_1-\cos\psi_2&=2\sin A\sin\theta\sin\phi\end{aligned} \tag{33}$$

the factor in square brackets becomes

$$\Big[\Big((2-2\cos A\cos\theta)\sin A\cos\theta\sin\phi-2\sin A\sin^2\theta\sin\phi\cos A\Big)^2$$

$$+(2-2\cos A\cos\theta)^2\sin^2 A\cos^2\phi\Big] \tag{34}$$

$$=4\sin^2 A\Big[(1-\cos\psi_1)(1-\cos\psi_2)\Big].$$

Hence,

$$K^2=64\frac{I_0^2\sin^2 A}{\beta^2}\frac{\sin^2\frac{a\beta}{2}(1-\cos\psi_1)\cdot\sin^2\frac{a\beta}{2}(1-\cos\psi_2)}{(1-\cos\psi_1)(1-\cos\psi_2)} \tag{35}$$

or,

$$K^2=16\frac{I_0^2\sin^2 A}{\beta^2}\frac{(1-\cos a\beta\,(1-\cos\psi_1))(1-\cos a\beta(1-\cos\psi_2))}{(1-\cos\psi_1)(1-\cos\psi_2)}. \tag{36}$$

This function applies to an isolated antenna. When the effect of the earth is considered, the function is unchanged if it is regarded as representing an inverted V antenna and its image. In this case the $Y$ axis will be the vertical direction. The appropriate zenith distance and azimuth $\theta''$, $\phi''$ are related to $\psi_1$, $\psi_2$ by the equations

$$\begin{aligned} \cos \psi_1 &= \cos A \sin \theta'' \cos \phi'' + \sin A \cos \theta'' \\ \cos \psi_2 &= \cos A \sin \theta'' \cos \phi'' - \sin A \cos \theta'' \end{aligned} \tag{37}$$

where the $Z$ axis is the initial line for $\phi''$.

In the case of the horizontal rhombic antenna the radiation vector of the image antenna referred to 0 is

$$\overline{F}_i = -\overline{F} e^{i2\beta H \cos (\pi - \theta')} \tag{38}$$

where $H$ is the height of the antenna above the ground and $\theta'$ is the zenith distance of the direction of radiation. The total radiation vector is

$$F_2 = F_i + F = F(1 - e^{-i2\beta H \cos \theta'}). \tag{39}$$

Hence,

$$\begin{aligned} K_2^2 &= (F_\theta F_\theta^* + F_\phi F_\phi^*)(1 - e^{i2\beta H \cos \theta'})(1 - e^{-i2\beta H \cos \theta'}) \\ &= K^2(2 - 2 \cos (2\beta H \cos \theta')) = 4 \sin^2 (\beta H \cos \theta') \cdot K^2 \end{aligned} \tag{40}$$

If $\phi'$ is the azimuth corresponding to $\theta'$ and is measured from the principal axis of the antenna as initial line

$$\begin{aligned} \cos \psi_1 &= \sin \theta' \cdot \cos (\phi' - A) \\ \cos \psi_2 &= \sin \theta' \cdot \cos (\phi' + A) \end{aligned} \tag{41}$$

and the complete radiation function for the horizontal rhombic antenna may be written

$$K_2^2 = 64 \frac{I_0^2 \sin^2 A}{\beta^2} \sin^2 (\beta H \cos \theta') \cdot \frac{[1 - \cos a\beta(1 - \sin \theta' \cdot \cos (\phi' - A))][1 - \cos a\beta(1 - \sin \theta' \cos (\phi' + A))]}{(1 - \sin \theta' \cdot \cos (\phi' - A))(1 - \sin \theta' \cdot \cos (\phi' + A))} \tag{42}$$

or,

$$K_2^2 = 256 \frac{I_0^2 \sin^2 A}{\beta^2} \sin^2 (\beta H \cos \theta') \cdot \frac{\sin^2 \frac{a\beta}{2} (1 - \sin \theta' \cdot \cos (\phi' - A)) \cdot \sin^2 \frac{a\beta}{2} (1 - \sin \theta' \cdot \cos (\phi' + A))}{(1 - \sin \theta' \cdot \cos (\phi' - A))(1 - \sin \theta' \cdot \cos (\phi' + A))}. \tag{43}$$

## III. Properties of the Radiation Functions

The radiation functions of the inverted V antenna and of the closely related horizontal rhombic antenna depend on the size and shape of the structure, the wave length, and the direction, as well as the current. The radiation function of the horizontal rhombic antenna depends also on the height. Let the dependence of these two functions on the several variables be indicated by

$$K^2 = f(I_0, \lambda, a, A, \theta', \phi') \tag{44}$$

$$K_2^2 = g(H, \lambda, \theta') \cdot K^2. \tag{45}$$

The outstanding features of the radiation functions are revealed by discussing their maxima and minima. Consider first the radiation function of the isolated rhombus in empty space or an inverted V above a perfect ground. The same function also appears as a factor in the radiation function of the horizontal rhombic antenna.

The directional maxima of any antenna of fixed size and shape are given by

$$f'_{\theta'} = 0; \qquad f'_{\phi'} = 0; \qquad [I_0, \lambda, a, A \text{ constant}]. \tag{46}$$

If, on the other hand, we desire to find the design which will provide the highest intensity in a chosen direction, the conditions are

$$f_a' = 0; \qquad f_A' = 0; \qquad [I_0, \lambda, \theta', \phi' \text{ constant}]. \tag{47}$$

We shall require also to find the optimum value of $A$ consistent with (46) for a certain azimuth and altitude. In this case we have

$$f_A' = 0; \qquad [I_0, \lambda, \theta', \phi', \text{constant}] \tag{48}$$

and,

$$[a = \text{function of } A, \text{ through (46)}].$$

Equation (35) may be written

$$K^2 = 16\, I_0^2 a^2 \sin^2 A \frac{\sin^2 u}{u} \frac{\sin^2 v}{v}; \qquad \begin{aligned} u &\equiv \pi \frac{a}{\lambda} (1 - \cos \psi_1) \\ v &\equiv \pi \frac{a}{\lambda} (1 - \cos \psi_2) \end{aligned} \tag{49}$$

and $\cos \psi_1$, $\cos \psi_2$ may be expressed in terms of any convenient orthogonal co-ordinates such as $\theta'$, $\phi'$ when required. Collected, these relations are

$$\begin{aligned} \cos \psi_1 &= \sin \theta' \cos (\phi' - A) = \cos A \cos \theta + \sin A \sin \theta \sin \phi \\ &= \cos A \sin \theta'' \cos \phi'' + \sin A \cos \theta'' \end{aligned} \tag{50}$$

$$\begin{aligned} \cos \psi_2 &= \sin \theta' \cos (\phi' + A) = \cos A \cos \theta - \sin A \sin \theta \sin \phi \\ &= \cos A \sin \theta'' \cos \phi'' - \sin A \cos \theta''. \end{aligned} \tag{51}$$

Differentiating (49) partially with respect to $\theta'$ and $\phi'$, and equating the derivatives to zero

$$f_{\theta'}' = f_u' u_{\theta'}' + f_v' v_{\theta'}' = 0 \tag{52}$$

$$f_{\phi'}' = f_u' u_{\theta'}' + f_v' v_{\theta'}' = 0. \tag{53}$$

The roots of these two simultaneous equations, when $J(u, v)/(\theta', \phi') \neq 0$, are given by

$$f_u' = 16 I_0^2 a^2 \sin^2 A \frac{\sin^2 v}{v} \sin u \cos u \cdot (2u - \tan u) = 0 \tag{54}$$

$$f_v' = 16 I_0^2 a^2 \sin^2 A \frac{\sin^2 u}{u} \sin v \cos v \cdot (2v - \tan v) = 0. \tag{55}$$

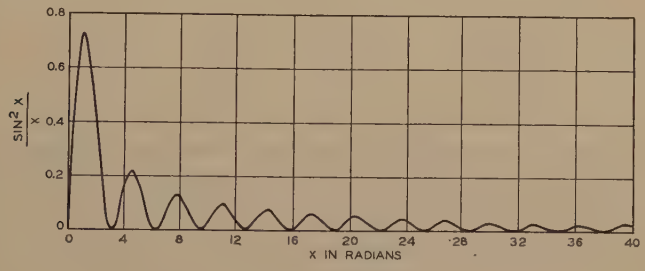


Fig. 2—Graph of the factor $\sin^2 x/x$.

The Jacobian $J(u, v)/(\theta', \phi') = -(\pi a/\lambda)^2 \frac{1}{2} \sin 2\theta' \sin 2A$ vanishes when $\theta' = 0$ and $\theta' = \pi/2$. The critical directions are given by

$$\sin u = 0 \tag{56}$$

$$\sin v = 0 \tag{57}$$

$$2u - \tan u = 0; \qquad 2v - \tan v = 0. \tag{58}$$

The last pair of equations generally correspond to maxima. The radiation function vanishes when either (56) or (57) is satisfied. (If $\psi_1$ and $\psi_2$ had been taken as independent variables, the same equations for the critical directions would have been obtained, subject to $J(u, v)/(\psi_1, \psi_2) \neq 0$; and this Jacobian vanishes only for $\psi_1 = 0, \pi$; $\psi_2 = 0, \pi$.) The roots of (58) are

$$\begin{aligned} u &= [0], \quad 0.3710\pi, \quad 1.466\pi, \quad 2.480\pi, \quad 3.486\pi, \quad \text{etc.} \\ v &= [0], \quad 0.3710\pi, \quad 1.466\pi, \quad 2.480\pi, \quad 3.486\pi, \quad \text{etc.} \end{aligned} \tag{59}$$

The pair of roots $u = 0$, $v = 0$ are directions of no radiation. The other roots, by pairs, correspond to a diminishing series of maxima, the greatest of which is at $u = v = 0.3710\pi$, the next at $u$ (or $v$) $= 0.371\pi$ and $v$ (or $u$) $= 1.466\pi$, and so on. (Fig. 2.)

In terms of $\psi_1$ and $\psi_2$, the maxima of $K^2$ are determined by the intersections of the two sets of cones

$$\cos\psi_1 = 1-\frac{\lambda}{a}0.3710,\ 1-\frac{\lambda}{a}1.466,\ 1-\frac{\lambda}{a}2.480,\ 1-\frac{\lambda}{a}3.486,\text{etc.}$$
$$\cos\psi_2 = 1-\frac{\lambda}{a}0.3710,\ 1-\frac{\lambda}{a}1.466,\ 1-\frac{\lambda}{a}2.480,\ 1-\frac{\lambda}{a}3.486,\text{etc.,} \tag{60}$$

and the minima (zeros) occur when *either* of the following conditions is satisfied:

$$\cos\psi_1 = 1,\quad 1-\frac{\lambda}{a},\quad 1-\frac{2\lambda}{a},\quad 1-\frac{3\lambda}{a},\quad \cdots,\quad 1-\frac{N\lambda}{a}$$
$$\cos\psi_2 = 1,\quad 1-\frac{\lambda}{a},\quad 1-\frac{2\lambda}{a},\quad 1-\frac{3\lambda}{a},\quad \cdots,\quad 1-\frac{N\lambda}{a} \tag{61}$$

where $N$ is the integral part of $2a/\lambda$. For example, if $a=4.6\lambda$, $N=9$, and there are ten values of $\psi_1$, and ten of $\psi_2$, between 0 and $\pi$ (including zero) for which $K^2$ vanishes. And there are nine critical values of $\psi_1$ and nine of $\psi_2$ which combine in pairs to determine directions of maximum radiation. The number of such directions is $2N^2$ minus twice the number of pairs $(\psi_1, \psi_2)$ which satisfy either of the following conditions: $\psi_1+\psi_2<2A$; $|\psi_2-\psi_1|>A$. The first maximum to disappear when $\psi_1+\psi_2<2A$ is the principal one: $\psi_1=\psi_2=\cos^{-1}(1-0.371\ \lambda/a)$. The limiting condition for existence of the principal maximum is $\cos A=1-0.371\,\lambda/a$. In that case a single principal maximum is directed along the principal axis of the antenna. The smallest number of maxima is obtained when $a/\lambda$ is small enough (or $A$ small enough) so that $|\psi_2-\psi_1|>A$ for all $\psi$'s except the pairs of type $\psi_1=\psi_2$ which determine $2N$ maxima, all in the meridian plane. These considerations suggest one way to suppress the most important subordinate maxima. This will be discussed later when the stereographic representation of the functions is given.

In general the maxima occur in quadruplets. For every maximum at $(\psi_1^m, \psi_2^n)$ there is an equal maximum at $(\psi_1^n, \psi_2^m)$, where the superscripts indicate the values of $\psi_1$, $\psi_2$ determined by the $m$th and $n$th roots of (58). However, if $m=n$, there are only two directions and they lie in the plane $\psi_1=\psi_2$. The principal maximum is of this class. The radiation function is symmetrical with respect to the plane of the antenna and also with respect to the perpendicular plane through the principal axis (meridian plane) as may be seen also from the fact that the function is unchanged when $\theta'$ is changed to $\pi-\theta'$, or $\phi'$ is changed to $-\phi'$.

The radiation function of the horizontal rhombic antenna is that of the inverted V antenna multipled by a factor that measures the effect of interference between the direct and the reflected radiation. That factor, $4 \sin^2 (\pi(2H \cos \theta'/\lambda))$ oscillates between four and zero as the zenith distance goes from zero to $\pi/2$. The factor vanishes when

$$\cos\theta' = 0, \quad \frac{1}{2}\frac{\lambda}{H}, \quad \frac{\lambda}{H}, \quad \frac{3}{2}\frac{\lambda}{H}, \cdots \quad \frac{N'\lambda}{2H}; \tag{62}$$

where $N'$ is the integral part of $\dfrac{2H}{\lambda}$

and is equal to four when

$$\cos\theta' = \frac{1}{4}\frac{\lambda}{H}, \quad \frac{3}{4}\frac{\lambda}{H}, \quad \frac{5}{4}\frac{\lambda}{H}, \cdots, \quad \frac{(2N''+1)}{4}\frac{\lambda}{H}; \tag{63}$$

where $N''$ is the integral part of $\left(\dfrac{2H}{\lambda} - \dfrac{1}{2}\right)$.

From (60), (61), (62), and (63) it will be seen that the directions for vanishing and maxima of one factor of $K_2^2$ depend only on the ratio $\lambda/a$, while the corresponding directions for the other factor depend only on $\lambda/H$. The effect of the factor, $4 \sin^2 (\pi(2H \cos \theta'/\lambda))$, on the other factor, $K^2$, depends on the relation between $\lambda/a$ and $\lambda/H$.

In order that interference with the reflected wave may have the most favorable effect in the direction of the principal maximum of $K^2$ the following relations must be satisfied simultaneously

$$(\cos\psi_1 = \cos\psi_2) \equiv \sin\theta' \cos A = 1 - \frac{\lambda}{a}\,0.371$$
$$\cos\theta' = \frac{2N''+1}{4}\cdot\frac{\lambda}{H}; \qquad N'' = 0, 1, 2, \text{ etc.} \tag{64}$$

Eliminating $\theta'$,

$$\left(\frac{1 - \dfrac{\lambda}{a}\,0.371}{\cos A}\right)^2 + \left(\frac{2N''+1}{4}\frac{\lambda}{H}\right)^2 = 1 \tag{65}$$

Ordinarily it will be required that (65) be satisfied. But it may also be desirable simultaneously to require that some subordinate maximum of $K^2$, say the first, be suppressed as much as possible by interference. The first subordinate maxima of $K^2$ are in the directions $(\psi_1, \psi_2)$, $(\psi_2, \psi_1)$ given by,

$$\cos \psi_{1,(2)} = 1 - \frac{\lambda}{a} 0.3710 \equiv P; \tag{66}$$

$$\cos \psi_{2,(1)} = 1 - \frac{\lambda}{a} 1.466 \equiv Q. \tag{67}$$

Solving (66) and (67) for $\theta'$, $\phi'$

$$\tan \phi_{12}' = \cot A \cdot \frac{P - Q}{P + Q}; \quad \sin \theta_{12}' = \sqrt{1 + \tan^2 \phi_{12}'} \cdot \sec A \cdot \frac{P + Q}{2}$$
$$\therefore \sin \theta_{12}' = \sqrt{1 + \cot^2 A \cdot \left(\frac{P - Q}{P + Q}\right)^2} \cdot \sec A \cdot \frac{P + Q}{2}. \tag{68}$$

Suppression of this radiation is obtained when

$$\cos \theta_{12}' = \frac{N'\lambda}{2H} \quad [N' = 1, 2, \text{etc.}]. \tag{69}$$

Eliminating $\theta_{12}'$ between (68) and (69), the height is given by

$$1 - \left(\frac{N'\lambda}{2H}\right)^2 = \left(1 + \cot^2 A \cdot \left(\frac{P - Q}{P + Q}\right)^2\right) \sec^2 A \cdot \left(\frac{P + Q}{2}\right)^2. \tag{70}$$

Complete suppression of the first subordinate maxima together with maximum reinforcement of the principal maximum is possible when (70) and (65) can both be satisfied; i.e., when

$$\left(\frac{4}{2N'' + 1}\right)^2 (1 - P^2 \sec^2 A) = \frac{4}{N^2}\left[1 - \left(1 + \cot^2 A \cdot \left(\frac{P - Q}{P + Q}\right)^2\right) \sec^2 A \left(\frac{P + Q}{2}\right)^2\right]. \tag{71}$$

Consider next the design of the antenna which will emit the greatest intensity in a chosen direction, for a given current. Equating to zero the partial derivatives of $K^2$ with respect to $a$ and $A$,

$$f_a' = 64 I_0^2 a \sin^2 A \frac{\sin u}{u} \frac{\sin v}{v} (v \sin u \cos v + u \cos u \sin v) = 0 \tag{72}$$

$$f_A' = 16 I_0^2 a^2 \frac{\sin u}{u} \frac{\sin v}{v} \left[\pi \frac{a}{\lambda} \sin \theta' \sin^2 A \left(\frac{\sin u(2v \cos v - \sin v)}{v} \sin (\phi' + A) - \frac{\sin v(2u \cos u - \sin u)}{u} \sin (\phi' - A)\right) + 2 \sin u \sin v \sin A \cos A\right] = 0. \tag{73}$$

A common solution is $\cos u = 0$, $\cos v = 0$. Or

$$u = (2R + 1)\frac{\pi}{2}; \qquad R = 0, 1, 2, \text{ etc.}$$
$$v = (2S + 1)\frac{\pi}{2}; \qquad S = 0, 1, 2, \text{ etc.} \tag{74}$$

These equations require that

$$\frac{a}{\lambda} = \frac{2R + 1}{2(1 - \cos \psi_1)} = \frac{(2S + 1)}{2(1 - \cos \psi_2)}. \tag{75}$$

When these relations are put in (35), we obtain the set of maximum values of $K^2$ with respect to $a$ and $A$:

$$K^2_{\max} = \frac{4I_0^2\lambda^2 \sin^2 A}{\pi^2} \cdot \frac{\sin^2 (2R + 1)\frac{\pi}{2} \cdot \sin^2 (2S + 1)\frac{\pi}{2}}{\sin^2 \tfrac{1}{2}\psi_1 \sin^2 \tfrac{1}{2}\psi_2}. \tag{76}$$

Since $\psi_1$, $\psi_2$ are fixed, these maxima are all of the same magnitude. The one of most interest, however, from the standpoint of economy is the one for which $a/\lambda$ is least. This means that either $R$ or $S$ is equal to zero. If one of them, say $R$, vanishes

$$\frac{a}{\lambda} = \frac{1}{4 \sin^2 \tfrac{1}{2}\psi_1} = \frac{2S + 1}{4 \sin^2 \tfrac{1}{2}\psi_2}. \tag{77}$$

This is only satisfied by certain pairs of values of $\psi_1$ and $\psi_2$; and if $S \neq 0$ the directions are far removed from the principal directional maximum, which ordinarily is undesirable from the point of view of gain. The antenna will therefore be oriented best with respect to the chosen direction when $R = 0$ and $S = 0$, and this requires also that the direction be in the meridian plane $\psi_1 = \psi_2$.

The requirements are thus reduced to $u = \pi/2$, $v = \pi/2$, which require that

$$\phi' = 0; \qquad a = \frac{\lambda}{2(1 - \sin \theta' \cos A)}. \tag{78}$$

The directional maximum is not pointed in the chosen direction; but it is as near as we can get it, if we insist that the intensity be as great as possible in the chosen direction.

The corresponding optimum value of $A$ is obtained by putting $u = v = \pi/2$ in $f_A' = 0$. We obtain thus a relation between $A$ and $\theta'$

$$\cos A - \sin \theta' = 0. \tag{79}$$

When this relation is satisfied, the relation (65) between $\lambda/a$ and $\lambda/H$ for maximum reinforcement of the principal directional maximum by ground reflection becomes

$$\left(\frac{2N''+1}{4}\right)^2 \cdot \frac{\lambda^2}{H^2} = \frac{\lambda}{a}\, 0.371. \tag{80}$$

The design at which we have just arrived has the disadvantage that the direction of greatest intensity does not coincide with the chosen direction of transmission. From the standpoint of gain, the most desirable design would be that which would aim the principal directional maximum in the direction in which the signal is to be transmitted. In the latter case we have found

$$u = v = 0.371\pi \tag{81}$$

while for the design which gives greatest intensity in a given direction

$$u = v = 0.5\pi. \tag{82}$$

Comparing intensities in the same direction we find

$$K^2_{u=v=0.5\pi} : K^2_{u=v=0.371\pi} :: 1 : \sin^4 0.371\pi = \text{antilog}_{10}\, 0.14672. \tag{83}$$

The loss in signal intensity due to using the smaller properly aimed antenna is only 1.5 decibels.

The angle $A$ which will result in the greatest intensity in the direction of the principal directional maximum for a chosen altitude is obtained by putting $u=v=0.371\pi$ in $K^2$ before differentiating (since the condition makes $a$ a function of $A$). We obtain the same result as before (cf. (79))

$$\cos A = \sin \theta' = 0. \tag{84}$$

(This result is obtained whenever $u=v=$ any constant.)

So far we have discussed mainly the isolated rhombic or inverted V antenna. Turning now to consideration of the corresponding properties of the horizontal rhombic antenna, we have for the critical direction

$$gf'_{\theta'} + fg_{\theta'}' = 0 \tag{85}$$

$$gf_{\theta'}' = 0 \tag{86}$$

and the largest maxima will occur when $f_{\theta'}'=0$, $f_{\phi'}'=0$, $g_{\theta'}'=0$; which are the same conditions that we have considered, together with the additional condition $g_{\theta'}'=0$.

Also, for the design which gives maximum intensity in a given direction we have

$$gf_a' = 0; \qquad gf_A' = 0; \tag{87}$$

the solutions of which are the same as for the isolated antenna. The optimum value for $A$ when the principal maximum is aimed in a chosen direction will also be the same as before, because $g$ is not a function of $a$ or $A$. Thus the properties of the horizontal antenna are very simply related to those of the isolated antenna.

It is sometimes desirable to have the variation of the direction of the principal maximum with wave length as small as possible. The rate of change of zenith distance with wave length is

$$\frac{d\theta'}{d\lambda} = -\frac{0.371}{\sqrt{\cos^2 A - \cos^2 \psi}}; \text{ where}$$
$$\cos \psi \doteq \sin \theta' \cos A = 1 - \frac{\lambda}{a} 0.371. \tag{88}$$

The most unfavorable condition is when $\cos A = \cos \psi$, or $\theta' = \pi/2$. In order for the principal maximum to exist, $\cos A$ must be equal to or greater than $\cos \psi$. The rate of change therefore approaches its least value when $A$ approaches zero and $\psi$ approaches $\pi/2$. It will be noted that the azimuthal angle covered by the major lobe is $2[\cos^{-1}(1-0.371\lambda/a)-A]$, and the vertical angle extends from $\theta' = \pi/2$ to $\theta' = \text{arc sin } (1 - \lambda/a)/\cos A$, unless extinguished sooner by interference, in which case it extends only to $\theta' = \text{arc cos } \lambda/2H$.

## IV. Stereographic Representation of the Radiation Pattern

The properties of rhombic antennas and the effects due to variation of design and frequency will be illuminated by the use of a simple graphical representation of the directions of the zeros and maxima of the radiation function. The facts are most clearly shown when the radiation function of the isolated antenna and the ground interference factor are treated separately.

If the directions of zeros and maxima of $K^2$ are plotted on a spherical blackboard with the rhombus at the center, they consist of a coaxial system of small circles, of alternating maxima and zeros defined by (60) and (61), around one arm of the antenna as axis, and an identical system of circles around the other arm of the antenna. The angle between the axes of the circles is the angle $2A$ of the rhombus. The heights of the two sets of zones marked out by the null circles are all equal. Consequently all zones subtend the same solid angle at the center. This pattern on the sphere is ideally suited to representation on the plane by means of the stereographic projection. The calculations required for the plotting are thereby made extremely simple and brief.

The stereographic projection is commonly used in cartography

and crystallography; but since it is not well known to engineers, a short account of its properties and the way it is used will be given.

When the sphere is projected on the plane of one of its circles, this plane is called the primitive plane, and the circle is called the primitive circle. In the stereographic projection, the center of projection is taken at a pole of the primitive. The projection of any point of the sphere is found by drawing a straight line from the given point to the center of projection. The intersection of this line with the primitive plane is the required point. Ordinarily the primitive circle is a great circle. The

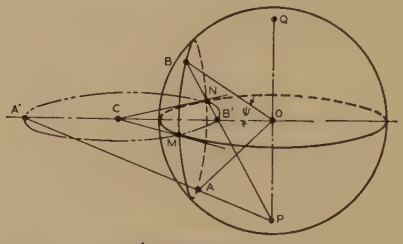


(a) PERSPECTIVE

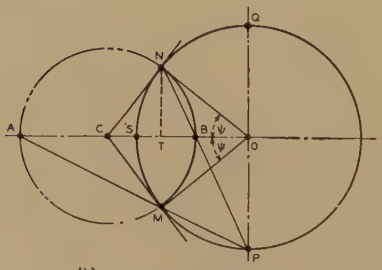


(b) PRACTICAL CONSTRUCTION

Fig. 3—Stereographic projection for the direct radiation factor.

most important properties of this projection are: (1) the projection of a circle is a circle; (2) angles on the sphere are unchanged in the projection.

Consideration of methods of construction may be limited to two special cases which include all that will be encountered here. Case (1): The plane of the given circle is perpendicular to the primitive plane. Case (2): The plane of the given circle is parallel to the primitive plane.

In connection with Figs. (3) and (4), it should be remarked that in the practical construction a single plane is used to represent both the primitive plane and the plane at right angles to it through the axes of the given circle and the primitive circle. In Case (1) the given circle and the primitive circle are at right angles where they intersect. As the angle of intersection is unchanged in the projection, the center of the

required circle is found by drawing the tangents $MC$ and $NC$. Alternatively the lines of projection $PN$, $PM$ may be drawn to intersect the line of measures in $A$ and $B$. The center is then obtained by bisecting $AB$. The construction in the other case is apparent from the figures.

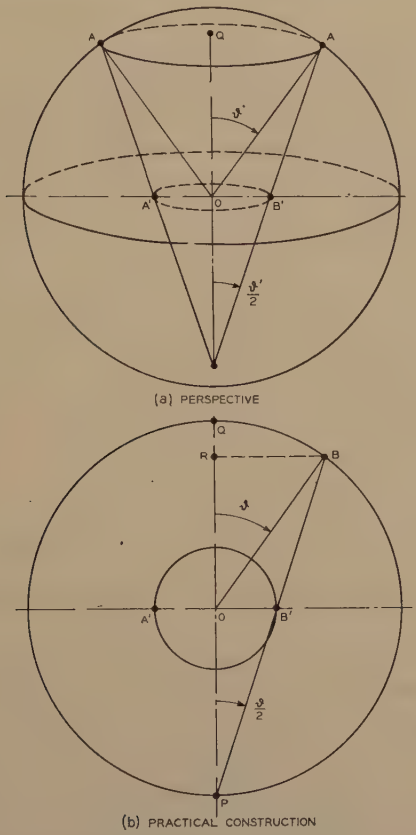


Fig. 4—Stereographic projection for the ground reflection factor.

Fortunately the forms of (60), (61), (62), and (63) are such as to make possible the complete and accurate stereographic mapping of the antenna characteristics with almost no computation, and without the use of tables. Referring to Fig. 3(*b*), if the sphere is of unit radius, the distance $ST$ is equal to $(1-\cos\psi)$. If, therefore, a series of points, $T$, are plotted along the line of measures, $OS$, such that $ST=\lambda/a$, $2\lambda/a$, $3\lambda/a$, etc., the corresponding points, $N$, will determine a series of angles $\psi$, which satisfy (61). Similarly the set of $\psi$'s which satisfy (60) are determined by plotting the points, $T$, for which $ST=r_1\lambda/a$, $r_2\lambda/a$, etc.,

where $r$ is the coefficient of $\pi$ in the roots of $\tan x = 2x$. Again in Fig. 4(b), if a series of points $R$ are plotted along $OQ$ in equal steps of length $\lambda/4H$ measured from 0, the $\theta'$'s so determined by erecting the perpendicular $RB$ satisfy (62) and (63), the nulls alternating with the maxima at equal intervals of $\cos \theta'$.

As an illustration, let us construct part of the stereographic radiation pattern of an antenna for which $\lambda/a = 0.5$; $\lambda/H = 1$. (Fig. 5). The unprimed $T$'s are plotted along the horizontal diameter at intervals of $0.5 \times 5$ centimeters (5 centimeters being the radius of the primitive circle). These points locate the null circles, of which only the first, corresponding to $T_1$, is shown. The primed $T$'s, which locate the maxi-

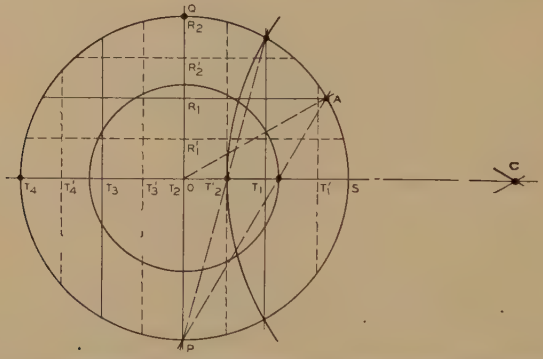


Fig. 5—Graphical construction of a distribution pattern.

mum circles, are plotted at distances from $S$ equal to $0.371 \times 0.5 \times 5$ centimeters, $1.466 \times 0.5 \times 5$ centimeters, etc. For the higher orders it will be seen that they fall almost exactly between the null $T$'s. To locate the ground reflection interference circles the vertical diameter $PQ$ is divided into equal segments of length $\frac{1}{4} \times 5$ centimeters beginning at 0. The primed $R$'s refer to maxima and the unprimed letters to zeros. Only the first null circle inside the horizon is drawn. The altitude of this circle above the horizon is equal to the angle $SOA$. The diagram is completed by drawing an identical system of circles whose centers lie on another axis making an angle with the other equal to the angle $2A$ of the rhombus.

Fig. 6 shows one half of the pattern of an antenna for which $a = 3.25\lambda$. It will be observed that as the length of the antenna is increased or the frequency is increased the number of zones into which the sphere is divided is increased and the radius of the principal maximum circle (on the right in the figure) diminishes. The altitude of the principal maximum attainable by varying the angle of the antenna is

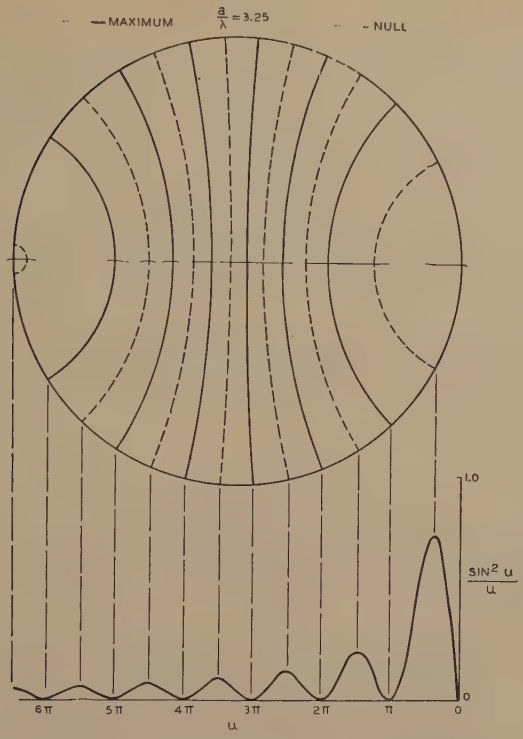


Fig. 6—A portion of a distribution pattern.

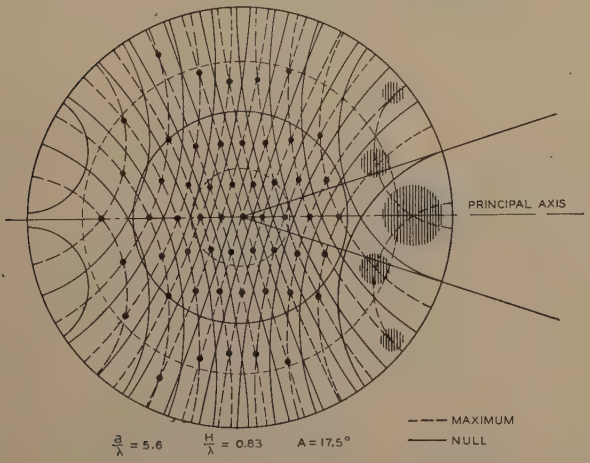


Fig. 7—Complete stereographic pattern for a horizontal rhombus.

limited to the radius of this circle. If this figure is copied on tracing cloth and placed directly over the original at various angles the effects

on the complete pattern of varying the antenna angle are easily seen.

A complete pattern for a horizontal antenna is shown in Fig. 7. This design is one which gives the strongest signal which can be emitted at an altitude of 17.5 degrees. Disregarding ground interference, the intensities of the six largest maxima are proportional to the areas of the shaded circles. Note, however, that in this case the (1, 3) pair of lobes fall so close to the zeroth ground interference null that they will be considerably attenuated while the (1, 1) and (1, 2) lobes are close to the first ground interference maximum and are reinforced accordingly. The dots in the figure locate the peaks of the minor lobes. The relatively large minor peaks (1, 4) and (1, 5) are missing.

The relative magnitudes of the directional maxima of $K^2$ are independent of the design of the antenna. The maximum values of $(\sin^2 x)/x$ are

| $n$ | 1 | 2 | 3 | 4 | 5 | 6 | 7 | 8 | 9 | 10 | 11 |
|---|---|---|---|---|---|---|---|---|---|---|---|
| $\frac{\sin^2 x}{x}$ | 0.7246 | 0.2147 | 0.1278 | 0.0911 | 0.0708 | 0.0579 | 0.0490 | 0.0425 | 0.0375 | 0.0335 | 0.0303. |

Beyond the fifth these numbers are given to this degree of accuracy by $1/x$. The intensities of the maxima in the meridian plane are proportional to the squares of these numbers; the others are measured by products. For example, the peak corresponding to the first maximum of $(\sin^2 u)/u$ and the second maximum of $(\sin^2 v)/v$, indicated by the symbol (1, 2), is proportional to the product, $0.7246 \times 0.2147$. The relative magnitudes of the directional maxima are shown in the following table in which $m$ indicates the order of a maximum of $(\sin^2 u)/u$ and $n$ the order of a maximum of $(\sin^2 v)/v$.

| $n$ | 1 | 2 | 3 | 4 | 5 | 6 | 7 | 8 | 9 | 10 | 11 |
|---|---|---|---|---|---|---|---|---|---|---|---|
| $m$ | | | | | | | | | | | |
| 1 | 0.52506 | | | | | | | | | | |
| 2 | 0.15554 | 0.04608 | | | | | | | | | |
| 3 | 0.09264 | 0.02744 | 0.01635 | | | | | | | | |
| 4 | 0.06604 | 0.01956 | 0.01165 | 0.008306 | | | | | | | |
| 5 | 0.05132 | 0.01520 | 0.009055 | 0.006455 | 0.005016 | | | | | | |
| 6 | 0.04197 | 0.01243 | 0.007406 | 0.005279 | 0.004103 | 0.003355 | | | | | |
| 7 | 0.03550 | 0.01052 | 0.006264 | 0.004465 | 0.003470 | 0.002838 | 0.002401 | | | | |
| 8 | 0.03077 | 0.009114 | 0.005429 | 0.003870 | 0.003007 | 0.002459 | 0.002080 | 0.001803 | | | |
| 9 | 0.02714 | 0.008041 | 0.004789 | 0.003414 | 0.002653 | 0.002170 | 0.001835 | 0.001591 | 0.001403 | | |
| 10 | 0.02429 | 0.007195 | 0.004286 | 0.003055 | 0.002374 | 0.001942 | 0.001642 | 0.001423 | 0.001256 | 0.001124 | |
| 11 | 0.02198 | 0.006511 | 0.003878 | 0.002764 | 0.002148 | 0.001757 | 0.001486 | 0.001288 | 0.001136 | 0.001017 | 0.0009199 |

As the order is increased these maxima occur at values of $u$ or $v$ nearer and nearer to an integral number of $\pi/2$'s. Even the fifth root of $\tan u = 2u$ occurs at a value of $u$ only two degrees less than $9/2\pi$.

It is easy to see that the gain increases when the ratio $a/\lambda$ is increased. But at the same time the solid angle covered by the principal beam is diminished, the beam is depressed, and greater height is required. The solid angle may become so small that the resulting increase

in fading will annul the advantage in gain. Therefore it is desirable to increase the gain by means which will not affect the solid angle or the altitude of the principal beam. A design in which the gain is increased by suppressing subordinate maxima is shown in Fig. 8. The (1, 3) pair of peaks are made to vanish by depressing them to the horizon. The height is adjusted so that the first ground interference null passes through the (1, 2) pair of maxima and the first interference maximum goes through the (1, 1) maximum. This particular example of a design which gives high gain with a fairly broad principal beam does not

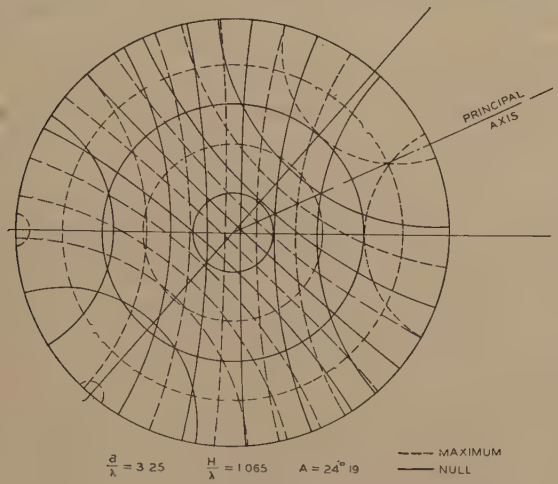


Fig. 8—A design in which several large subordinate maxima have been suppressed.

satisfy the condition $A = \pi/2 - \theta'_{(1,1)}$ demanded by the requirement of highest intensity for a given current. But a design which effects a reduction of the radiation resistance permits the use of a larger antenna current without increasing the expenditure of power.

It may be shown that the necessary relation between $\lambda/a$ and the zenith distance of the principal lobe when a certain subordinate maximum $(1, n)$ is on the horizon is

$$\left[2\left(1 - r_1\frac{\lambda}{a}\right)^3 - \sin^2\theta'_{(1,1)}\left(2 - \frac{\lambda}{a}(r_1 + r_n)\right)\right]^2 \cdot \sin^2\theta'_{(1,1)}$$
$$= 4\left(1 - r_1\frac{\lambda}{a}\right)\left(\sin^2\theta'_{(1,1)} - \left(1 - r_1\frac{\lambda}{a}\right)^2\right)\left(1 - \left(1 - r_1\frac{\lambda}{a}\right)^2\right). \quad (89)$$

Then only those peaks $(1, m)$ can exist for which $m<n$. When we say that a peak vanishes by interference, we do not mean to imply that the entire corresponding lobe is wiped out, but only a major portion of it.

## V. States of Polarization and Applicability of the Reciprocation Theorem

Because of the symmetry of the radiation function, one may expect to find that the electromotive intensity is either parallel or perpendicular to the plane of the rhombus and the meridian plane for directions of radiation which lie in these planes, but not elsewhere. If a formula giving the directional properties of the antenna in reception is obtained on the assumption of a certain polarization of the received wave, it must not be supposed that the directional properties in transmission can be inferred from such a formula on the basis of the reciprocation theorem except in that range of direction for which the assumption regarding polarization is satisfied in transmission. For this reason the reception formula due to Bruce, Beck, and Lowry will not yield the directional properties of a transmitting antenna. If reciprocity exists at all, it will be confined to certain limited ranges of direction, which depend on the state of polarization of the transmitted ray. This we now proceed to investigate.

The components of the complex electromotive intensity of the transmitted wave are expressible in the forms

$$E_{\theta'} = -120\pi i\beta A_{\theta'} \tag{90}$$

$$E_{\phi'} = -120\pi i\beta A_{\phi'} \tag{91}$$

where $A_{\phi'}$ and $A_{\theta'}$ are the components of the complex magnetic vector potential. Hence, from the definition of the radiation vector, we have

$$E_{\theta'} = -120\pi i\beta \frac{e^{-i\beta r}}{4\pi r} F_{\theta'} \tag{92}$$

$$E_{\phi'} = -120\pi i\beta \frac{e^{-i\beta r}}{4\pi r} F_{\phi'}. \tag{93}$$

The spherical components of the radiation vector in terms of the rectangular components are given by

$$F_{\theta'} = -F_x \sin\theta' + F_y \cos\theta' \sin\phi' + F_z \cos\theta' \cos\phi' \tag{94}$$

$$F_{\phi'} = F_y \cos\phi' - F_z \sin\phi'. \tag{95}$$

Substituting the values of $F_y$ and $F_z$, we find

$$F_{\theta'} = I \cos\theta' \cdot 2ie^{i(a\beta/2)(\cos\psi_1+\cos\psi_2-2)} \frac{\sin\frac{a\beta}{2}(1-\cos\psi_1)\cdot\sin\frac{a\beta}{2}(1-\cos\psi_2)}{(1-\cos\psi_1)(1-\cos\psi_2)} \times \frac{2}{\beta}\left[\left(2-(\cos\psi_1+\cos\psi_2)\right)\sin A\sin\phi' + (\cos\psi_1-\cos\psi_2)\cos A\cos\phi'\right] \quad (96)$$

$$F_{\phi'} = I\,2ie^{i(a\beta/2)(\cos\psi_1+\cos\psi_2-2)} \frac{\sin\frac{a\beta}{2}(1-\cos\psi_1)\cdot\sin\frac{a\beta}{2}(1-\cos\psi_2)}{(1-\cos\psi_1)(1-\cos\psi_2)} \times \frac{2}{\beta}\left[\left(2-(\cos\psi_1+\cos\psi_2)\right)\sin A\cos\phi' - (\cos\psi_1-\cos\psi_2)\cos A\sin\phi'\right]. \quad (97)$$

(Note that $(\cos\psi_1-\cos\psi_2) = 2\sin\theta'\sin\phi'\sin A$;

$(\cos\psi_1+\cos\psi_2) = 2\sin\theta'\cos\phi'\cos A$).

We see that $F_{\theta'}$ vanishes and $F_{\phi'}$ remains finite when $\phi'=0$ or $\theta'=\pi/2$. In other words, the electric vector is parallel to the plane of the antenna only for radiation directed in the meridian plane or the plane of the antenna.

By means of these equations the direction of the electric vector may be calculated for any direction of the ray. The most important direction is that of the principal maximum; and it is shown that for this ray the electric vector is horizontal for a horizontal rhombus and vertical for an inverted V antenna.

The formula for the complex current in the receiver given by Bruce, Beck, and Lowry, when translated into the symbols used in this paper, is

$$I_r = i\frac{\epsilon\lambda}{4_\pi Z_0}\left[\frac{\sin(\phi'+A)}{1-\cos(\phi'+A)\cdot\sin\theta'} - \frac{\sin(\phi'-A)}{1-\cos(\phi'-A)\cdot\sin\theta'}\right] \times\left[1-e^{-ia\beta(1-\cos(\phi'-A)\cdot\sin\theta')}\right]\left[1-e^{-ia\beta(1-\cos(\phi'+A)\cdot\sin\theta')}\right] \times\left[1+e^{-i2\beta H\cos\theta'}\right] \quad (98)$$

when the ground is perfect. The square of the modulus of the current is

$$|I_r|^2 = \frac{\epsilon^2\lambda^2}{16\pi^2 Z_0^2}\left[\frac{\sin(\phi'+A)}{1-\sin\theta'\cdot\cos(\phi'+A)} - \frac{\sin(\phi'-A)}{1-\sin\theta'\cdot\cos(\phi'-A)}\right]^2 \tag{99}$$

$$\cdot 4\sin^2\frac{a\beta}{2}(1-\sin\theta'\cdot\cos(\phi'-A))\cdot 4\sin^2\frac{a\beta}{2}(1-\sin\theta\cdot\cos(\phi'+A))$$

$$\cdot 4\sin^2(\beta H\cos\theta').$$

Comparing this with the corresponding function for radiation we see that they differ as functions of direction only in that

$$\left[\frac{\sin(\phi'+A)}{(1-\cos\psi_2)} - \frac{\sin(\phi'-A)}{(1-\cos\psi_1)}\right]^2$$

appears as a factor in $|I_r|^2$ instead of the factor

$$\frac{1}{(1-\cos\psi_1)(1-\cos\psi_2)} \equiv \frac{1}{(\cos\phi'-\sin\theta'\cos A)^2+\sin^2\phi'\cos^2\theta'}$$

of $K_2^2$. After some reduction we find that

$$\left[\frac{\sin(\phi'+A)}{1-\cos\psi_2} - \frac{\sin(\phi'-A)}{1-\cos\psi_1}\right]^2 \tag{100}$$

$$= 4\sin^2 A\cdot\left[\frac{\cos\phi'-\sin\theta'\cos A}{(\cos\phi'-\sin\theta'\cos A)^2+\sin^2\phi'\cos^2\theta'}\right]^2.$$

The two factors are seen to be identical only when $\phi'=0$ or $\theta'=\pi/2$, a result which we have already predicted from the restrictions on the validity of the reciprocation theorem and the fact that the receiving equation is based on an electric vector which is normal to the plane of incidence.

It cannot be maintained that this receiving formula will be correct for a receiving antenna when it is receiving radiation directly from any of the lobes of a rhombic transmitting antenna other than those in its meridian plane. While the receiving antenna will not respond to a vertical component of $E$, it will respond to the horizontal component of $E_{\theta'}$ (as well as to $E_{\phi'}$ which is wholly horizontal). The component $E_{\phi'}$ is in the plane of the wave front; but the horizontal component of $E_{\theta'}$ is in the plane of incidence.

## VI. Note on the Radiation Resistance and the Gain

The radiation resistance is given by

$$R = \frac{30\pi}{I_0^2\lambda^2} \int K^2 \, d\Omega \tag{101}$$

for the inverted V, and by

$$R = \frac{30\pi}{I_0^2\lambda^2} \int K_2^2 \, d\Omega \tag{102}$$

for the horizontal rhombic antenna. The differential, $d\Omega$, signifies an element of solid angle; and the integration is to be carried out over all directions.

The absolute gain in decibels is

$$10 \log_{10} 4\pi \frac{K^2_{\max}}{\int K^2 d\Omega} \tag{103}$$

where $K_{\max}^2$ indicates the value of $K^2$ (or $K_2^2$) evaluated at the principal maximum. Difficulty of performing the indicated integrations has prevented general calculation of the radiation resistance and gain. The calculation can be performed for any particular case by mechanical integration.

*Proceedings of the Institute of Radio Engineers*
*Volume 25, Number 10* *October, 1937*

# CHARACTERISTICS OF THE IONOSPHERE AT WASHINGTON, D. C., AUGUST, 1937*

By

T. R. Gilliland, S. S. Kirby, N. Smith, and S. E. Reymer
(National Bureau of Standards, Washington, D. C.)

FIG. 1 shows the critical frequency and virtual height data for August, 1937. The characteristics of the ionosphere showed the effects of the seasonal advance toward winter in that the daytime values of $f_{F_2}$ were greater, the rise of $f_{F_2}$ at sunrise was more rapid, and

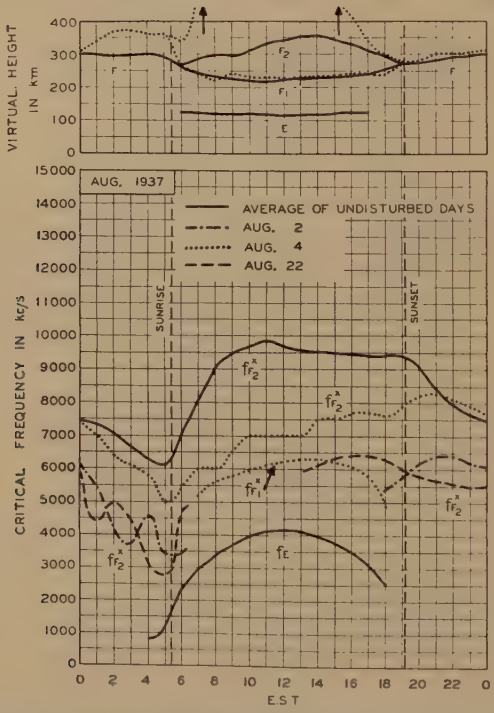


FIG. 1. Virtual heights and critical frequencies of the E, $F_1$, $F_2$, and F layers of the ionosphere for August, 1937. The solid line graphs represent averages for the quiet days. The graphs for August 2, 4, and 22 represent conditions for days of ionosphere storms.

the $f_{F_1}$ on quiet days was more poorly defined than during July. The $f_{F_1}$ was so poorly defined on quiet days during August that the values could not be accurately determined and for this reason they are not

* Decimal classification: R113.61. Original manuscript by the Institute, September 9, 1937. Publication approved by the Director of the National Bureau of Standards of the U. S. Department of Commerce.

shown in the figure. The critical frequencies for the undisturbed days in August, 1937, exceeded those for August, 1936, by approximately the following amounts: noon $f_E$—250 kc, noon $f_{F_2}$—1100 kc, midnight $f_F$—1100 kc.

Out of 366 hours of observations from 0000 to 1100, E.S.T., strong sporadic E reflections up to 4400 kilocycles or higher were present seven per cent of the time and up to 6200 kilocycles or higher 2.5 per cent of the time. Out of 353 hours of observations from 1200 to 2300, E.S.T., strong sporadic E reflections up to 4400 kilocycles or higher were present fourteen per cent of the time and up to 6200 kilocycles or higher six per cent of the time. Around sunset on a few days, especially August 18, strong sporadic E reflections up to 11,000 kilocycles were present.

TABLE I
IONOSPHERE STORMS

| Date 0000–2400, E.S.T. | $h_F$ before sunrise km | Max. $f_{F_2}{}^x$ during day (near sunset) kc | Min. $f_{F_2}$ during day (before sunrise) kc | Magnetic Character[1] | |
|---|---|---|---|---|---|
| | | | | 0000–1200 G.M.T. | 1200–2400 G.M.T. |
| Aug. 22 | 415 | 6400 | 2800 | 1.7 | 1.1 |
| Aug. 2 | 420 | 6400 | 3350 | 1.4 | 0.7 |
| Aug. 4 | 352 | 8300 | 5000 | 1.0 | 0.4 |
| Aug. 28 | 313 | 8700 | 4750 | 0.2 | 0.4 |
| Aug. 29 | 315 | 9200 | 5300 | 0.3 | 0.0 |
| Aug. 23† | 333 | near normal | 4400 | 0.4 | 0.1 |
| Aug. 3† | 329 | normal | 5000 | 0.4 | 0.6 |
| Average of undisturbed days | 298 | 9870 | 6070 | 0.14 | 0.2 |

[1] American character figure. Average of seven observatories, two of which are operated by Carnegie Institution of Washington and five of which are operated by the United States Coast and Geodetic Survey.

† The ionosphere storms of August 2–3 and 22–23 ended shortly after sunrise on August 3 and 23, respectively.

Ionosphere disturbances associated with magnetic storms will hereafter be called ionosphere storms. In Table I ionosphere storms are listed approximately in the order of their severity together with other related data.

Out of 182 hours of night measurements of $f_F{}^x$ between 0000 and 0500, E.S.T., twenty-four values were more than twenty per cent below the undisturbed average. All of these occurred on the ionosphere storm days of August 2, 3, 4, 22, 23, and 28. During this same period forty values of $f_F{}^x$ were more than ten per cent below the undisturbed average for August. All but seven of these occurred on the dates listed in Table I. Of these night measurements no values were over twenty per cent above, two values were over fifteen per cent above, and twelve values over ten per cent above the undisturbed average.

Out of sixty-eight hours of observations between 0600 and 2200, E.S.T., on Wednesdays nine values were over twenty per cent below and fourteen values over fifteen per cent below the undisturbed average. All of these occurred on the ionosphere storm day of August 4. Between

these hours on the quiet days of August 11, 18, and 25 all values were within ±10 per cent of the undisturbed average.

Emissions from station W8XAL, 6060 kilocycles, 650 kilometers, were propagated regularly by the F layer at night except for short periods between midnight and 0600, E.S.T., on the ionosphere storm days of August 2, 3, and 4. The ionosphere storm day of August 22 was Sunday and the W8XAL transmissions did not begin until 0800, E.S.T., which was too late to indicate an early morning failure of F layer transmissions. During August E layer transmission began on the average at 0628 and ended at 1821, E.S.T.

Transmissions from W1XK, 9570 kilocycles, 600 kilometers, during August were undergoing a transition from summer to winter type propagation. For ten days of the summer type, normal E layer transmission began on the average at 0828 and ended on the average at 1443, E.S.T. On five of these days F layer transmission was observed to begin at an average of 1752, E.S.T. On eleven winter type days F layer transmission began on the average at 0640, E.S.T. The average ending time of F layer transmission on twenty-two days was 2104, E.S.T. These transmissions were not received by F layer on August 2, 4, 21, 22, 27, and 28. Sporadic E transmissions obscured the beginning and ending of normal E and F layer transmission on several occasions.

Transmissions from DJB, Berlin, 15,200 kilocycles, 6700 kilometers, were propagated regularly by the F layer on ionospherically quiet nights. These transmissions were made regularly from 1700 to 2300, E.S.T., or 2300 to 0500, Berlin time. They failed completely on the nights of August 3–4, 22–23, 27–28, failed during the later hours of transmission on the nights of August 1–2, 19–20, and 28–29, and were very poor on the night of August 4–5. These periods of poor propagation were, except for August 19–20, all times of ionosphere storms.

Sudden disturbances of the ionosphere were not as numerous during August, 1937, as during July. They were marked by the following radio fade-outs, observed at Washington:[2]

TABLE II

| Date | Beginning of fade-out | Beginning of recovery | Recovery complete | Location of transmitter | Minimum intensity |
|---|---|---|---|---|---|
| Aug. 1 | 1740 | — | 1756 | Ohio, D.C. | 0.2 |
| Aug. 1 | 1820 | — | 2005 | Ohio, Mass. | 0.5 |
| Aug. 6 | 2152 | 2201 | 2209 | Ohio | 0.01 |
| Aug. 7 | 1400 | 1432 | 1540 | Ohio, Mass., D.C. | 0.02 |
| Aug. 10 | 1420 | — | 1530 | Ohio | 0.5 |
| Aug. 11 | 1905 | 1915 | 1922 | Ohio | 0.05 |
| Aug. 14 | 1816 | 1829 | 1838 | Ohio | 0.0 |
| Aug. 18 | 1727 | 1735 | 1800 | Ohio, Mass. | 0.0 |
| Aug. 27 | 2047 | — | 2140 | Ohio, D.C. | 0.01 |
| Aug. 28 | 1924 | 2006 | 2050 | Ohio, Mass., D.C. | 0.0 |

[2] All times G.M.T. Minimum intensities given in terms of transmissions from W8XAL, frequency 6060 kilocycles, distance 650 kilometers.

# CONTRIBUTORS TO THIS ISSUE

**Dellinger, J. H.:** Born July 3, 1886, at Cleveland, Ohio. Educated at Western Reserve University, 1903–1907; received A.B. degree, George Washington University, 1908; Ph.D. degree, Princeton University, 1913; D.Sc. degree, George Washington University, 1932. Joined staff of National Bureau of Standards as physicist, 1907; chief engineer, Federal Radio Commission, 1928–1929; chief of radio section, research division, aeronautics branch, Department of Commerce, 1926–1934; chief of radio section, National Bureau of Standards, 1919 to date. United States representative at numerous international radio and electrical conferences, 1921 to date. Vice president, Institute of Radio Engineers, 1924; president, 1925. Fellow, Institute of Radio Engineers, 1923.

**Foster, Donald:** Born March 19, 1900, at West Torbrook, Nova Scotia, Canada. Assistant in chemistry, Acadia University, 1918–1919; topographer and assistant geologist, Geological Survey of Canada, 1918–1920; assistant in chemistry, Acadia University, 1918–1919; assistant in physics, Yale University, 1920–1921; teacher of physics and mathematics in preparatory schools, New Haven, Connecticut, 1921–1924; Loomis Fellow, Yale University, 1921–1924; received Ph.D. degree, Yale University, 1924. Optical engineer, research and development department, Eastman Kodak Company, 1924–1925; research department, Bell Telephone Laboratories, Inc., 1925–1936; physicist, Westinghouse Electric and Manufacturing Company, 1936 to date. Nonmember, Institute of Radio Engineers.

**Goddard, DeWitt R.:** Born November 30, 1904, at New York, New York. Received B.S. degree in electrical engineering, Worcester Poly-Technic Institute, 1929. Communication receiver research and development, RCA Communications, Inc., 1929 to date. Associate member, Institute of Radio Engineers, 1931.

**Morrison, John F.:** See PROCEEDINGS for June, 1937.

***Norton, K. A.:** Born February 27, 1907, at Rockwell City, Iowa. Received B.S. degree, University of Chicago, 1928. Inspection development laboratory Western Electric Company, 1929. Columbia University, 1930–1931. Radio Section, Bureau of Standards, July, 1929, to September, 1930, and June, 1931, to December, 1934. Federal Communications Commission, December, 1934, to date. Associate member, Institute of Radio Engineers, 1929.

**Peterson, Harold O.:** Born November 3, 1899, at Blair, Nebraska. Received B.S. degree in electrical engineering, University of Nebraska, 1921. Testman, General Electric Company, 1921–1922. Engaged in development of radio communications equipment, Radio Corporation of America, 1922–1929; in charge, radio communication receiver development laboratory, RCA Communications, Inc., 1929 to date. Associate member, Institute of Radio Engineers, 1922; Member, 1931.

* Paper published in September, 1937, issue of the PROCEEDINGS

**Roberts, W. van B.:** Born 1893. Received B.S. degree, Princeton University, 1915; E.E. degree, 1917; Ph.D. degree, 1924. Student engineer, Western Electric Company, summer, 1916; head of radio and signaling department, School of Military Aeronautics, U. S. Signal Corps, 1917; technical officer of sound ranging, Section 1, Engineer Corps, A.E.F., 1918; instructor in physics and communication theory, school of electrical engineering, Princeton University, 1919–1923. Radio Corporation of America, 1924 to date. Associate member, Institute of Radio Engineers, 1922; Fellow, 1929.

**Samuel, Arthur L.:** Born December 5, 1901, at Emporia, Kansas. Received B.A. degree, College of Emporia, 1923; received S.B. and S.M. degrees, Massachusetts Institute of Technology, 1926. General Electric Company (intermittently), 1923–1927; instructor, electrical engineering department, Massachusetts Institute of Technology, 1926–1928; technical staff, Bell Telephone Laboratories, Inc., 1928 to date. Member, American Physical Society and American Institute of Electrical Engineers. Associate member, Institute of Radio Engineers, 1924.